2012-03-08

Novel Phosducin-Like Protein Binding Partners: Exploring Chaperone and Tumor Suppressor Protein Interactions

Amy Jetaun Gray
Brigham Young University - Provo

Novel Phosducin-Like Protein Binding Partners:

Exploring Chaperone and Tumor Suppressor

Protein Interactions

Amy J. Gray

A dissertation submitted to the faculty of
Brigham Young University
in partial fulfillment of the requirements for the degree of

Doctor of Philosophy

Barry M. Willardson, Chair
Laura C. Bridgewater
Gregory F. Burton
Steven W. Graves
John T. Prince

Department of Chemistry and Biochemistry

Brigham Young University

April 2012

ABSTRACT

Novel Phosducin-Like Protein Binding Partners:
Exploring Chaperone and Tumor Suppressor
Protein Interactions

Amy J. Gray
Department of Chemistry and Biochemistry, BYU
Doctor of Philosophy

Many proteins cannot fold into their native state without the assistance of one or more molecular chaperones. Chaperonins are an essential class of chaperones that provide an isolated chamber for proteins to fold. CCT, a group II chaperonin found in eukaryotes assists in the folding of actins, tubulins, and many other cellular proteins. PhLP1 is a member of the phosducin protein family that assists CCT in the folding of Gβ and its subsequent assembly with Gγ. However, previous studies have not addressed the scope of PhLP1 and CCT-mediated Gβγ assembly. The data presented in Chapter 2 shows that PhLP1 plays a vital role in the assembly of all Gγ subunits that form dimers with Gβ2 and the assembly of Gγ2 with Gβ1-4, without affecting the specificity of the Gβγ interactions. These findings suggest that PhLP1 has a general role for the assembly of all Gβγ combinations.

Although the role of PhLP1 as a co-chaperone for Gβγ assembly has been established, other possible functions for PhLP1 either as a co-chaperone or otherwise are yet to be investigated. A known tumor suppressor protein, PDCD5, was found to interact with PhLP1 in a co-immunoprecipitation proteomics screen. The data presented in Chapter 3 show that PDCD5 binds PhLP1 indirectly through a ternary complex with CCT. Our results signify that the apoptotic function of PDCD5 is cytosolic, is phosphorylation dependent, and most likely involves CCT. Moreover, structural analysis suggests that over-expressed PDCD5 blocks β-actin from entering the CCT folding cavity, suggesting a co-chaperone role for PDCD5 in inhibiting or enhancing folding of yet-to-be determined CCT substrates.

Compared to PhLP1, the functions of other members of the phosducin family, PhLP2A, PhLP2B, and PhLP3, are poorly understood. They have no role in G-protein signaling, but appear to assist CCT in the folding of actin, tubulin and proteins involved in cell cycle progression. Chapter 4 investigates the possibility of PhLP2 and/or PhLP3 acting as co-chaperones in the folding and assembly of actins and tubulins. In addition, another mediator of cellular signaling, 14-3-3ε, was found to interact with PhLP2A in a phosphorylation dependent manner and relieve the inhibition of β-actin folding caused by PhLP2A over-expression.

Key words: Chaperonin, chaperone, G-protein signaling, phosducin-like protein, PDCD5

ACKNOWLEDGEMENTS

I wish to acknowledge and thank everyone who contributed to this work. I am especially grateful for my advisor, Dr. Barry Willardson, and his willingness to lead me in this research, and the Department of Chemistry and Biochemistry and Brigham Young University for granting me this opportunity. I have enjoyed working with an outstanding group of people in the Willardson lab. I would like to particularly acknowledge Alyson C. Howlett, Christopher M. Tracy, Rebecca L. Plimpton, and Nana Sono-Koree who contributed directly to this work. Finally, I owe deep gratitude to my family and my husband, Nathan W. Gray, as I could not have accomplished this goal without their patience, love, and support.

TABLE OF CONTENTS

LIST OF FIGURES AND TABLES

ABBREVIATIONS

A	Alanine
ADP	Adenosine diphosphate
ATP	Adenosine triphosphate
C-	Carboxy-terminus
CCT	Chaperonin containing tailless complex polypeptide 1
D	Aspartic acid
E	Glutamic acid
G	Heterotrimeric GTP binding protein
GDP	Guanosine diphosphate
GPCR	G-protein coupled receptor
GTP	Guanosine triphosphate
Gα	G-protein alpha subunit
Gβ	G-protein beta subunit
Gβγ	G-protein beta and gamma subunit dimer
Gγ	G-protein gamma subunit
HA	Hemagglutinin
HEK 293T cells	Human embryonic kidney 293 cells
Hsp	Heat shock protein
LCMSMS	Liquid chromatography coupled to tandem mass spectrometry
MS	Mass spectrometry
MSMS	Tandem mass spectrometry
N-	Amino-terminus
PCR	Polymerase chain reaction
Pdc	Phosducin
PDCD5	Programmed Cell Death Protein 5
PhLP1	Phosducin-like protein 1
PhLP 2A	Phosducin-like protein 2A
PhLP 2B	Phosducin-like protein 2B
PhLP 3	Phosducin-like protein 3
R7BP	R7 binding protein
RGS	Regulator of G protein signaling
RNAi	RNA interference
S	Serine
siRNA	Short interfering RNA
WT	Wild-type

CHAPTER 1 INTRODUCTION:

THE EUKARYOTIC CHAPERONIN COMPLEX COOPERATES WITH PHOSDUCIN-LIKE PROTEINS IN PROTEIN FOLDING AND ASSEMBLY

Summary

Many proteins cannot fold into their native state without the assistance of one or more molecular chaperones. Chaperonins are an essential class of chaperones that provide an isolated chamber for proteins to fold. CCT, a group II chaperonin found in eukaryotes assists in the folding of actins, tubulins, and many other cellular proteins. PhLP1 is a member of the phosducin protein family that assists CCT in the folding of Gβ and its subsequent assembly with Gγ. Other members of the phosducin family, PhLP2 and PhLP3, have no role in G protein signaling, but appear to assist CCT in the folding of actin, tubulin and proteins involved in cell cycle progression. In this study, other functions of phosducin-like proteins as co-chaperone or otherwise are investigated.

Introduction

In order for proteins to reach their native state, they must fold properly. The information for the native state is encoded in the amino acid sequence (*1*), however there is ample evidence showing that proteins fold co-translationally (*2*). In the past, it was generally thought that all proteins folded spontaneously *in vivo (3).* Small, single domain proteins usually fold efficiently because hydrophobic amino acid residues are buried quickly. However, when it was observed that proteins imported into the mitochondria needed to be unfolded to pass through the membrane (*4*), Hartl and Horwich subsequently discovered that these unfolded proteins required Hsp60, a structural homolog of GroEL, mediated by ATP for their refolding (*5-7*). Furthermore,

Hartl and colleagues found that chaperone-mediated folding actually consisted of a series of chaperone proteins (*8*). Today, it is understood that 65-85% of newly translated proteins fold spontaneously, but it is the larger proteins that tend to fold inefficiently due to exposure of hydrophobic regions which may cause aggregation (*9*). To overcome this problem, cells contain a complex chaperone system to assist in folding and prevention of aggregation. The three major molecular chaperone systems implicated in cytosolic protein folding in eukaryotes are the heat shock protein (Hsp) 70s along with their Hsp40 cofactors, the Hsp90 system, and the chaperonins (*2, 10*). Hsps are synthesized at increased levels in response to stress conditions and generally recognize hydrophobic residues and/or structural regions that are normally buried upon completion of folding (*9*). Hsp70s and chaperonins participate in protein folding through cycles of substrate binding and release and are regulated by adenosine triphosphatase (ATPase) activity and cofactor proteins. Moreover, deregulation of the chaperone system could result in accumulation of toxic protein aggregates that can lead to several human diseases including Alzheimer's, Huntington's, Parkinson's and amyotrophic lateral sclerosis (*9*).

Group I and group II chaperonins

Chaperonins are a class of high molecular weight protein complexes (800-1000 kDa) that are involved in the folding of specific proteins that cannot be folded by simpler chaperone systems (*11*). There are two groups of chaperonins: group I chaperonins are found in prokaryotic cells and endosymbiotic organelles, and group II chaperonins are found in Archaea and Eukarya (*12*). Both groups have a unique ring-shaped structure which provides a substrate binding cavity where entire proteins or protein domains can fold while being sequestered from the cytosol. Chaperonins are comprised of two rings arranged back-to-back containing homologous 60 kDa protein subunits. These chaperonin subunits share a similar structure with three basic domains.

The equatorial domain binds ATP, the apical domain is involved in substrate binding, and the hinge domain connects the equatorial and apical domains allowing communication between the two. The apical domains have the most sequence divergence and contain substrate binding sites (*13*).

The most thoroughly studied chaperonin is GroEL, a group I chaperonin found in *Escherichia coli*. GroEL contains two homoheptameric rings consisting of 14 identical subunits. GroEL has a wide spectrum of folding substrates due to the non-specific hydrophobic regions in the apical domains in the binding cavity. The binding cavity of GroEL cannot close on its own, therefore a ring-shaped cofactor, GroES, is required for proper function (*14*). GroES acts as a removable lid that provides a chamber for the folding of substrates. Group II chaperonins such as CCT (chaperonin-containing TCP-1) in eukaryotes and the thermosome in archaea, are hetero-oligomeric complexes containing eight or nine subunits in each ring (*1*). Group II chaperonins do not require a co-chaperone for cavity closure, but have a built-in lid made of the helical extensions in their apical domains that carry out drastic conformational changes upon ATP binding.

Both groups of chaperonins have a general protein folding cycle that is driven by ATP hydrolysis. During the folding cycle, the chaperonins assume two main conformations. The chaperonin adopts an open structure and a high affinity for the substrate when ADP is bound, and the ATP-bound conformation assumes a closed structure that has a low affinity for the substrate. Thus, the substrate binds the chaperonin in the open state. Subsequently, nucleotide binding induces a conformational change that leads to cavity closure (with the help of cofactors in group I chaperonins or by the helical protrusions in the case of group II chaperonins) and

release of the substrate inside the cavity. The substrate is then allowed to fold in its isolated environment (*1*).

The eukaryotic cytosolic chaperonin CCT

The chaperonin containing tailless complex polypeptide 1 (CCT) (also known as TRiC) is an essential group II chaperonin that has been estimated to interact with 9-15% of all newly synthesized cytosolic proteins (*15, 16*). Thus, many of these proteins may require CCT for their folding or assembly. CCT has eight different yet homologous subunits α, η, δ, θ, γ, β, ζ, and ε, in which the order within the ring structure has been debated (*17, 18*). The subunits share about 30% sequence identity (*19*). CCT has a much narrower substrate spectrum than does GroEL in the *E. coli* cytosol (*15*). This is due to extended regions present in the apical domains that are important in cavity closure induced by ATP binding. Despite its narrower substrate spectrum, CCT is thought to specifically recognize many different substrates by its different individual subunits through both hydrophobic and electrostatic interactions (*12*).

The mechanism of CCT closure differs slightly from the general chaperonin mechanism. ATP binding alone does not induce closure of the lid, but the current understanding is that hydrolysis of ATP is the driving force of lid closure. Supporting evidence of this mechanism came when non-hydrolyzable analogs of ATP did not promote lid closure. However, when the transition state analog ADP-AlF_x is bound to CCT, a closed conformation is assumed. Thus, the hydrolysis of ATP is what actually induces lid closure (*12*). Another unique folding mechanism of CCT is that some substrates do not release into the cavity like GroEL substrates; instead, they remain bound to CCT during the folding process (*20*). Many substrates of CCT are homodimers (actin and tubulin) or heterodimers, such as Von Hippel-Lindau protein (VHL) composed of

VHL and elongins B and C. Interestingly, even after the γ-phosphate is released, these substrates are not released from CCT without their binding partners being present (*12*).

CCT has also been shown to cooperate with upstream chaperones in the folding of distinct protein classes. The co-chaperone prefoldin/GimC is required for efficient transfer of nascent actin or tubulin to the chaperonin (*21, 22*). Prefoldin (PFD) is a heterohexameric complex of six different proteins that is present in archaea and eukaryotes (*23*). The structure of PFD resembles a jellyfish, consisting of a double β-barrel and six coiled-coils protruding from the base. Unfolded proteins bind to the hydrophobic residues on the tips of these tentacles (*21*). PFD binds CCT by spanning the top of the complex and making contacts with two of the CCT subunits (*21*). PFD binds unfolded actin and then passes it off to CCT to continue actin folding. Not all CCT substrates are delivered to CCT by PFD, but use other chaperones to reach CCT. For example, a group of WD40 repeat proteins use an Ssb-type Hsp70 chaperone in their transfer (*22*). Thus, there could be many unknown chaperones that deliver a unique set of substrates to CCT.

Recently, a crystal structure of yeast CCT in complex with actin at 3.8 Å revealed an intrinsic asymmetry. Furthermore, all C- and N-termini of the subunits were observed to form a network of β-sheets to make the cavity floor and the ring-ring interface, except for the N-terminus of the CCTε subunit, which threads in from the outside of the complex through a channel that is formed from the neighboring subunits (*18*). This N-terminus is much longer than the other subunits and is conserved among orthologs, suggesting an important role in CCT function.

G protein subunit β is a substrate of CCT

The most studied substrates of CCT are the cytoskeletal proteins, actin and tubulin. It has been suggested that actins and tubulins occupy 50-60% of the CCT chaperonin capacity (*22*). CCT has been estimated to fold about 10% of the total protein in the cell. As such, an increasing number of substrates have been found. A recent mass spectrometric proteomics screen identified CCT substrates by releasing proteins in an ATP-dependent manner. Among the growing list are septin subunits, proteins involved in chromatin modification, and proteins involved in cell cycle networks (*24*). Other mass spectrometric proteomic screens reveal a set of CCT substrates that contain WD40 repeats (*16, 22, 25*). WD40 repeat proteins contain four or more copies of 40 amino acid stretches that typically end in Trp-Asp (WD). They are composed of β-sheets that form a β-propeller structure. One of the WD40 repeat proteins found to be folded by CCT is guanine nucleotide binding protein (G protein) β subunit (Gβ).

Gβ is an essential subunit of the G protein heterotrimer and is composed of two distinct regions: a short N-terminal α-helix domain and a WD40 repeat domain containing seven blades of a β-propeller structure. Gβ is unstable on its own requiring Gγ for stabilization. Gβγ is down-regulated when the CCTα subunit is knocked down, suggesting the necessary role of CCT in G protein signaling (*26*). Moreover, knockdown of the CCTζ subunit resulted in a decreased rate of Gβ1γ2 formation (*27*). The hydrophobic regions in the β-strands of Gβ are important in the Gβ-CCT interaction, and CCT protects Gβ from aggregation (*28*). In one study, Gβ was shown to bind to the entire complex of CCT (*19*), but CCT did not interact with Gγ subunits, indicating an interaction upstream of Gβγ assembly. Taken together, these data indicate that Gβ is a substrate of CCT.

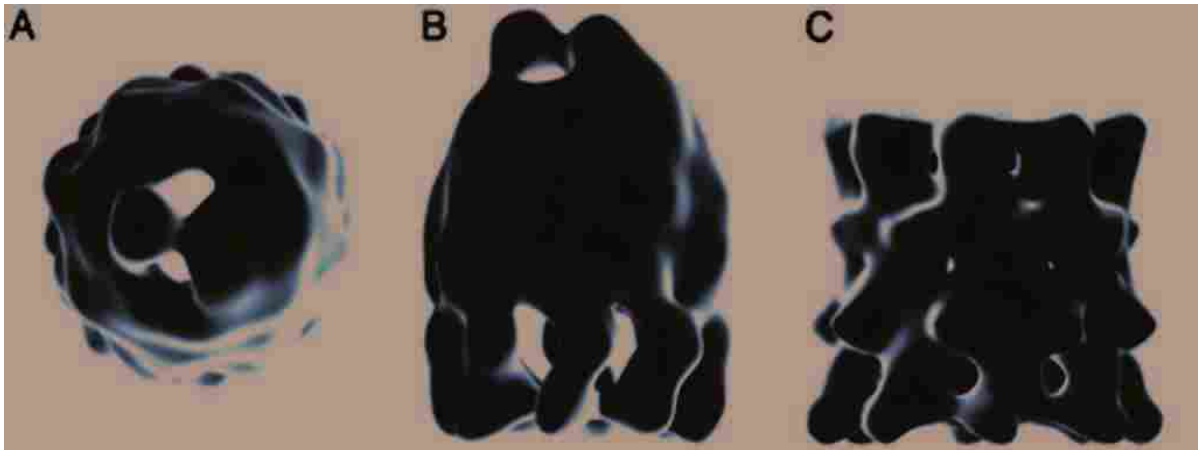

Figure 1-1. Cryo-EM structures of the PhLP1-CCT and apo-CCT complexes. A) Top view of the PhLP1-CCT complex from a cryo-EM 3D reconstruction. B) Side view of the PhLP1-CCT complex. C) Side view of apo-CCT. Reproduced with permission from *Proceedings of the National Academy of Sciences USA,* (*34*) copyright 2004. http://www.pnas.org.

PhLP1 acts as a co-chaperone in CCT-mediated Gβγ assembly

The phosducin family contains three different subgroups. Phosducin (Pdc) and Phosducin-like protein 1 (PhLP1) make up subgroup 1 of the Pdc gene family (*29*). Pdc and PhLP1 share 65% sequence homology and both associate with Gβγ dimers (*30*). They both share a perfectly conserved 11 amino acid sequence located in helix 1 that is a major site of Gβγ binding (*31*). The expression pattern of Pdc is restricted and found only in the photoreceptor cells of the retina and in the pineal gland (*32, 33*), suggesting a specific role in visual signaling. In contrast, PhLP1 is expressed in most tissues and cell types (*31, 34*), indicating a more general function in signaling.

Initially, PhLP1 was thought to be a down-regulator of G protein signaling. However, many observations were inconsistent with PhLP1 inhibiting G protein signaling. For example, when *phlp1* was deleted in *Dictyostelium*, G protein signaling was completely abolished (*29*), indicating an essential role of PhLP1 in G protein signaling. Clues to the function of PhLP1 came when a proteomics screen of PhLP1 revealed a high affinity interaction with CCT (*35*).

Interestingly, Pdc did not share the ability to bind CCT with PhLP1. PhLP1 was subsequently found to bind CCT not as a substrate, but rather in its native form, suggesting that PhLP1 has a regulatory role in CCT-mediated folding (*35*).

The structure of the PhLP1-CCT complex determined by cryo-electron microscopy (*36*) has provided valuable insight into the function of the PhLP1-CCT interaction (see Figure 1-1). Unlike folding substrates of CCT, such as actin and tubulin which bind CCT within the folding cavity, PhLP1 binds above the cavity only making contact with the tips of the apical domains of the CCT subunits. PhLP1 sits above the folding cavity in manner analogous to prefoldin (*21, 36*). These findings led to additional studies that directly measured the role of PhLP1 and CCT in the folding and assembly of Gβγ (*19, 26, 37-39*). One study demonstrated that when PhLP1 is knocked down using siRNA, the levels of Gβ1 expression are significantly reduced (*39*). Additionally, the rate of Gβγ dimer assembly was reduced 5-fold when cells were depleted of PhLP1 by 90% and increased 4-fold when PhLP1 was over-expressed (*39*). Gβ bound to CCT in *in vitro* translation assays, and the addition of Gγ decreased binding of Gβ to CCT while increasing its binding to Gγ in an ATP-dependent manner (*19*). Collectively, these findings indicate that PhLP1 acts as a co-chaperone in the CCT-mediated folding and assembly of the Gβγ dimer.

PhLP1 must be phosphorylated by protein kinase CK2 at the serine residues 18-20 (S18-20) in order to catalyze Gβγ dimer formation (*39*). This was shown with an S18-20A alanine substitution variant. When PhLP1 S18-20A was over-expressed in HEK293 cells, the rate of Gβγ dimer assembly decreased 15-fold compared to WT PhLP1 and by 4-fold compared to an empty vector control (*39*). Not only did PhLP1 S18-20A inhibit Gβγ assembly, it also blocked the ability of endogenous PhLP1 to catalyze the assembly in a dominant negative manner. Later,

an N-terminal 75 amino acid truncation of PhLP1 (PhLP1 Δ1-75) was found to be a more effective dominant negative inhibitor than PhLP1 S18-20A. Consequently, this truncated variant has been a useful tool in understanding PhLP1-mediated Gβγ assembly. This variant lacks the conserved Gβγ binding region corresponding to Helix 1 in Pdc as well as the S18-20 phosphorylation site. When PhLP1 Δ1-75 was over-expressed, the Gβγ assembly process was completely blocked since it could not be phosphorylated and bound Gβ poorly (*39*). Interestingly, PhLP1 Δ1-75 is similar to a naturally occurring PhLP1 splice variant (designated as PhLP1S) lacking the first 83 amino acids on the N-terminal end (*31, 40*). Similar to PhLP1 Δ1-75, when PhLP1S is over-expressed Gβ and Gγ expression is blocked and Gβγ signaling is strongly inhibited (*40*).

These data demonstrate the need for PhLP1 in CCT-mediated Gβγ assembly, however, they do not provide a mechanism to how this is accomplished. The cryo-EM structure of PhLP1-CCT reveals that PhLP1 binds on the top of the CCT complex and not inside the cavity (*36*). This orientation would allow nascent Gβ to bind inside the folding cavity with PhLP1 on top forming a ternary complex. Over-expression of PhLP1 causes a decrease in Gβ binding to CCT rather than the increase that this hypothesis would suggest (*38*). However, the over-expression of PhLP1 S18-20A and Δ1-75 variants cause significant increases in Gβ binding to CCT (*38*), suggesting that when PhLP1 is not phosphorylated, a stable PhLP1-Gβ-CCT ternary complex is formed and phosphorylation of PhLP1 may destabilize this ternary complex resulting in the release of a PhLP1-Gβ intermediate. This PhLP1-Gβ intermediate could subsequently associate with Gγ. Many pieces of evidence support a PhLP1-Gβ intermediate. First, PhLP1 was found to bind Gβ in the absence of Gγ (*39*). Second, Gγ does not accelerate the PhLP1-mediated release of Gβ from CCT (*38*). Lastly, Gγ does not bind CCT directly or in complex with CCT (*19, 38*).

From these observations, a mechanistic model of PhLP1-mediated Gβγ dimer assembly has been proposed (*38, 41*) as shown in Figure 1-2. In this model, PhLP1 forms a stable ternary complex with CCT and nascent Gβ. Once Gβ is folded and PhLP1 is phosphorylated on Ser 18-20, then PhLP1-Gβ complex is released from CCT. The PhLP1-Gβ intermediate can then pick up Gγ which is probably being held by another chaperone, possibly DRiP78 (*42*). Gα then competes with PhLP1 for binding to the stable Gβγ dimer.

This model, provides a general mechanism for PhLP1-mediated Gβγ dimer assembly, however it does not address whether PhLP1 is used for the assembly of all combinations of Gβγ dimers. Chapter 2 will discuss the specificity of PhLP1-mediated Gβγ assembly. Another question that may arise concerning the function of PhLP1 is whether the only function of PhLP1 is in the folding and assembly of Gβγ. Other possible functions for PhLP1, either as a co-chaperone or otherwise, are yet to be investigated. Chapter 3 will describe investigations into other functions of PhLP1.

The emerging roles of PhLP2 and PhLP3 as co-chaperones

Other members of the Pdc family were first discovered in yeast (*43*). They were first designated as Plp1 and Plp2; however, phylogenetic analysis placed Plp1 in subgroup III and Plp2 in subgroup II, so group II subfamily members are designated as PhLP2 and group III members are designated as PhLP3 (*29*). As explained above, PhLP1 plays an important role in G protein signaling, so it seems logical that the other phosducin family subgroups could also play a role in G protein signaling. In support of this hypothesis Plp2 and Plp1 have been shown to bind Gβγ in yeast (*43*). However, mammalian PhLP2 and PhLP3 do not share the conserved α-helix 1 found in Pdc and PhLP1 important in Gβγ dimer binding, and they have been found to bind Gβγ poorly (*43*). Additionally, PhLP2 and PhLP3 appear to be unrelated to Gβγ signaling because no

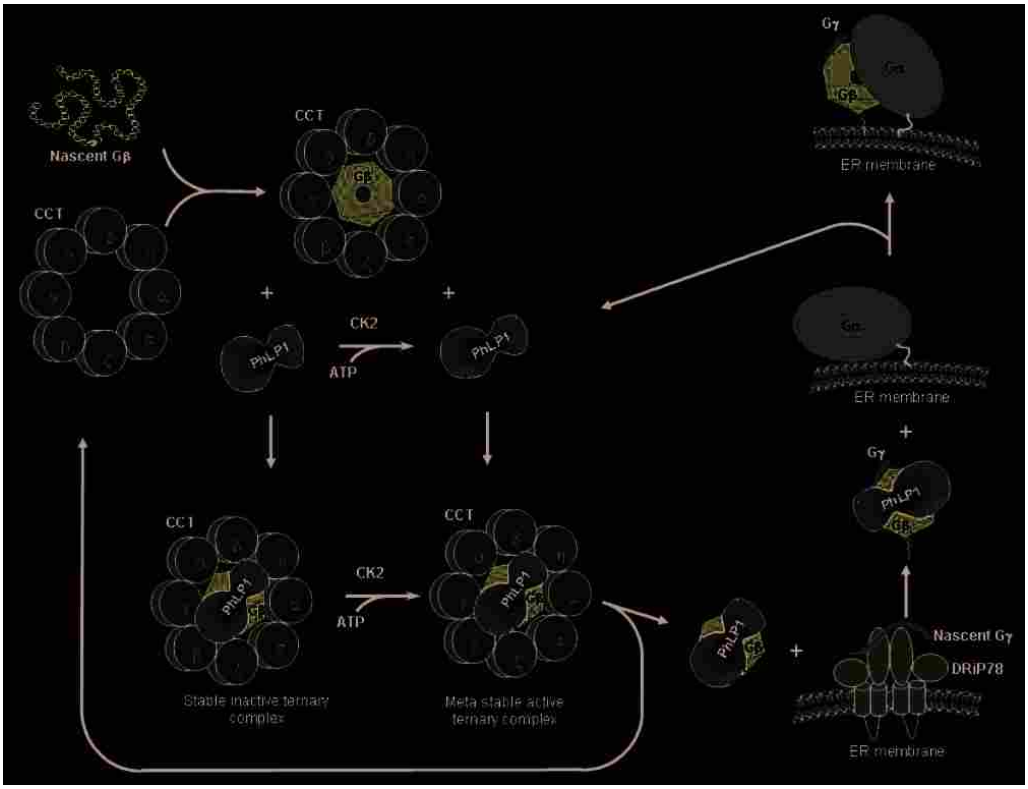

Figure 1-2. Model of PhLP1-mediated Gβγ dimer assembly. Nascent Gβ binds CCT within the folding cavity and PhLP1 associates above Gβ, forming a ternary complex. If PhLP1 is not phosphorylated within the S18-20 sequence by CK2, the ternary complex is stable and inactive in Gβγ assembly. If PhLP1 is phosphorylated at this site, then a PhLP1-Gβ complex is released from CCT and interacts with Gγ bound to DriP78, forming the Gβγ dimer. PhLP1 is released when Gβγ associates with Gα and the ER membrane, and the G protein heterotrimer is then trafficked to the plasma membrane. PhLP1 is then free to catalyze another round of Gβγ assembly (*41*).

effect was observed on the Gβγ-dependent mating pheromone response in yeast with PhLP2 and PhLP3 over-expression or with *phlp3* deletion and temperature sensitive *phlp2* mutants (*43, 44*).

One unique characteristic that all mammalian phosducin-like proteins have is their ability to interact with CCT in their native state (*35, 44, 45*). PhLP1 and PhLP3 share a conserved N-terminal region that is not shared by Pdc. This N-terminal region and the C-terminus of PhLP3 were observed to be important in binding to CCT. Cryo-EM images reveal that PhLP3 binds CCT in a manner similar to PhLP1 by binding across the chaperonin cavity (*45*). The PhLP2A-CCT interaction was also confirmed through GST-fusion pull-downs (*44*). These observations

lead to the conclusion that all PhLP proteins share a similar binding mechanism to CCT (*45*). It is also likely that they all act as co-chaperones in concert with CCT.

In human and mice, there are two members of subgroup 2 designated as PhLP2A and PhLP2B (*29*). These two members share 57% sequence homology, but differ in their expression patterns (*46*). PhLP2A is ubiquitously expressed (*46*), whereas, PhLP2B is expressed in germ cells undergoing meiotic maturation (*47*). Members of subgroup 2 are the only phosducin members to be shown essential for life. Disruption of the yeast PhLP2, plp2, resulted in haploid spores that failed to grow, but disruption of yeast PhLP3, yielded viable spore products (*43*). Additionally, disruption of PhLP2A in *Dictostelium*, resulted in decreased growth rate and cell culture collapse after 16-17 cell divisions (*29*). Moreover, over-expression of plp1 does not rescue the deletion of plp2 (*43*). Interestingly, PhLP2B expression rescued the lethal phenotype of yeast *phlp2*Δ (*47*), indicating an evolutionarily-conserved function. Given their sequence similarity, distinct expression patterns, and compensatory effects, it is believed that PhLP2A and PhLP2B have similar yet tissue-specific functions. PhLP2 has been thought to be involved in the folding of several CCT substrates involved in cytoskeletal morphogenesis and cell cycle progression (*44*).

Subgroup 3 of the phoducin family contains one member in mammals, designated as PhLP3. PhLP3 only has 15% identity and 37% similarity to human PhLP1 (*45*). Unlike PhLP2, PhLP3 is not considered essential in yeast (*43*) or *Dictyostelium* (*29*). However, when PhLP3 is disrupted in *C. elegans* by RNA interference, embryonic cell division fails. Additionally, the embryos have short microtubules suggesting an important role of PhLP3 in microtubule organization (*48*). A role for PhLP3 in microtubule organization agrees with the implications of PhLP3 involved in actin and tubulin folding (*43, 45*). One genetic analysis suggested a role for

PhLP3 in β-tubulin folding when deletion of *phlp3* protected the cells against the toxic effects of excess free β-tubulin (*49*). In contrast, the folding of β-tubulin *in vitro* is significantly inhibited by PhLP3 (*45*). PhLP3 forms a ternary complex with CCT and actin or tubulin (*45*); again indicating a role of PhLP3 in actin and tubulin folding. It is unclear how PhLP3 is involved in tubulin folding, but it is clear that it does play some role.

Conclusion

It has been clear for some time now that many proteins require chaperone-assisted folding in order to reach their native state and avoid aggregation. CCT is a eukaryotic group II chaperonin that provides a chamber that entropically favors the folding of hydrophobic proteins while being sequestered from the cytosol. Other chaperones such as PFD and Hsp70 proteins are involved in the folding process upstream of CCT. It is clear that PhLP1 acts as a co-chaperone in the folding of Gβ and the subsequent assembly of the Gβγ dimer, however the extent of the specificity of PhLP1 has yet to be investigated. The other subgroups of the phosducin family are hypothesized to also act as co-chaperones with CCT. As of yet, no specific CCT substrates, besides Gβγ have been found to require any of the phosducin-like proteins for their folding or assembly. PhLP2 has been implicated in the folding of cell cycle control proteins and PhLP3 has been shown to participate in the folding of actin and tubulin, but very little is known about the mechanism. The following studies describe the specificity of PhLP1 in the assembly of different combinations of Gβγ dimers and discuss other possible functions of the PhLP proteins.

CHAPTER 2:

SPECIFICITY OF PHOSDUCIN-LIKE PROTEIN 1-MEDIATED G PROTEIN βγ ASSEMBLY

Summary

In order for G protein signaling to occur, the G protein heterotrimer must first be assembled from its individual subunits. Recent studies have shown that phosducin-like protein (PhLP1) works as a co-chaperone with the cytosolic chaperonin complex (CCT) to fold Gβ and mediate its interaction with Gγ. These studies have only focused on the most common Gβγ dimer, and the extent of PhLP1-mediated Gβγ assembly has not yet been addressed. This is an important question considering that there are 4 Gβs that form various dimers with 12 Gγ subunits. This chapter demonstrates that PhLP1 plays a vital role in the assembly of all Gγ subunits that form dimers with Gβ2 and the assembly of Gγ2 with Gβ1-4, without affecting the specificity of the Gβγ interactions. These findings suggest that PhLP1 has a general role for the assembly of all Gβγ combinations.

Introduction

Eukaryotic cells translate changes in extracellular conditions into intracellular responses by utilizing receptors coupled to heterotrimeric GTP-binding proteins (G proteins). Mammalian genomes contain nearly 1,000 G protein-coupled receptors (GPCRs) (*50*). GPCRs are involved in many physiological functions including neurotransmission, hormone and enzyme release from endocrine and exocrine glands, immune response, blood pressure regulation, taste and olfactory responses, and vision (*50*). Upon ligand binding to the GPCR, GDP is exchanged for GTP on the G protein heterotrimer (consisting of Gα, Gβ, and Gγ subunits) and Gα-GTP releases from

the Gβγ dimer. The signal is then amplified by Gα-GTP and Gβγ interacting with downstream effectors such as effector enzymes and ion channels (*51*). The duration and amplitude of the signal is tightly regulated. One way the signal is controlled is by phosphorylation of the receptor coupled with β-arrestin binding and internalization (*52*). Another element of signaling control is through regulators of G protein signaling (RGS) proteins. RGS proteins initiate the intrinsic GTPase activity of the Gα subunit (*53*). When GTP is hydrolyzed to GDP, the inactive Gα-GDP and Gβγ reassociate and the heterotrimer can enter a new cycle (*51*).

In order for G protein signaling to occur, the heterotrimer must first assemble post-translationally from its nascent polypeptides. It has been established that the Gβγ obligate dimer assembles first followed by the subsequent association of Gα (*54*). Phosducin-like protein 1 (PhLP1) has been shown to not only bind the G protein β subunit, but to also be a co-chaperone in the CCT-mediated folding of Gβ and the subsequent binding of Gγ (*39*). CCT is a group II chaperonin that assists in the folding of actin, tubulin, and many other cytosolic proteins including many β-propeller proteins like Gβ (*16*).

Previous studies on the mechanism of PhLP1-mediated Gβγ assembly have focused on the most common dimer, Gβ1γ2, thus leaving open questions about the role of PhLP1 in the assembly of the other Gβγ combinations. In humans, there are 5 genes that code for Gβ and 12 for Gγ along with some splice variants (*55, 56*). This leaves room for over 60 different Gβγ dimer combinations. Gβs 1-4 are broadly expressed and share 80-90% sequence identity (*55, 56*). Gβ5 is only expressed in the central nervous system and retina and shares only 53% sequence identity with Gβ1 (*57*). Gβ5 carries a longer N-terminal domain and binds RGS proteins instead of Gγ (*57*). The Gγ protein family is separated into 5 subfamilies and is more structurally diverse than the Gβ family with the sequence identity of the 12 different Gγs extending from 10-

70% (*58*). All Gγ subunits are post-translationally modified on the C-terminus with isoprenyl groups. Subfamily I are farnesylated, while the other subfamilies are geranylgeranylated (*59*). These isoprenyl modifications contribute to their association with the cell membrane, GPCRs, Gαs, and effectors (*54*).

There is some inherent selectivity in the assembly of different Gβγ combinations, but in general Gβs 1-4 can form dimers with most Gγ subunits (*60*). The purpose of these many Gβγ dimers has puzzled researchers for many years. A great deal of research indicates that GPCRs and effectors prefer to couple to a subset of Gβγ combinations based on sequence complementarity, cellular expression patterns, subcellular localization, and post-translational modifications (*56*). In contrast to Gβs 1-4, Gβ5 does not interact with Gγ subunits *in vivo*, but instead forms irreversible dimers with RGS proteins of the R7 family including RGS6, RGS7, RGS9, and RGS11 (*61*).

All Gβ isoforms are able to interact with CCT to some extent (*19*). Gβ4 and Gβ1 bind CCT better than Gβ2 and Gβ3 while Gβ5 binds CCT poorly (*19*). These results would suggest that the CCT-mediated folding of Gβ4 and Gβ1 may be more dependent on PhLP1 than the other Gβs because the co-chaperone role of PhLP1 was discovered with Gβ1γ2. However, another report has indicated that Gγ2 assembly with Gβ1 and Gβ2 is more PhLP1-dependent than with Gβ3 and Gβ4 (*42*). Thus, it is not clear from current information whether PhLP1 plays a general role in Gβγ dimer formation or whether it specifically catalyzes assembly of only a subset of these complexes. This chapter addresses the specificity of PhLP1 in acting as a co-chaperone for the assembly of many different Gβγ combinations. This study reveals that PhLP1 has a wide breadth of function in Gβγ dimerization. PhLP1 was found to be necessary for Gβ2 assembly

with all 12 Gγ subunits that form dimers with Gβ2 and for the assembly of Gγ2 with four of the five Gβ subunits. Overall, PhLP1 does not appear to influence Gβγ specificity.

Experimental Procedures

Cell culture

HEK293T cells were cultured in 1:1 DMEM/F-12 growth media containing 2.5 mM L-glutamine and 15 mM HEPES supplemented with 10% fetal bovine serum. The cells were subcultured regularly to maintain growth but were only used to 25 passages.

Preparation of cDNA constructs

The pcDNA3.1 vectors containing N-terminally FLAG-tagged human Gβs 1-4, Gβ5short, and N-terminally HA-tagged Gγs 1-5 and 7-13 were purchased from the Missouri University of Science and Technology cDNA Resource Center (www.cdna.org). C-terminally c-myc-tagged human PhLP1 and Δ1-75 truncation variant of PhLP1 were constructed in pcDNA3.1/myc-His B vector using PCR as described (*39*).

RNA interference experiments

Short interfering RNAs (siRNAs) were chemically synthesized (Dharmacon) to target nucleotides 608–628 of human lamin A/C (*39*) and nucleotides 345–365 of human PhLP1 (*39*). HEK 293T cells were grown in 12-well plates to 50–70% confluency at which point they were transfected with siRNA at 100 nM final concentration using Oligofectamine reagent (Invitrogen) as described previously (*39*). 24 h later, the cells were transfected with 0.5 μg each of FLAG-Gβ and HA-Gγ in pcDNA3.1(+) using Lipofectamine 2000 according to the manufacturer's protocol (Invitrogen). The cells were harvested for subsequent immunoprecipitation experiments 72 h

later. 10 μg of cell lysate were immunoblotted with an anti-PhLP1 antibody (*39*) to assess the percent PhLP1 knockdown.

Dominant interfering mutant experiments

HEK 293T cells were plated in 6-well plates and grown to 70-80% confluency. The cells were then transfected with Lipofectamine 2000 (Invitrogen) according to the manufacturer's instructions. Each well was transfected with 1.0 μg of the empty vector control, wild-type PhLP1-myc, or PhLP1 Δ1-75-myc along with 1.0 μg each of the indicated Flag-Gβ and HA-Gγ cDNAs. The cells were harvested for immunoprecipitation 48 hours after transfection.

Immunoprecipitation experiments

Transfected HEK 293T cells were washed with phosphate-buffered saline (PBS) (Fisher) and solubilized in immunoprecipitation buffer (PBS pH 7.4, 2% NP-40 (Sigma)), 0.6 mM PMSF, 6 μl/ml protease inhibitor cocktail per mL buffer (Sigma P8340)). The lysates were passed through a 25-gauge needle 10 times and centrifuged at maximum speed for 10-12 minutes at 4ºC in an Eppendorf microfuge. The protein concentration for each sample was determined using the DC Protein Assay Kit II (Bio-Rad) and equal amounts of protein were used in the subsequent immunoprecipitations. Approximately 150 μg of total protein were used in immunoprecipitations from cells in 12 well plates and 450 μg from cells in 6 well plates. The clarified lysates were incubated for 30 minutes at 4°C with 2.5 μg anti-FLAG antibody (clone M2, Sigma), for lysates from 12-well plates or with 6.25 μg of anti-FLAG for lysates from 6-well plates. Next, 30 μl of Protein A/G Plus agarose slurry (Santa Cruz Biotechnology) were added, and the mixture was incubated for 30 minutes at 4°C. The immunoprecipitated proteins were solubilized in SDS sample buffer and resolved on 10% Tris-Glycine-SDS or 16.5% Tris-Tricine-SDS gels. The proteins were transferred to nitrocellulose and immunoblotted using an

anti-FLAG (clone M2, Sigma), anti-c-myc (BioMol), anti-HA (Roche), or an anti-PhLP1 antibody (*39*). Immunoblots were incubated with the appropriate anti-rabbit, anti-mouse, (Li-Cor Biosciences), or anti-rat (Rockland) secondary antibody conjugated with an infrared dye. Blots were scanned using an Odyssey Infrared Imaging System (Li-Cor Biosciences), and protein band intensities were quantified using the Odyssey software. The data are presented as the mean value +/- standard error from at least three experiments.

Results

It has been shown previously that PhLP1 must bind Gβγ with high affinity in order to mediate Gβγ assembly (*38, 39*). To determine the ability of PhLP1 to catalyze the different Gβγ dimer formations with the five Gβ subunits, we began by measuring the interaction of PhLP1 with all five Gβ subunits in complex with Gγ2 by co-immunoprecipitation. Gβs 1-4 co-immunoprecipitated similar amounts of PhLP1, whereas Gβ5 co-immunoprecipitated significantly less, indicating that PhLP1 binds Gβ5 with a lower affinity than it does Gβ1-4. The differences in binding cannot be attributed to different expression levels because each Gβ subunit expressed similarly under these conditions (Fig 2-1A).

The effect of siRNA-mediated PhLP1 knockdown on the five Gβ isoforms and Gγ dimerization were measured by co-immunoprecipitation of Gγ2 with the Gβs. Gγ2 was chosen because it is a common isoform that associates with all of the Gβ subunits *in vitro* (*60*). HEK 293T cells were treated with a mock treatment of no siRNA, a control siRNA to Lamin A/C, or PhLP1 siRNA and then co-expressed with HA-Gγ2 and one of the five FLAG-Gβ subunits. The lysates were immunoprecipitated with anti-FLAG antibody and the precipitate was immunoblotted with anti-HA and anti-FLAG antibodies to detect the amount of Gγ2 bound to each Gβ subunit. Fig 2-1B shows that a 75% knockdown in PhLP1 resulted in a 50% decrease in

Gβ1 and an 85% decrease in Gγ compared to the Lamin A/C control. A similar pattern was seen with the other Gβ subunits except for Gβ5, which had no detectable Gγ2 bound under these conditions (Fig 2-1C). In order to compare the effect of PhLP1 knockdown on Gγ2 assembly with the different Gβ subunits more directly, the Gγ2/Gβ1-4 ratio was determined for the three siRNA conditions (Fig 2-1C). In each case, much less Gγ2 associated with Gβ when PhLP1 was knocked down ranging from a 64 to 84% decrease. These results indicate that PhLP1 assists with the formation of Gβγ complexes containing Gβs 1-4 and Gγ2.

An alternative method was also used to examine the role of PhLP1 in Gβγ assembly with different Gβ subunits. It has been shown previously that an N-terminally truncated PhLP1 variant (PhLP1 Δ1-75), where the first 75 amino acids are removed, acts in a dominant interfering manner to block Gβγ assembly (*38, 39*). PhLP1 Δ1-75 forms a stable ternary complex with Gβ-CCT that does not release Gβ from CCT for association with Gγ (*38, 39*). When PhLP1 Δ1-75 was co-expressed with FLAG-Gβ1 and HA-Gγ2, the amount of Gγ2 in the Gβ1 immunoprecipitate was greatly reduced compared to with wild-type PhLP1 and an empty vector control (Fig. 2-2A). This pattern was also similar among Gβs 1-4. PhLP1 Δ1-75 caused the Gγ2/Gβ ratios to decrease by 75-92% in the Gβ1-4 immunoprecipitates (Fig. 2-2B). Once again no Gβ5γ2 complex was detected under these conditions. Interestingly, co-expression of wild-type PhLP1 increased the amount of Gβ and Gγ2 in the FLAG-Gβ immunoprecipitates by 30-50% for all five Gβ isoforms (see Figs. 2-2A and 2-4A). This observation is consistent with a PhLP1-mediated enhancement of Gβγ formation, resulting in a stabilization of Gβ and Gγ expression. Collectively, these findings confirm the siRNA knockdown results by showing that PhLP1 is important in the assembly and Gβs 1-4 with Gγ2.

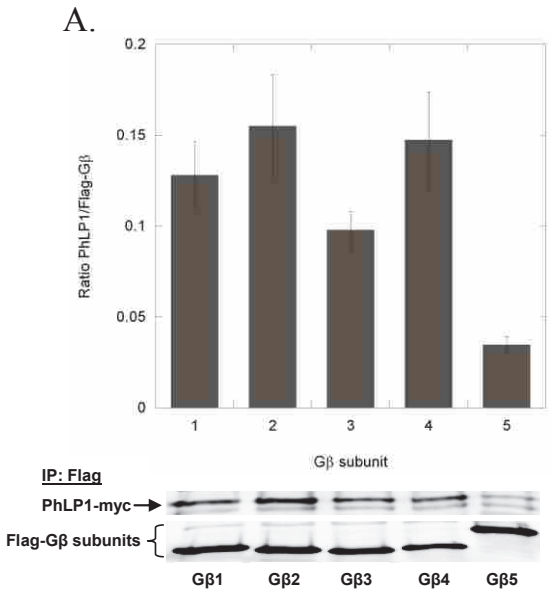

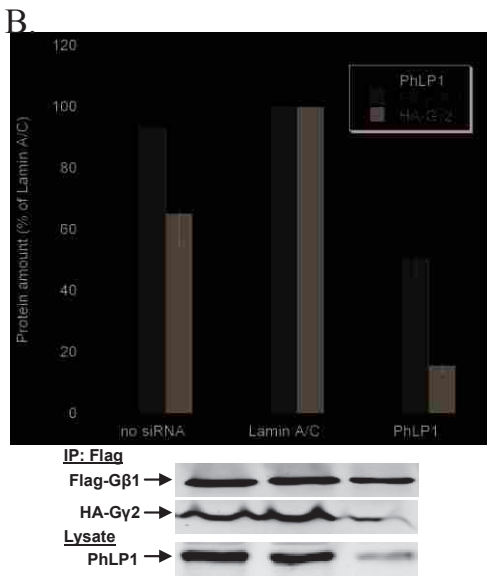

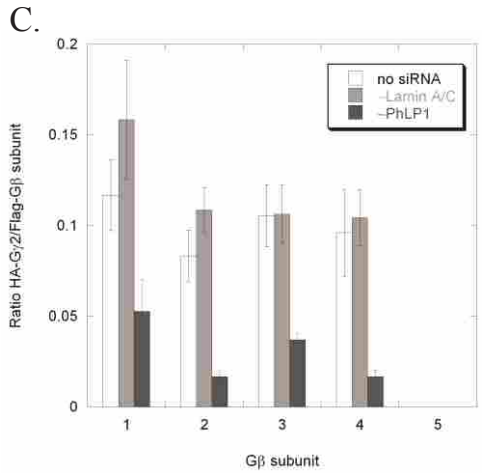

Figure 2-1. Effects of PhLP1 knockdown on the assembly of all Gβ subunits with Gγ2. HEK 293T cells were treated as follows: A) Cells were transfected with PhLP1-myc, HA-Gγ2 and the indicated FLAG-Gβ cDNAs. After 48 hours, cells were lysed, immunoprecipitated with an anti-FLAG antibody and immunoblotted with anti-myc or anti-FLAG antibodies. The graph represents the ratio of the PhLP1-myc/FLAG-Gβ band intensities for all 5 Gβs. Bars represent the average ± standard error from 3 separate experiments. A representative blot is shown below the graph. B, C) Cells were treated with siRNA against PhLP1, lamin A/C, or no siRNA as indicated. Twenty-four hours later, cells were transfected with the indicated FLAG-Gβ subunit and HA-Gγ2 cDNAs. After 72 additional hours, cells were lysed, immunoprecipitated with an anti-FLAG antibody and immunoblotted with anti-FLAG or anti-HA antibodies. Bands were quantified and expressed as a percentage of the lamin A/C control for Gβ1γ2 in (B) or as the ratio of HA-Gγ2/Flag-Gβ for all five Gβs in (C). PhLP1 knockdown was measured by quantifying the PhLP1 band intensity in immunoblots of 10 μg of whole cell lysate. The average PhLP1 knockdown was between 60-76% compared to the lamin A/C control. Bars represent the average ± standard error from 3-5 separate experiments. If no bar is shown, then no complex was detected for that particular Gβγ species. A representative blot for Gβ1γ2 is shown below the graph in (B).

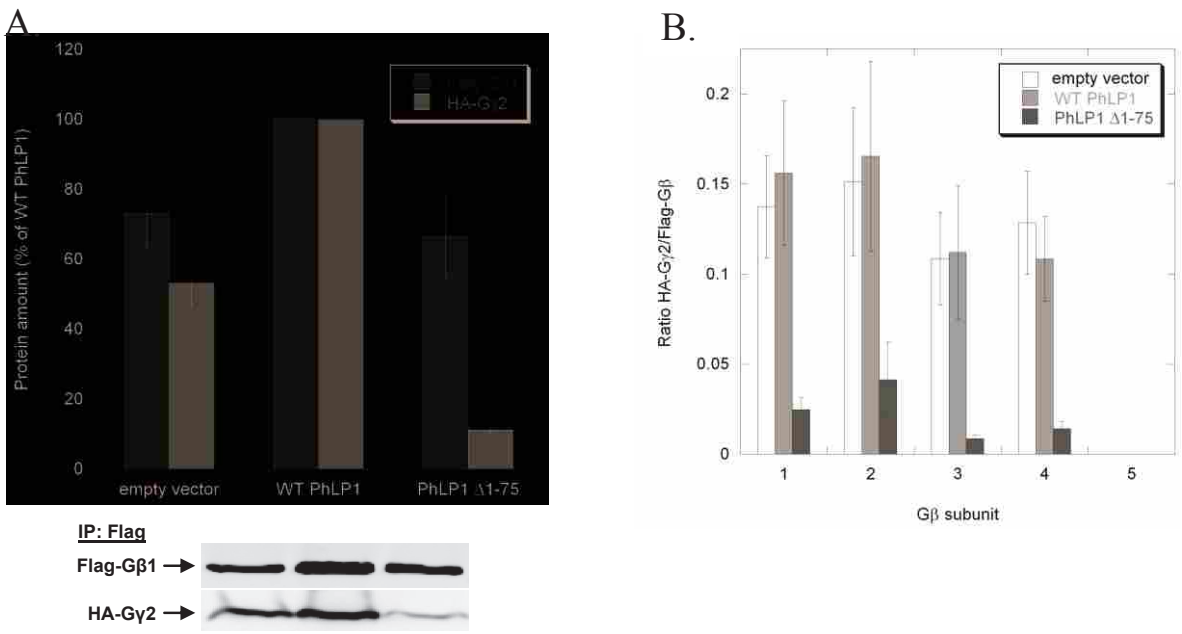

Figure 2-2. Effects of PhLP1 Δ1-75 expression on the assembly of all Gβ subunits with Gγ2. HEK 293T cells were transfected with either wild-type PhLP1, PhLP1 Δ1-75, or an empty vector control along with the indicated Flag-Gβ subunits and HA-Gγ2 cDNAs. After 48 hours, cells were lysed, immunoprecipitated with an anti-Flag antibody and immunoblotted with anti-Flag or anti-HA antibodies. Bands were quantified and expressed as a percentage of the wild-type PhLP1 control for Gβ1γ2 in (A) or as the ratio of HA-Gγ2/Flag-Gβ for all five Gβs in (B). Bars represent the average ± standard error from 3-5 separate experiments. If no bar is shown, then no complex was detected for that particular Gβγ species. A representative blot for Gβ1γ2 is shown below the graph in (A).

Another question regarding the scope of PhLP1-mediated Gβγ assembly is whether all Gγs or just a subset require PhLP1 to associate with Gβ. In order to address this question, the effects of siRNA-mediated PhLP1 knockdown and PhLP1 Δ1-75 over-expression on the association of Gβ2 with all twelve Gγ subunits were also measured. Gβ2 was chosen because it associates with most Gγ isoforms, yet it does show selectivity between different isoforms (*60*). HEK 293T cells were treated with siRNA in the same manner in Fig. 2-1 and then co-transfected with FLAG-Gβ2 and each of the 12 HA-tagged Gγ subunits. Cell lysates were immunoprecipitated with FLAG antibody as in Fig. 2-1 and the precipitates were immunoblotted with anti-HA and anti-FLAG antibodies to detect the amount of Gγ that associated with Gβ2. Fig. 2-3A shows the amount of PhLP1 in the cell extracts and the amounts of Gβ2 and Gγ2 in the

immunoprecipitate. The results were similar to the Gβ1γ2 experiments. When PhLP1 was knocked down 80%, it caused a 30% decrease in Gβ2 and a 90% decrease in Gγ2 compared to the lamin A/C control (Fig. 2-3A). A similar pattern was seen with all the other Gβ2γ combinations that formed dimers. Gβ2 decreased by 20-50% while the Gγs decreased by 80-95% (data not shown). The Gγ/Gβ2 band intensity ratios for the three siRNA conditions for all Gγ subunits are shown in Fig. 2-3B. All ratios were significantly reduced when PhLP1 was knocked down compared to the no siRNA and Lamin A/C controls, except for Gγs 1, 11, and 13 where no complex was detected. These results show that PhLP1 is important in the assembly of all Gβ2γ dimers.

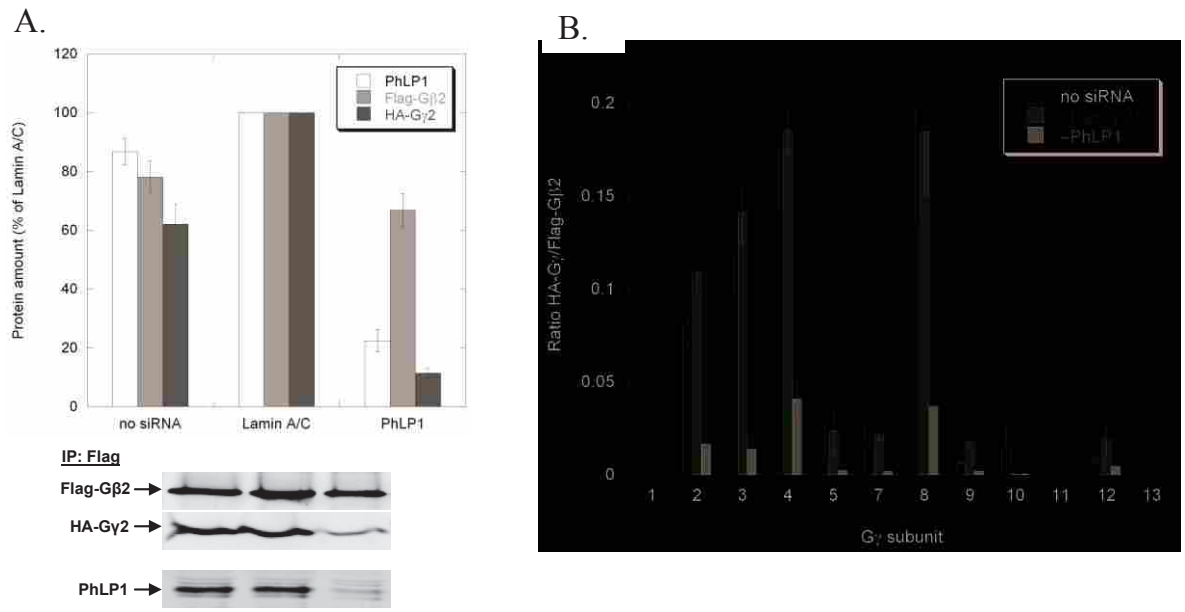

Figure 2-3. Effects of PhLP1 knockdown on the assembly of all Gγ subunits with Gβ2. HEK 293T cells were treated with siRNA against PhLP1, lamin A/C, or no siRNA as indicated. Twenty-four hours later, cells were transfected with the indicated HA-Gγ subunit and Flag-Gβ2 cDNAs. After 72 additional hours, cells were lysed, immunoprecipitated with an anti-Flag antibody and immunoblotted with anti-Flag or anti-HA antibodies. Bands were quantified and expressed as a percentage of the lamin A/C control for Gβ2γ2 in (A) or as the ratio of HA-Gγ/Flag-Gβ2 for all 12 Gγs in (B). PhLP1 knockdown was measured by quantifying the PhLP1 band intensity in immunoblots of 10 μg of whole cell lysate. The average PhLP1 knockdown was between 66-90% compared to the lamin A/C control. Bars represent the average ± standard error from 3-14 separate experiments. If no bar is shown, then no complex was detected for that particular Gβγ species. A representative blot for Gβ2γ2 is shown below the graph in (A).

The dominant interference experiments were also performed with all the Gβ2γ combinations. Co-expression of PhLP1 Δ1-75 with FLAG-Gβ2 and HA-Gγ2 resulted in a 50% reduction in the amount of Gβ2 and a 95% reduction in the amount of Gγ2 in the FLAG immunoprecipitate compared to the wild-type PhLP1 control (Fig. 2-4A). Additionally, the co-expression of wild-type PhLP1 increased Gβ2 and Gγ2 levels by 50%, similarly to Gβ1γ2 (Fig. 2-2A). For the other Gγs, Gβ2 decreased 20-50% while the co-immunoprecipitating Gγs decreased by 80-95% (data not shown). In Fig. 2-4B, the effect of PhLP1 Δ1-75 on the Gγ/Gβ2 ratios was similar for all the Gγs that formed dimers with Gβ2. For every Gγ that formed a dimer with Gβ2, the Gγ/Gβ2 ratio decreased 81-100% compared to the lamin A/C control. Gγs 1, 11, and 13 did not form a dimer with Gβ2. These results, combined with the PhLP1 knockdown data clearly indicate that all Gβ2γ dimers depend on PhLP1 for their assembly.

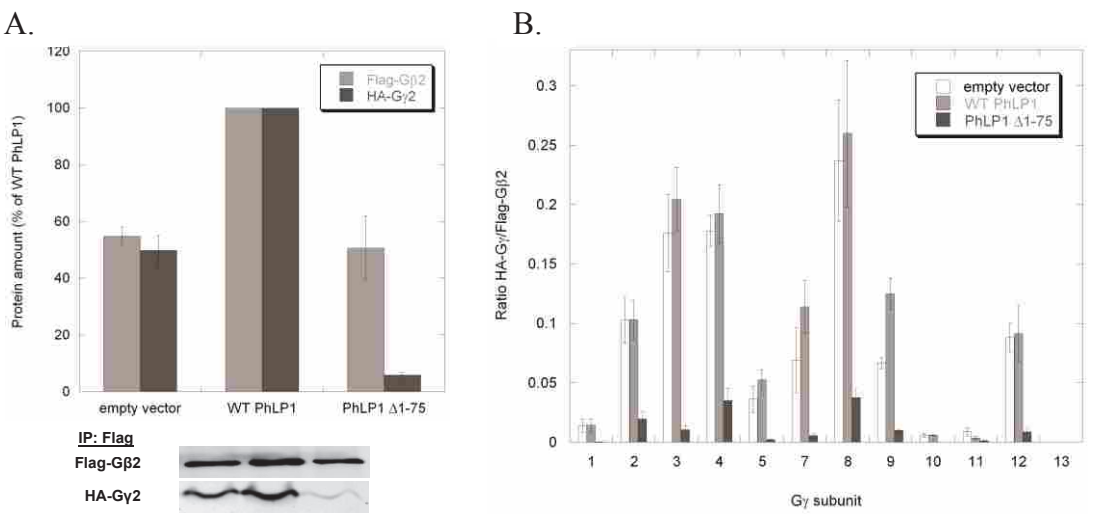

Figure 2-4. **Effects of PhLP1 Δ1-75 expression on the assembly of all Gγ subunits with Gβ2.** HEK 293T were transfected with either WT PhLP1, PhLP1 Δ1-75, or an empty vector control along with the indicated HA-Gγ subunit and Flag-Gβ2 cDNAs. After 48 hours, cells were lysed, immunoprecipitated with an anti-Flag antibody and immunoblotted with anti-Flag or anti-HA antibodies. Bands were quantified and expressed as a percentage of the wild-type PhLP1 control for Gβ2γ2 in (A) or as the relative ratio of HA-Gγ/Flag-Gβ2 for all 12 Gγs in (B). Bars represent the average ± standard error from 3-6 separate experiments. If no bar is shown, then no complex was detected for that particular Gβγ species. A representative blot for Gβ2γ2 is shown below the graph in (A).

The Gγ subunits can be divided genetically into five subfamilies as shown in the phylogenetic tree in Fig. 2-5A. The Gγ/Gβ2 ratios in the PhLP1 knockdown and PhLP1 Δ1-75 dominant interfering experiments were averaged based on the subfamilies they belonged to (Fig 2-5B and Fig. 2-5C). The data show that the binding affinity of Gγ subfamilies with Gβ2 is as follows: II > III > I/IV with no dimer formation found in subgroup V. This pattern is similar to the pattern of Gβ2γ specificity reported previously *in vitro (60)*. Even though Gβ2 preferentially binds different Gγ subunits, the data indicate that PhLP1 does not influence the Gβ2γ affinity. This conclusion is evidenced by the fact that the percent decrease in the amount Gβ2γ complex formed relative to the Lamin A/C control was the same for all Gγ subgroups when PhLP1 was depleted with siRNA. Similarly, when PhLP1 Δ1-75 was over-expressed, the percent decrease was the same for all Gγ subgroups. Thus, it appears that PhLP1 does not affect which Gγ will interact with Gβ2.

Discussion

Post-translational assembly of the heterotrimer is necessary for G protein signaling. The mechanism of how Gβ and Gγ subunits form stable dimers has recently been described (*19, 38, 39*). PhLP1 acts as a co-chaperone with CCT allowing the folding of Gβ and the assembly with Gγ. However, most studies have focused on the common dimer Gβ1γ2 and have not addressed whether this is a general mechanism or only for a subset of Gβγ dimers. This study focuses on the specificity of the co-chaperone role of PhLP1 on many different Gβγ dimer combinations. The results clearly show that PhLP1 is a general co-chaperone for all Gβγ dimer assembly. All of the Gβ subunits require PhLP1 for their association with Gγ2 (Fig 2-1 and 2-2). Additionally, all of the Gγ subunits that form a dimer with Gβ2 also require PhLP1 for their association (Fig 2-3 and 2-4). All of the Gβ subunits have been shown to bind CCT with Gβ5 binding with less

affinity than the other Gβ subunits (*19*). It seems very likely that other combinations of Gβγ dimers would also require PhLP1 for their assembly. Thus, it appears that all Gβγ dimers follow a similar mechanism of formation.

Understanding why some Gβγ combinations form dimers and some do not has been of interest for some time (*56*). Biochemical studies have suggested that the G protein α, β, and γ subunits may form preferred trimers *in vivo*, however, little is known of the mechanism of specific assembly (*56*). Many studies have shown that G protein α, β, and γ subtypes show cell-specific expression, thus one mechanism of controlling the assembly of specific G protein trimers could be by expressing specific subunits in particular cell types (*56*). It has also been suggested that cellular components such as PhLP1 could influence Gβγ specificity (*60*); however, this does not appear to be the case. As illustrated above, the specificity of Gβγ dimer formation was not changed by increases or decreases in PhLP1 activity. Apparently, PhLP1 is acting as a catalyst in Gβγ assembly by facilitating the association of Gβγ dimers that are intrinsically stable and not influencing which Gβ and Gγ subunits can bind.

It is interesting to note that inhibition of PhLP1 activity through siRNA-mediated knockdown or over-expression of the PhLP1 Δ1-75 dominant negative variant resulted in a surprisingly small decrease in Gβ expression (~50%), despite the fact that very little of this residual Gβ was associated with Gγ (Figs. 2-1 through 2-4). This observation indicates that Gβ can exist in the cell unassociated with Gγ. It is likely that this pool of undimerized Gβ is associated with CCT because it has been previously shown that Gβ-CCT complexes are relatively stable in the absence of PhLP1 and Gγ (*38*). Thus, it appears that the role of CCT is to fold Gβ and protect it from aggregation or proteolytic degradation until it can be released by PhLP1 to interact with Gγ.

A.

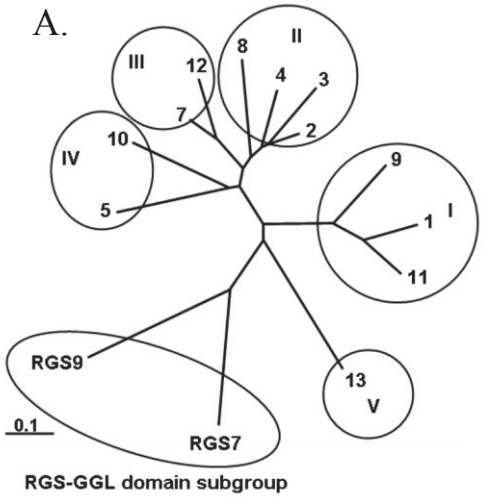

B.

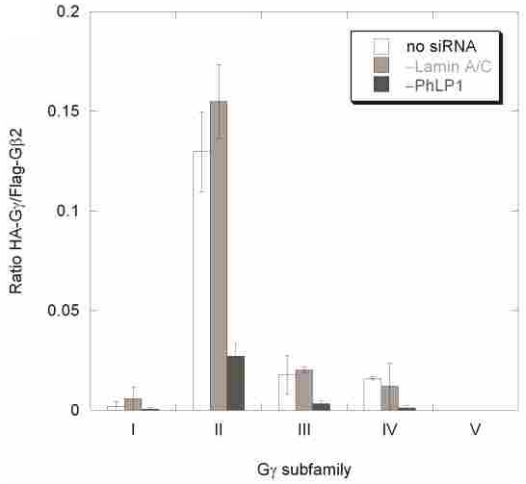

C.

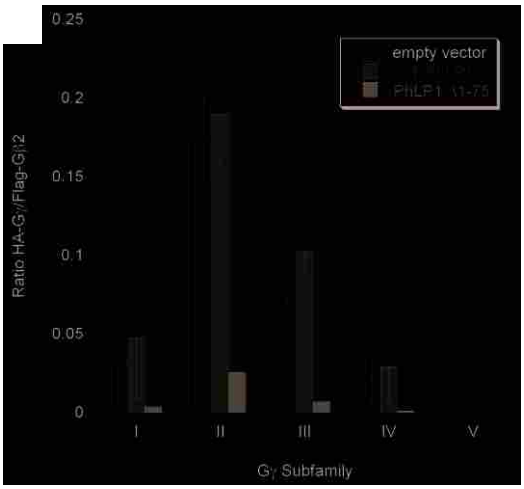

Figure 2-5. Effects of PhLP1 knockdown on the specificity of Gβ2 dimerization with Gγ subfamilies. A) The phylogenetic relationship between human Gγ subunits and RGS7 and 9 is depicted. An unrooted dendrogram was made using TreeView from a Gγ family sequence alignment created with ClustalX. The Gγ family can be separated into 5 subfamilies as indicated. The scale bar represents a substitution rate of 0.1 per amino acid. B) The Gγ/Gβ2 ratios within each Gγ subfamily under the different siRNA conditions from Fig. 3B were averaged and plotted to show the effects of PhLP1 knockdown on the subfamily specificity of Gβ2Gγ dimer formation. Error bars represent the standard error of the mean within each subfamily. C) A similar average of the Gβ2Gγ ratios for each subfamily under the different PhLP1 over-expression conditions from Fig. 4B was calculated and plotted. If no bar is shown, then no complex was detected for that particular Gβγ species.

In conclusion, this work expands the role of PhLP1 as an essential co-chaperone in the assembly of all Gβγ combinations. The data provide additional insight into the broad role PhLP1 assumes to bring the unstable β-propeller fold of Gβ subunits together with their complementary Gγ to create stable Gβγ dimers in order to perform their vital functions in G protein signaling.

CHAPTER 3:

INTERACTION OF PHLP1 AND CCT WITH PDCD5

Summary

Phosducin-like protein 1 (PhLP1) has been recently shown to be a co-chaperone with the cytosolic chaperonin complex (CCT) in the folding and assembly of nascent G protein βγ subunit dimers and Gβ5-RGS proteins. However, other possible functions for PhLP1 either as a co-chaperone or otherwise are yet to be investigated. Using PhLP1 as bait, a co-immunoprecipitation proteomics screen indicated that PhLP1 interacts with a known tumor suppressor, programmed cell death 5 protein (PDCD5). Subsequent experiments showed that PDCD5 binds PhLP1 indirectly through a ternary complex with CCT. Additional findings disagree with previous reports suggesting that PDCD5 translocates rapidly from the cytoplasm to the nucleus during the initial stages of apoptosis. Instead, our results indicate that the apoptotic function of PDCD5 is cytosolic, most likely involving CCT. Moreover, PDCD5 phosphorylation on S118, a reported CK2 phosphorylation site, was found to increase its binding to CCT during apoptosis. Structural and biochemical analysis suggests that over-expressed PDCD5 blocks β-actin from entering the CCT folding cavity. We propose that PDCD5 binds inside the folding cavity of CCT, not as a substrate, but as a co-chaperone or inhibitor of yet-to-be determined CCT substrates involved in cell cycle progression or apoptosis.

Introduction

Phosducin-like protein 1 (PhLP1) has been shown to act as a co-chaperone in CCT-mediated Gβγ dimer assembly (*38, 39*). Gβ is a well-studied CCT substrate containing a characteristic β-propeller fold. It is estimated that CCT folds 10% of all cellular proteins (*15*).

Indeed, CCT substrates have been linked to many cellular processes such as cytoskeletal function, chromatin modification, and cell cycle networks (*24*). Thus, it is possible that PhLP1 could act as a co-chaperone in the folding and assembly of other CCT substrates besides Gβ. Other functions of PhLP1 as a co-chaperone or otherwise have yet to be explored. This chapter begins with an investigation of novel functions of PhLP1. In a mass spectrometry proteomics screen, PhLP1 was found to interact with programmed cell death 5 (PDCD5), a tumor suppressor protein involved in apoptosis. This observation then led to the discovery of a novel PDCD5-CCT interaction. These observations link CCT to a potentially important role in apoptosis.

Cells protect themselves from environmental hazards by many different mechanisms. In response to DNA damage, the cell will either trigger a series of cellular changes which may lead to repair or tolerance of the damaged DNA, or the cell responds by removing itself from the cell population by death. Apoptosis is a natural programmed cell death process that occurs in multi-cellular organisms. In addition to the importance in protecting the organism from DNA damage, apoptosis is also an important process during development. Defects in apoptotic signals may result in different types of human diseases. Excessive apoptosis causes atrophy, whereas, insufficient apoptosis may cause proliferative diseases such as cancer.

PDCD5 was first cloned from TF-1 cells undergoing apoptosis (*62*). In early studies recombinant PDCD5 was shown to accelerate apoptosis in many tumor cells (*62*), and significantly increased levels of PDCD5 have been reported in cells undergoing apoptosis (*63*). Additionally, siRNA knockdown of PDCD5 promoted cell proliferation and reduced apoptotic stimulation that was induced by Bax over-expression (*64*). Moreover, it has been suggested that PDCD5 is uniformly distributed throughout a normal cell, and then translocates rapidly to the nucleus in the early stages of apoptosis (*63*). However, the mechanism of nuclear translocation

of PDCD5 during apoptosis is puzzling because PDCD5 does not contain a nuclear localization signal (*63*). A predicted nucleic acid binding region in the PDCD5 structure provides evidence in favor of apoptosis-induced nuclear localization of PDCD5, however the only reported evidence of nuclear translocation comes from immunofluorescence experiments (*63*) which can easily produce false positives. Thus, additional evidence is necessary to confirm nuclear localization of PDCD5.

Phosphorylation of serine 118 (S118) on PDCD5 by casein kinase 2 (CK2) has been reported *in vitro* and in HEK 293T cells (*65*). An unphosphorylated PDCD5 variant, S118A, was observed to impair the apoptotic potential of PDCD5; suggesting that phosphorylation of PDCD5 is essential in promoting apoptotic activity (*65*). PDCD5 consists of two flexible N-terminal α-helices, a core region containing a 3-helix bundle, and an unstructured C-terminal region (*66*). One group has suggested that the C-terminal region of PDCD5 contains the apoptotic activity and is also likely responsible for cell translocation (*66*). S118 is positioned in the C-terminal unstructured region, suggesting that S118 phosphorylation is important in the apoptotic activity of PDCD5. In contrast, another study demonstrated that the deletion of the N-terminal helical portion decreases the apoptotic activity of PDCD5 (*67*). Yet again, further studies are required to better understand the role of PDCD5 in apoptosis.

In the current study, PDCD5 was found to interact with PhLP1 in a proteomics screen. The PDCD5-PhLP1 interaction was not direct, but was further described as a ternary complex with CCT. Furthermore, assembly assays and cryo-EM data demonstrate that PDCD5 does not associate with CCT as a substrate, but instead accumulates inside the CCT folding cavity over time and is released by CCT during apoptosis. Contrary to previously reported data (*63*), PDCD5 was not detected in the nucleus before or after apoptosis. Additionally, PDCD5 was

found to interact specifically to β-tubulin, a well-characterized substrate of CCT, but interestingly not α-tubulin. Our findings link CCT as a key player in apoptosis and contradict the current belief that PDCD5 is a nuclear protein.

Experimental Procedures

Cell culture

HEK 293T and U2OS cells were cultured in 1:1 DMEM/F-12 growth media containing 2.5 mM L-glutamine and 15 mM HEPES supplemented with 10% fetal bovine serum. The cells were subcultured regularly to maintain growth but were only used to 20 passages.

Preparation of cDNA constructs

FLAG-tagged human PDCD5 and tubulin binding protein co-factor A (TBCA) cDNA sequences (Open Biosystems) were cloned in pcDNA3.1/myc-His B vector (Invitrogen) using PCR. Single and double point mutation variants of PDCD5 were prepared by site-directed mutagenesis. C-terminally c-myc-tagged human PhLP1 and the Δ1-75 truncation variant of PhLP1 were constructed in pcDNA3.1/myc-His B vector using PCR as described (*39*). His-PDCD5-FLAG was cloned into the first multiple cloning site of the bacterial expression vector pETDuet, and PhLP1-myc-His was cloned into the bacterial expression vector pET15b (Novagen) using PCR and utilizing unique endonuclease restriction sites near the substitution site. The integrity of all constructs was confirmed by sequence analysis. The N-terminally hemagglutinin (HA)-tagged Gγ2 and FLAG epitope-tagged Gβ1 cDNAs also in the pcDNA3.1 vector were obtained from the UMR cDNA Resource Center.

Protein Expression and Purification

Escherichia coli DE3 cells were transformed with human PhLP1 or PDCD5 in the pETDuet vector. The recombinant proteins were then purified using nondenaturing Co^{2+} affinity chromatography as previously described for Nickel-chelate chromatography (*30*). The purified proteins were concentrated and exchanged into 20 mM HEPES, pH 7.2, 150 mM NaCl by ultrafiltration and were stored in 50% glycerol at -20°C. Protein concentrations were determined using BCA protein assay reagent (Pierce). CCT was purified from bovine testis using a sucrose gradient (*21*).

CK2 Phosphorylation of PhLP

Purified PhLP1 (50 μM) was phosphorylated by CK2 (10 units/μl, Calbiochem) in 20 mM HEPES, pH 7.5, 100 mM KCl, 20 mM NaCl, 5 mM $MgCl_2$, 5 mM dithiothreitol, and 1mM ATP for 1 h at 37 °C. The phosphorylation was confirmed by SDS-PAGE using 10% gels.

Cryo Electron Microscopy

For cryo-EM, purified CCT and PDCD5 were combined in a buffer containing 10 mM Tris-HCl pH 7.5, 10 mM NaCl, 5 mM $MgCl_2$. 5-μl aliquots of the CCT:PDCD5 solution (in the absence of ATP) were applied to Quantifoil 2-μm holey carbon grids for 1 min, blotted for 3 s and frozen rapidly in liquid ethane at −180 °C. The samples were loaded into an FEI Tecnai G2 FEG200 electron microscope through a Gatan side-entry cryo-holder. For the ATP-free CCT, about 100 images were acquired using a 200kV emission voltage with a defocus range of 2–3.5 μm at 84k magnification on a 4K × 4K Eagle CCD camera (Gatan Inc.). A total of 6000 particles (down-sampled to 3.5 Å per pixel) were selected, normalized and CTF-corrected using standard XMIPP procedures.

RNA interference experiments

HEK 293T cells were grown in 12-well or 6-well plates to 50–70% confluency at which point they were transfected with CCTζ (Dharmacon), PhLP1 (Dharmacon), PDCD5 (Ambion), or negative control siRNA #1 (Ambion) at 100 nM final concentration using Oligofectamine reagent (Invitrogen) as described previously (*39*). In some cases, the cells were transfected 24 h later with 0.5 μg (12-well) or 1.0 μg (6-well) each of PDCD5-FLAG or PhLP1-myc in pcDNA3.1 using Lipofectamine 2000 according to the manufacturer's protocol (Invitrogen). Cells were harvested for subsequent immunoprecipitation experiments 4 days after the knockdown. 10 μg of cell lysates were immunoblotted with an anti-CCTζ antibody (Santa Cruz), anti-PhLP1, or anti-PDCD5 antibodies to assess the percent knockdown.

Transient transfections

HEK 293T and U2OS cells were grown in 6-well plates, 60-mm dishes, or 100-mm dishes to 80-90% confluency at which point they were transfected with 1 μg (6-well plate), 2 μg (60-mm dishes), or 6 μg (100-mm dishes) each of the indicated vectors using Lipofectamine 2000 according to the manufacturer's protocol (Invitrogen). 48 hours later, the cells were harvested for immunoprecipitation, mass spectrometry, or radiolabel pulse-chase experiments.

Mass spectrometry sample preparation

HEK 293T cells were transfected with empty vector or c-terminally myc-tagged phosducin, PhLP1, or PhLP2A containing TEV cleavage sites. After an immunoprecipitation with anti-myc antibody (Enzo), proteins were released via TEV protease cleavage according to the manufacturer's protocol (Promega). The released co-immunoprecipitates were then digested into peptides with enzyme-grade trypsin (Promega) and were analyzed by MS-MS on an Orbitrap mass spectrometer.

U2OS cells were transfected with empty vector or FLAG-TEV-PDCD5. 30 hours after transfection, the cells were irradiated with 60 J/m^2 UV-C radiation or were left untreated. After an additional 14-16 hours, cells were harvested and the lysates were immunoprecipitated in ATP-depletion buffer (PBS, 1% NP-40, 1 mM Azide, 5 mM EDTA, supplemented with 6 ul/ml protease inhibitor (Sigma) and 0.6 mM PMSF) using anti-FLAG antibody (Sigma). Immunoprecipitates were incubated with TEV protease overnight at 4°C. Cleaved immunoprecipitates were then prepared for mass spectrometry analysis.

Immunoprecipitates from U2OS cells were purified, reduced with DTT, and treated with iodoacetamide in a 10 kDa filter. Samples were then digested with 0.8 μg proteomic grade trypsin (Promega) overnight at room temperature. Samples were analyzed by LC-MS using an Orbitrap mass spectrometer. Peptides were identified using the MASCOT software (*68*).

Radiolabel pulse-chase assays

Transfected HEK 293T cells in 6-well plates were washed and incubated in methionine-free DMEM media (Mediatech Inc.) supplemented with 4 mM $_L$-glutamine (Sigma), 0.063 g/l $_L$-cystine dihydrochloride (USB) and 10% dialyzed fetal bovine serum (Invitrogen). The media was discarded and the cells were pulsed with 800 μl of new media supplemented with 200 μCi/ml radiolabeled $_L$-[^{35}S] methionine (Perkin-Elmer) for 10 min. After the pulse phase, the cells were washed and incubated in DMEM/F-12 growth media supplemented with an extra 4 mM $_L$-methionine (Sigma) and 4 μM cyclohexamide to discontinue the [^{35}S] methionine incorporation. After the indicated chase times, the cells were harvested for immunoprecipitation experiments.

Immunoprecipitation experiments

Transfected or untreated HEK 293T or U2OS cells were washed with phosphate-buffered saline (PBS) (Fisher) and solubilized in IP buffer (PBS, pH 7.4, 1% NP-40 (Sigma)), β-tubulin IP buffer (50 mM Na_2HPO_4, pH 7.5, 10mM NaCl, 0.1% Tween 20, 1mM GTP), Actin IP buffer (20mM HEPES, pH 7.4, 50mM KCl, 1mM DTT, 0.2 mM $CaCl_2$, 0.5% NP-40, 4 uM cyclohexamide, 40 mM glucose), or ATP-depletion buffer (PBS pH 7.4, 1% NP-40, 100 mM deoxy-glucose, 1mM sodium azide, 5 mM EDTA) supplemented with 0.6 mM PMSF and 6 µl/ml protease inhibitor cocktail (Sigma P8340). The lysates were passed through a 25-gauge needle 10 times and centrifuged at maximum speed for 10 minutes at 4ºC in an Eppendorf microfuge. The protein concentration for each sample was determined using the DC Protein Assay Kit II (Bio-Rad) and equal amounts of protein were used in the subsequent immunoprecipitations. In time sensitive immunoprecipitations, the protein concentrations were not determined, but equal volumes were used. In this case, samples were immunoblotted with anti-β-actin antibody (clone 8H10D10, Cell Signaling) as a loading control. The clarified lysates were incubated for 20-30 minutes at 4°C with 3 µg anti-myc (clone 9E10, Enzo Life Sciences), 0.3 µg anti-CCTε antibody (clone PK/29/23/8d, Serotec), 0.3 µl anti-TCP-1α (CCTα) antibody (clone 91a, Assay Designs), 3 µg anti-FLAG (clone M2, Sigma), anti-HA (clone 3F10, Roche) or polyclonal rabbit anti-PDCD5 antibody (Abcam). Next, 30 µl of Protein A/G Plus agarose slurry (Santa Cruz Biotechnology) were added, and the mixture was incubated for 20-30 minutes at 4°C. The agarose beads were washed 3 times in the appropriate buffer and the immunoprecipitated proteins were solubilized in SDS sample buffer.

Immunoprecipitated proteins and lysates were resolved on 10% or 14% Tris-Glycine-SDS gels or 16.5% Tricine-SDS gels. The proteins were transferred to nitrocellulose and

immunoblotted using the antibodies listed above or, anti-CCTζ (Santa Cruz), anti-β-actin (Cell Signaling), anti-PARP (cat# 9542, Cell Signaling), anti-phosphorylated H2A.X histone (pH2A.X) (clone 20E3, Cell Signaling), or anti-PhLP1 (*69*) antibodies. Immunoblots were incubated with the appropriate anti-mouse, anti-rat, anti-rabbit, or anti-goat (Li-Cor Biosciences) secondary antibody conjugated to an infrared dye. Blots were scanned using an Odyssey Infrared Imaging System (Li-Cor Biosciences), and protein band intensities were quantified using the Odyssey software. Radiolabeled gels were dried and incubated on a phosphoscreen (GE Healthcare). Radiographs were imaged on a Storm 860 phosphorimager and the band intensities were quantified using Image Quant software (GE Healthcare). The data are presented as the mean value +/- standard error from at least three experiments.

UV-C-induced apoptosis assay

U2OS cells were plated in 100mm dishes to 70-80% confluency. Cells were then washed with warmed PBS and were irradiated with 60 J/m^2 UV-C light using a UV Stratalinker 1800 (Stratagene). Fresh media was added and cells were returned to the 37°C incubator. 14-16 hours later, cell lysates were assessed for DNA damage and apoptosis by immunoblotting for pH2A.X, and PARP (Cell Signaling) antibodies. Where indicated, cell lysates were immunoprecipitated with PDCD5 antibody and immunoblotted for CCTε.

Nuclear Extractions

Non-treated or UV irradiated U2OS cells were lysed in hypotonic buffer (20 mM HEPES, pH 8.0, 1.5 mM $MgCl_2$, 5 mM KCl, 0.1 mM DTT) supplemented with 6 µl/ml protease inhibitor cocktail (Sigma) 0.6 mM PMSF and incubated for 10 min. Cells were then dounce homogenized and the nuclei were collected by centrifugation at 16,000g for 10 min at 4°C. The pellets were then washed in pre-nuclear extraction wash buffer (15 mM Tris, pH7.5, 1 mM

EDTA, 10% Sucrose, 1 mM DTT) two times. The nuclear pellets were then lysed in nuclear extraction buffer (15 mM Tric-HCl pH7.5, 1 mM EDTA, 0.4 M NaCl, 2 mM $MgCl_2$ 10% Sucrose, 1 mM DTT), supplemented with 0.6 mM PMSF, 6 µl/ml protease inhibitor cocktail (Sigma), and 250 U/ml Benzonase (EMD Chemicals). Pellets were incubated on ice for 30 min and the insoluble proteins were removed by centrifugation at 21,100g for 15 min. Cytosolic and nuclear fractions were separated by SDS-PAGE and blotted for various proteins. Anti-TATA-binding protein (TBP) (clone 1TBP18**,** Abcam) antibody was used as a nuclear control.

Results

A proteomics search for PhLP1 binding partners

To facilitate the identification of novel PhLP1 binding partners, an immunoprecipitation coupled with mass spectrometry strategy was employed. Pdc-TEV, PhLP1-TEV, PhLP2A-TEV with a C-terminal c-myc tag, or an empty vector control, was expressed in HEK 293T cells. Each Pdc family member was immunoprecipitated with an antibody against the c-myc tag and the samples were incubated with TEV protease. This procedure freed PhLP1 and any interacting partners from the antibody and protein A/G beads, removing these contaminants from the mass spectrometry analysis. The proteins were reduced, alkylated, acetone precipitated, and then digested with trypsin. The resulting peptides were analyzed by LCMSMS and protein identifications were assigned using the MASCOT software (*68*).

Table 3-1. A proteomics search for PhLP1 binding partners.

Control	Pdc-TEV-myc	PhLP1-TEV-myc	PhLP2-TEV-myc	Gene	Description	Protein ID
0	0	76	79	CCT8	T-complex protein 1 subunit theta	IPI00784090.2
2	1	76	70	CCT5	T-complex protein 1 subunit epsilon	IPI00010720.1
0	0	76	76	CCT1	T-complex protein 1 subunit alpha	IPI00290566.1
1	0	64	72	CCT2	T-complex protein 1 subunit beta	IPI00297779.7
1	0	68	70	CCT3	chaperonin containing TCP1, subunit 3 isoform b	IPI00290770.3
0	0	65	52	CCT4	Putative uncharacterized protein CCT4	IPI00893358.1
0	0	57	53	CCT7	T-complex protein 1 subunit eta	IPI00018465.1
0	0	0	49	PDCL2	Phosducin-like protein 2A	IPI00031629.1
0	0	41	38	CCT6A	T-complex protein 1 subunit zeta	IPI00027626.3
0	0	38	0	HSD17B4	Peroxisomal multifunctional enzyme type 2	IPI00019912.3
0	0	36	0	PDCL	Phosducin-like protein	IPI00298409.3
0	3	5	13	TUBB	Tubulin beta chain	IPI00011654.2
0	10	4	0	GNB1	Guanine nucleotide-binding protein G(I)/G(S)/G(T) subunit beta-1	IPI00026268.3
0	0	9	0	PDCD5	Programmed cell death protein 5	IPI00023640.3
0	7	3	0	GNB2	Guanine nucleotide-binding protein G(I)/G(S)/G(T) subunit beta-2	IPI00003348.3
0	3	0	0	RPL23	10 kDa protein	IPI00795751.1
0	3	0	0	GNB4	Guanine nucleotide-binding protein subunit beta-4	IPI00012451.3
0	1	0	0	GNG5	Guanine nucleotide-binding protein G(I)/G(S)/G(O) subunit gamma-5	IPI00027240.7
0	1	0	0	PDC	phosducin isoform b	IPI00021742.3

HEK293T cells were transfected with empty vector or phosducin-TEV-myc family members. 48 hours later, the cells were lysed and immunoprecipitated with an anti-myc antibody. Proteins were released via TEV protease cleavage. The co-immunoprecipitates then underwent a trypsin digest and were analyzed by MS-MS on an Orbitrap mass spectrometer. The table displays a selection of hits found in the proteomics screen. The numbers in the first four columns indicate the number of peptides identified in each sample. IPI represents the International Protein Index.

The proteins listed in Table 3-1 were found to interact with either the empty vector control, Pdc, PhLP1, or PhLP2A. All CCT subunits were found to interact with PhLP1 and PhLP2A, but not Pdc, in agreement with previous observations (*35, 36, 44, 45*). Multiple Gβ subunits and one Gγ subunit were also found in the proteomics screen. Two hits of particular interest were peroxisomal multifunctional enzyme type 2 (HSD17B4) and programmed cell death protein 5 (PDCD5), both of which were specific to PhLP1.

HSD17B4 and PDCD5 specifically interact with PhLP1

In order to confirm HSD17B4 and PDCD5 as PhLP1 binding partners, FLAG-tagged HSD17B4 or PDCD5 were over-expressed in HEK 293T cells along with members of the phosducin family or an empty vector control. HSD17B4 and PDCD5 were found to co-immunoprecipitate with PhLP1, but not with the other phosducin family members (Figure 3-

1A,B). These data indicate that HSD17B4 and PDCD5 interact specifically with PhLP1. PDCD5 has been reported to be an important regulator of apoptosis, and PDCD5 down-regulation has been observed in some human tumors (*62*). Moreover, recombinant PDCD5 was shown to induce cell death in human cancer cells (*70*). In response to these important findings we were prompted to further explore the PDCD5-PhLP1 interaction.

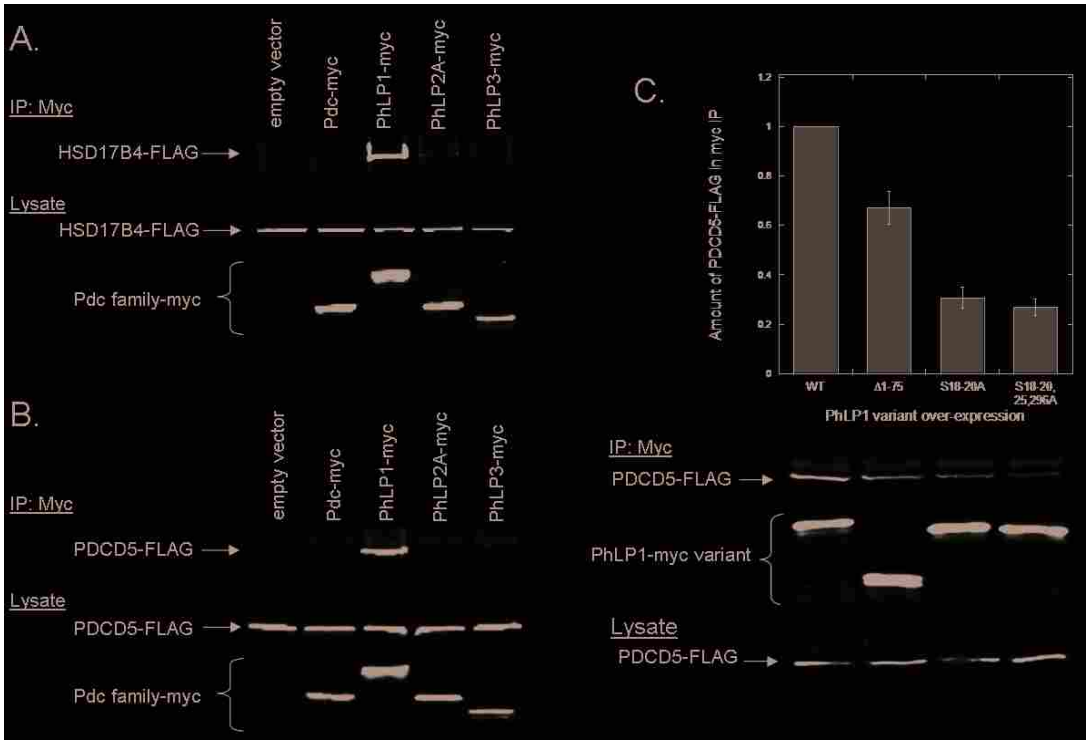

Figure 3-1. HSD17B4 and PDCD5 specifically interact with PhLP1. A) HEK 293T cells were transfected with HSD17B4-FLAG along with empty vector or a myc-tagged phosducin family member as indicated. After 48 hours, cells were lysed, immunoprecipitated with an anti-myc antibody, and immunoblotted with anti-myc or anti-Flag antibodies. B) Cells were transfected with PDCD5-FLAG along with empty vector or a myc-tagged Phosducin family member and were immunoprecipitated and immunoblotted as in (A). C) Cells were transfected with either PDCD5-FLAG along with PhLP1-myc variants and immunoprecipitated and immunoblotted as in A. The graph depicts the amount of PDCD5 in the myc IP in the presence of the PhLP1 variants and represents the average of at least three independent experiments.

The PDCD5-PhLP1 interaction is phosphorylation dependent

PhLP1 contains phosphorylation sites on serines 18-20 that have been shown to be important in its function as a co-chaperone in the release of Gβ from CCT (*38*). In order to investigate the contribution of PhLP1 phosphorylation to its interaction with PDCD5, the dominant interfering PhLP1 Δ1-75 and dephosphorylated PhLP1 mutants (S18-20A and S18-20, 25,296A) were over-expressed and the co-immunoprecipitation of PDCD5 was measured. The amount of PDCD5 interacting with PhLP1 Δ1-75 was about 30% less than WT PhLP1. Furthermore, PhLP1 S18-20A and PhLP1 S18-20,25,296A interacted with PDCD5 70% less than WT PhLP1 (Fig. 3-1C). These data clearly show that S18-20 phosphorylation of PhLP1 affects the interaction with PDCD5.

PhLP1 and CCT form a ternary complex with PDCD5

To determine whether PhLP1 and PDCD5 bind directly or indirectly through a common complex, recombinant PhLP1 and PDCD5 were co-immunoprecipitated *in vitro*. When PhLP1 or phosphorylated PhLP1 (p-PhLP1) were pulled down, no PDCD5 was co-immunoprecipitated (Fig. 3-2A). The reciprocal experiment revealed the same results when no PhLP1 or p-PhLP1 interacted with PDCD5 (data not shown). These results suggest that PhLP1 and PDCD5 do not interact directly, but instead are components of the same complex. Knowing that PhLP1 interacts with CCT as a co-chaperone and PhLP1 does not interact with PDCD5 directly, we hypothesized that PDCD5 could also interact with CCT. By pulling down over-expressed PDCD5, we were able to observe both endogenous PhLP1 and CCTε as co-immunoprecipitates (Fig. 3-2B). A reciprocal experiment confirmed this interaction when PhLP1 and PDCD5 co-immunoprecipitated with CCT (Fig. 3-2B).

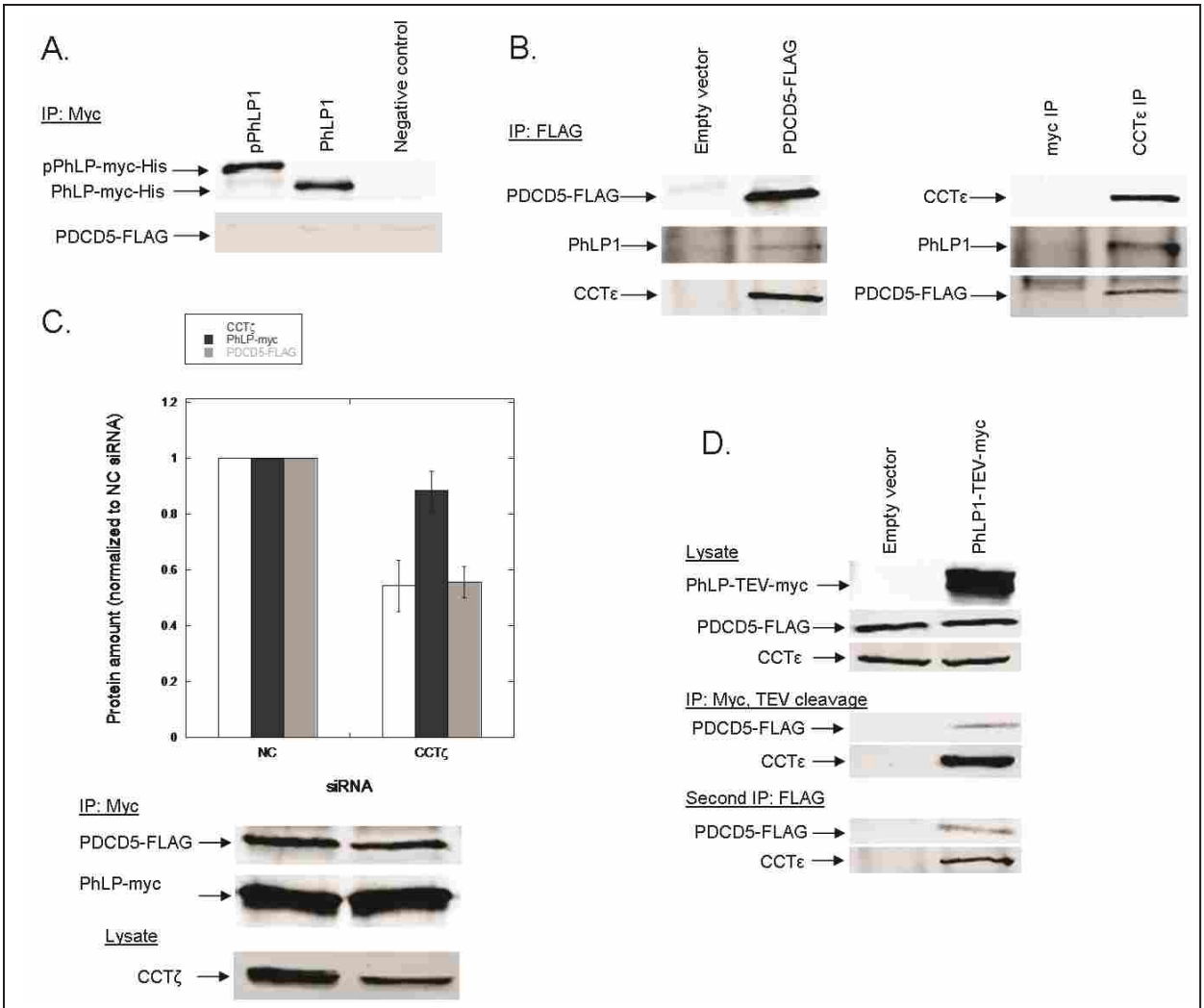

Figure 3-2. PDCD5, PhLP1, and CCT form a ternary complex. A) Recombinant PhLP1 and PDCD5 were purified from *E. coli* on a His-pur Co^{2+} column. PhLP1 was phosphorylated by CK2. pPhLP1, PhLP1, or no PhLP1 was incubated with PDCD5 as indicated and immunoprecipitated with myc antibody. B) HEK293T cells were transfected with empty vector or PDCD5-FLAG. The left panel shows PhLP1 and CCTε as co-immunoprecipiatates of a FLAG IP. The right panel shows PhLP1 and PDCD5-FLAG as co-immunoprecipitates of a CCTε IP, with the myc antibody acting as a negative control. C) HEK 293T cells were treated with negative control or CCTζ siRNA as indicated. 24 hours later, cells were transfected with PDCD5-FLAG and PhLP1-myc. Cells were lysed and immunoprecipitated with myc antibody. Immunoprecipitates and cell extracts were immunoblotted to determine the amount of proteins in the IP and the efficiency of the CCT knockdown, respectively. Bars represent the average ± standard error from at least three experiments. Representative blots are shown below the graphs. D) HEK 293T cells were transfected with PDCD5-FLAG along with empty vector or PhLP1-TEV-myc. 48 hours later, cells were lysed and immunoprecipitated with myc antibody. The immunoprecipitate was treated with TEV protease and subjected to a second IP with FLAG antibody. The top three blots represent the proteins present in the cell lysate, the middle two blots represent the proteins present after the first IP, and the bottom two blots represent the proteins present after the second IP.

In previous experiments, knocking down the CCTζ subunit using RNAi resulted in decreased expression of the entire CCT complex (*27*). By implementing this method, we were able to investigate the effect of diminished CCT expression on the amount of PDCD5 interacting with PhLP1. When CCT was knocked down 40%, the amount of PDCD5 interacting with PhLP1 also reduced 40% (Fig 3-2C). These results provide evidence that PhLP1 and CCT form a complex with PDCD5, meaning PhLP1 and PDCD5 are binding simultaneously to CCT. This idea was also tested in a double immunoprecipitation. Over-expressed PhLP1 with a C-terminal myc tag and TEV cleavage site was immunoprecipitated and released with TEV protease. This immunoprecipitate was then subject to another IP using a FLAG antibody. The IP results presented in Figure 3-2D indicate that the same CCT complexes that co-immunoprecipitated with PhLP1 were also bound to PDCD5. Together, these data confirm that PDCD5 and PhLP1 interact with CCT simultaneously. This series of experiments demonstrated that PDCD5 does not bind PhLP1 directly. Instead, we learned that PDCD5 forms a ternary complex with CCT and PhLP1.

Cryo-EM structure of the PDCD5-CCT complex

After observing an interaction between PDCD5 and CCT through immunoprecipitations in HEK 293T cells, we sought to explore the structure of the PDCD5-CCT complex to gain a better understanding of the nature of this interaction. Recombinant PDCD5 was purified from *E. coli*, and CCT was purified from bovine testis (*21*). The purified components were mixed and the resulting complex was analyzed using cryo electron microscopy (cryo-EM). Figure 3-3 shows negatively stained images of CCT, CCT:PDCD5, CCT:PDCD5:anti-CCTδ, and CCT:PDCD5:anti-CCTε complexes. Interestingly, the images show that PDCD5 binds deep inside the folding cavity similarly to CCT substrates (*20, 71, 72*). An antibody targeted to the

outside of the CCTδ subunit clearly indicates that PDCD5 specifically binds to the CCTδ subunit. Many structural and biochemical assays have been performed to determine the arrangement of the CCT subunits (*17, 18, 73, 74*). Originally, the order of the subunits around the CCT ring was reported to be α, ε, ζ, β, γ, θ, δ, and η (*74*). However, a different order of subunits has recently been proposed to be α, ζ, β, γ, θ, δ, ε, and η (*17*). The negative stained image of the CCT:PDCD5:CCTε antibody complex indicates that the ε subunit is three (clockwise direction) or five (counterclockwise direction) subunits away from the δ subunit. Thus, our results confirm the first reported subunit arrangement (*18*). Our results also point to the possibility of PDCD5 being a novel CCT substrate.

PhLP1 and PDCD5 bind CCT independently of each other

Since PhLP1 and PDCD5 bind CCT simultaneously, we hypothesized that they could bind CCT synergistically. To test this hypothesis, we looked at the effect of PDCD5 on the PhLP1-CCT interaction. When PDCD5 was over-expressed in HEK 293T cells, the amount of PhLP1 that co-immunoprecipitated with CCT did not change compared to an empty vector control where no PDCD5 was over-expressed (Fig. 3-4A). Additionally, when PDCD5 was knocked down with RNAi, the resulting 75% reduction of endogenous PDCD5 levels did not affect the amount of CCT that co-IPs with PhLP1 (Fig. 3-4B). Similarly, the PDCD5-CCT interaction was not affected by PhLP1 expression. When PhLP1 was over-expressed, the amount of PDCD5 that co-immunoprecipitated was not significantly different compared to an empty vector control (Fig. 3-4C). Furthermore, when PhLP1 was knocked down with RNAi, a 90% reduction of endogenous PhLP1 expression resulted in no significant change in the amount of CCT that co-immunoprecipitated with PDCD5 (Fig. 3-4D). Together, these data demonstrate that PDCD5 and PhLP1 simultaneously bind CCT independently of each other. Independent

binding indicates that PDCD5 and PhLP1 bind different sites on CCT that do not interact, either sterically or conformationally.

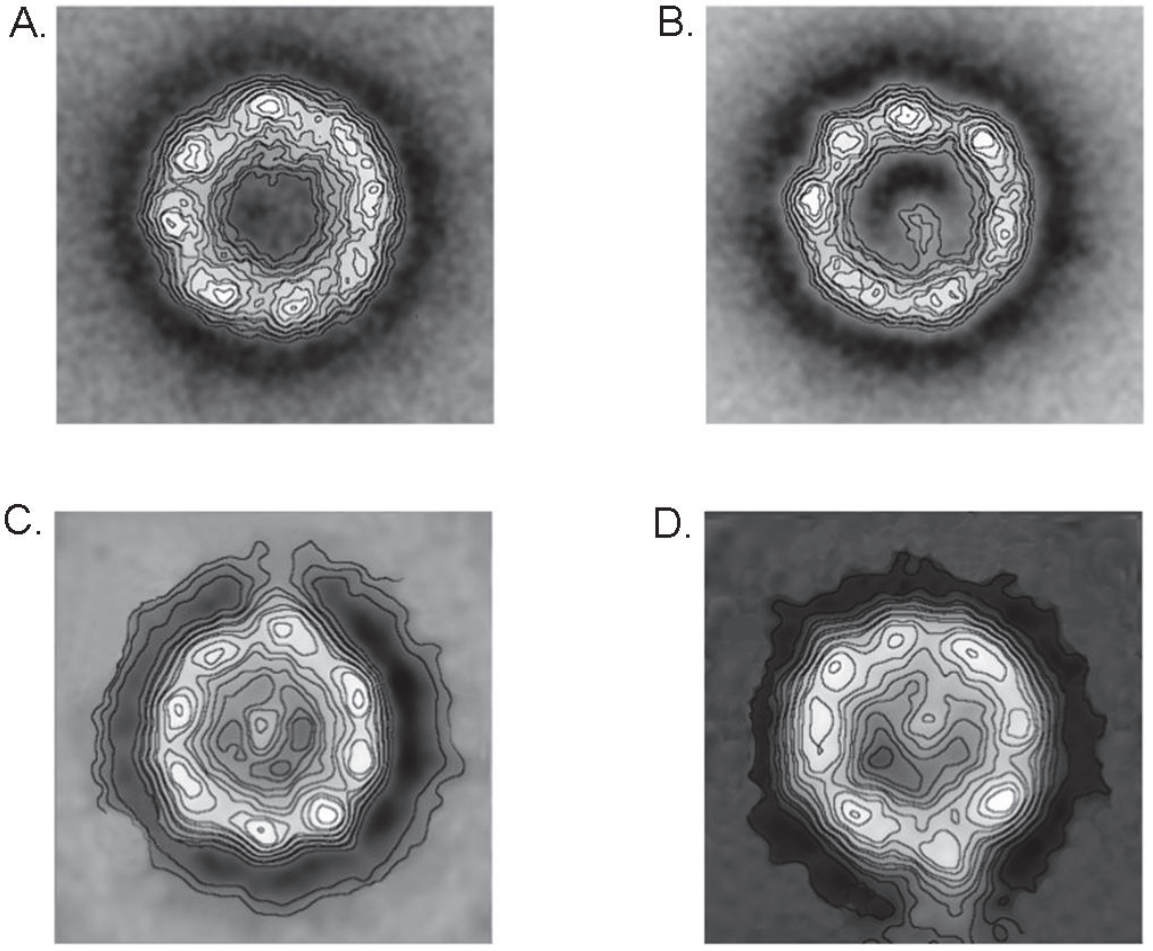

Figure 3-3. Cryo-EM of CCT-PDCD5 complex. Average images obtained from negatively stained CCT (A), CCT:PDCD5 (B), CCT:PDCD5:antiCCTdelta (C), and CCT:PDCD5:antiCCTepsilon (D) particles. Images were averaged from 1018, 1128, 1356, and 2014 particles respectively.

To determine whether PDCD5 and PhLP1 affect each other's expression, we used RNAi to knock down the endogenous levels of PDCD5 and measured the protein expression of PhLP1 and vice versa. When PhLP1 expression is reduced 80% there were no significant changes in endogenous PDCD5 levels (Fig. 3-5A). Additionally, when PDCD5 expression was reduced by 50%, there was no significant change in endogenous PhLP1 levels (Fig. 3-5B). From these data, we conclude that PhLP1 and PDCD5 do not affect the other's protein expression.

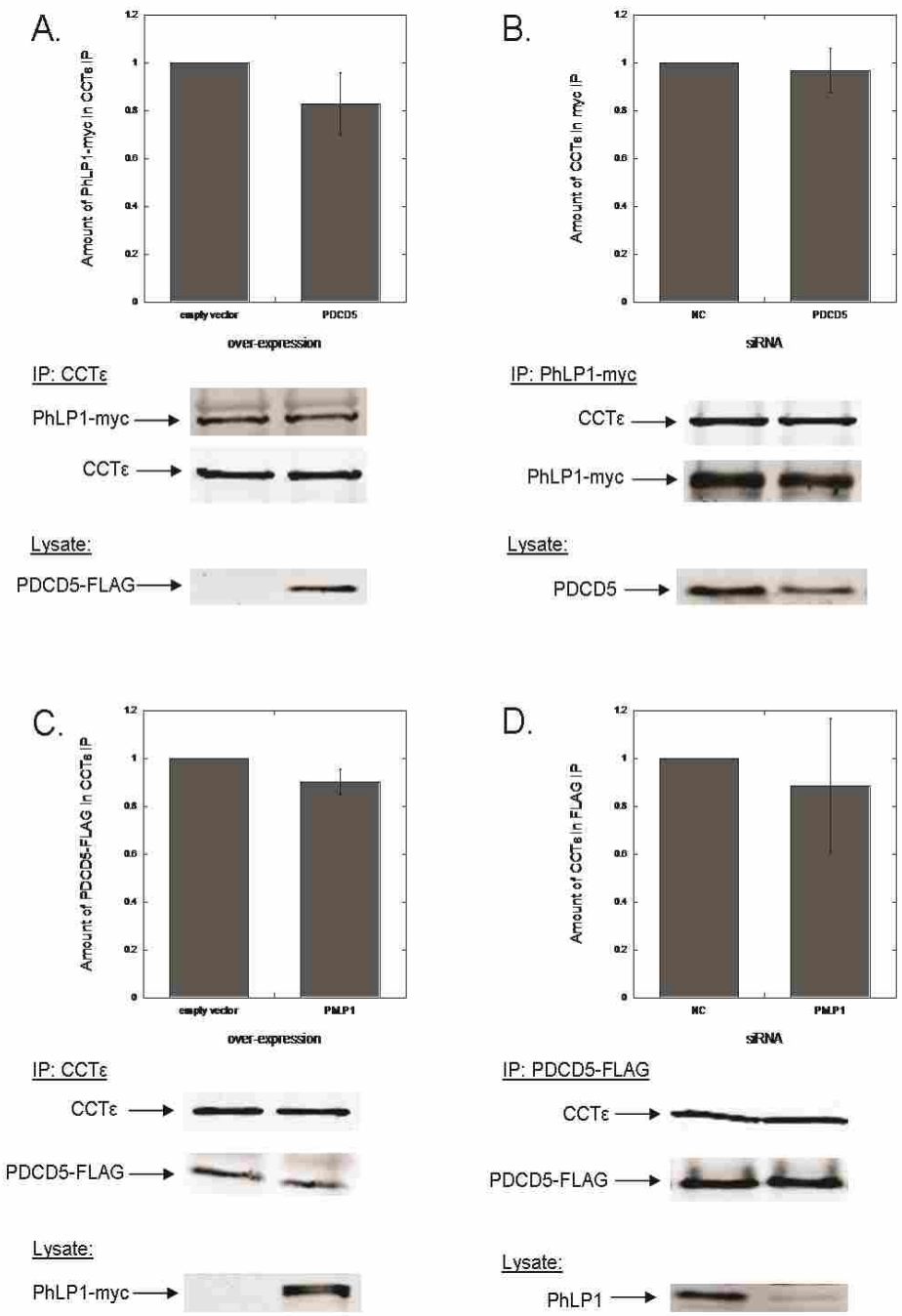

Figure 3-4. PhLP1 and PDCD5 bind CCT independently of each other. PDCD5 was either over-expressed (A) or knocked down (B), along with PhLP1-myc over-expression in HEK 293T cells. Cell lysates were immunoprecipitated with anti-CCTε (A) or anti-myc (B) and the ratio of co-immunoprecipitate to immunoprecipitate was measured compared to the negative controls. PhLP1 was either over-expressed (C) or knocked down (D), along with PDCD5-FLAG over-expression in HEK 293T cells. Cell lysates were immunoprecipitated with anti-CCTε (A) or anti-FLAG (B) and the ratio of co-immunoprecipitate to immunoprecipitate was measured compared to the negative controls. Bars represent the average ± standard error from at least three experiments. Cell lysates were blotted for PDCD5-FLAG, PDCD5, PhLP1-myc, or PhLP1 as indicated to verify the over-expression and knockdowns. Representative gels are shown below the graphs.

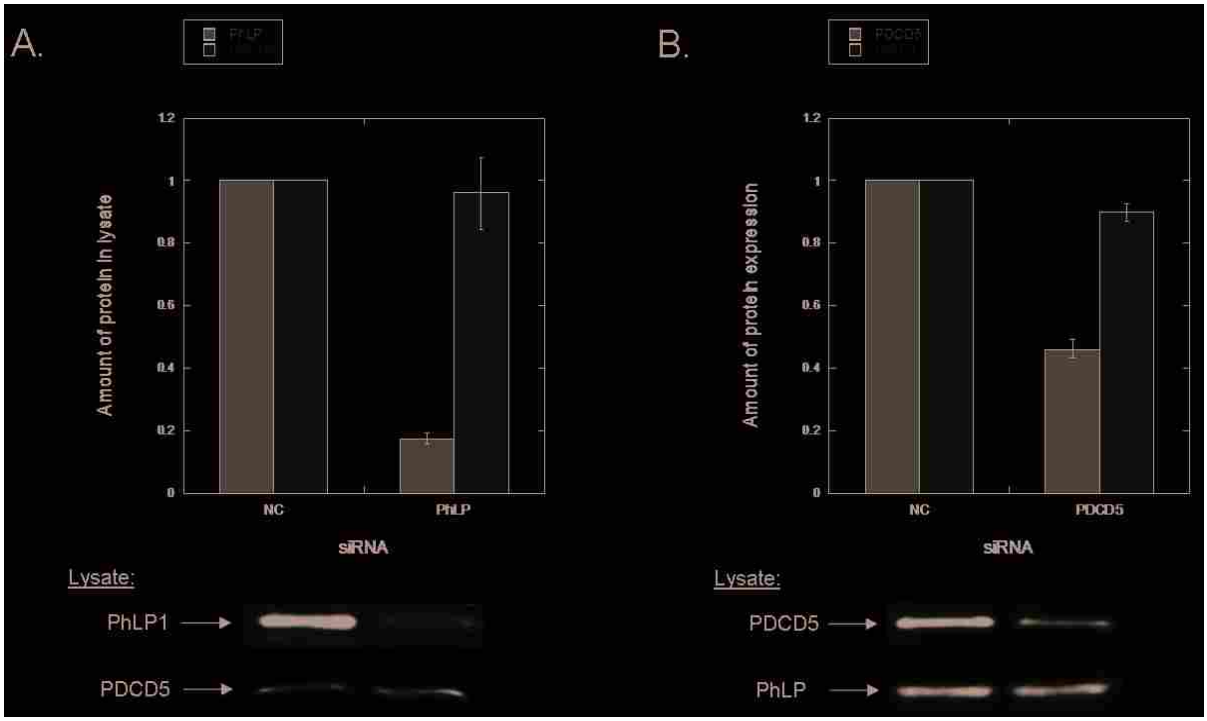

Figure 3-5. PhLP1 and PDCD5 do not affect the expression of the other. PhLP1 (A) or PDCD5 (B) were knocked down in HEK 239T cells using RNAi. 96 hours later, cell lysates were blotted for PhLP1 and PDCD5. The graphs indicate the relative expression of PhLP1 and PDCD5 compared to the negative siRNA controls. Bars represent the average ± standard error from at least three experiments. Representative gels are shown below the graphs.

PDCD5 is not involved in Gβγ assembly

PhLP1 has been shown to act as a co-chaperone in CCT-mediated Gβγ assembly (*27, 38, 39*). After observing PDCD5 and PhLP1 forming a ternary complex with CCT, we explored the possibility of PDCD5 also affecting Gβγ assembly. HEK 293T cells were transfected with Gβ1 and Gγ2 along with PhLP1, PDCD5, or a combination of PhLP1 and PDCD5, Gβ was immunoprecipitated and the amount of Gγ that co-immunoprecipitated was measured. PhLP1 Δ1-75, which acts as a dominant negative inhibitor of Gβγ assembly ((*27, 38, 39*), also see Chapter 2), was used as a positive control. A transfection of empty vector also served as a negative control. As was expected, Gβγ assembly was inhibited when PhLP1 Δ1-75 was over-

expressed compared to WT PhLP1. However, when PDCD5 was over-expressed with or without PhLP1, no changes in Gβγ assembly were detected (Fig. 3-6A).

To further test for a possible role of PDCD5 in Gβγ assembly, we also measured the amount of nascent Gβ bound to Gγ when endogenous levels of PDCD5 are knocked down using RNAi. When PDCD5 was knocked down 80%, there was no significant change in the amount of nascent Gβ bound to Gγ (Fig. 3-6B). Additionally, we found that PDCD5 knockdown had no effect on nascent PhLP1 bound to Gγ (Fig. 3-6B). Together, these data demonstrate that PDCD5 has no effect on Gβγ assembly or on PhLP1 binding to Gβγ. Consequently, is does not appear that PDCD5 is a co-chaperone in CCT-mediated Gβγ assembly nor is it influencing the role of PhLP1 as co-chaperone.

PDCD5 is not a substrate of CCT

Since PDCD5 binds inside the folding cavity of CCT, it was important to determine whether or not PDCD5 is a substrate of CCT. When newly synthesized substrates of CCT are measured in a pulse-chase experiment, the amount of substrate bound to CCT decreases over time as the substrate folds and releases (*75*). To measure the amount of nascent PDCD5 bound to CCT over time, HEK 293T cells transfected with PDCD5 were pulsed with [^{35}S] methionine and then chased with cold methionine for the times indicated. CCT was then immunoprecipitated using an antibody against the CCTε subunit. In the same experiment, CCT assembly was measured by quantifying the CCTα to CCTε ratio over time as an example of the behavior of a stable CCT interaction. In addition, the binding of a 50 kDa band (most likely tubulin) was monitored as an example of a CCT substrate that would be released over time (Fig 3-7A). Surprisingly, the amount of PDCD5 bound to CCT increased over time in a manner similar to CCTα and in contrast to the decrease observed for the 50 kDa tubulin band (Fig 3-7A).

This result indicates that PDCD5 is not a CCT substrate, but a stable CCT binding partner. Despite the fact that PDCD5 binds CCT within the folding cavity, it is not being folded by CCT. These observations suggest that PDCD5 is a co-chaperone with CCT like PhLP1.

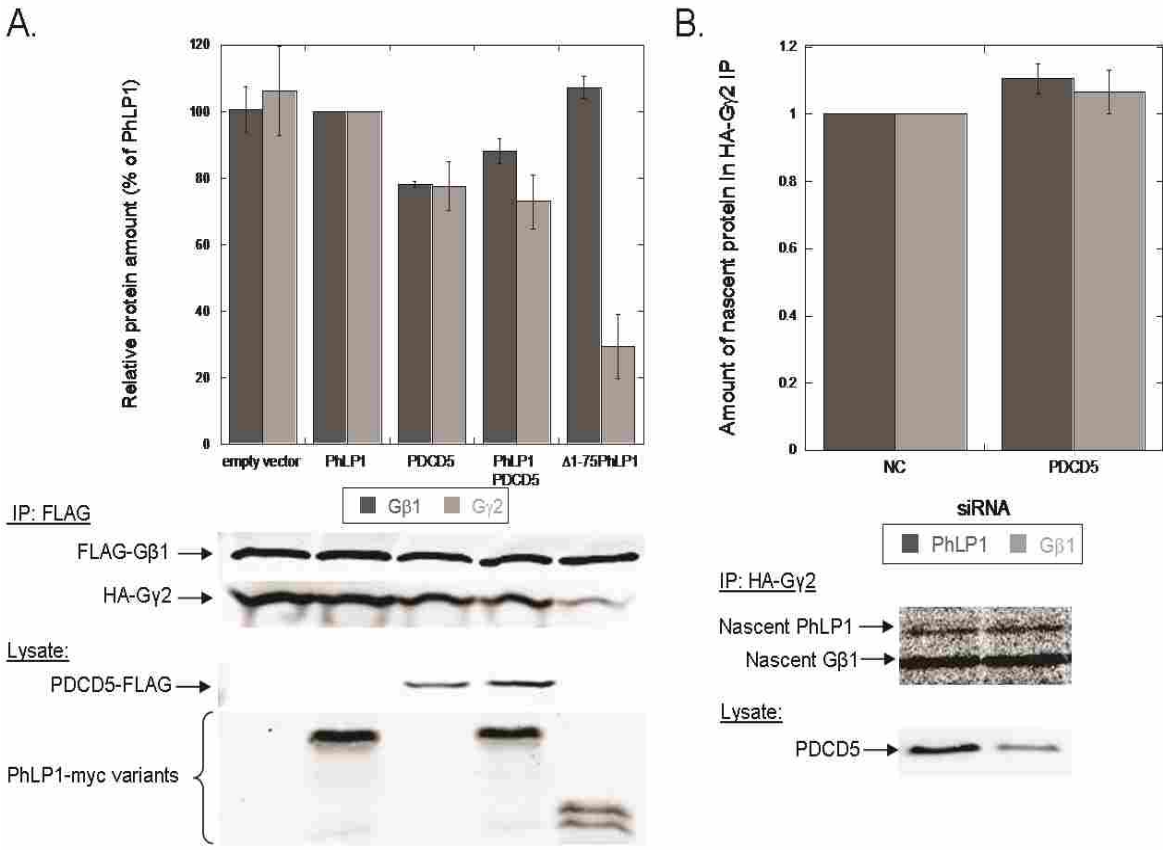

Figure 3-6. PDCD5 does not affect Gβγ assembly. A) HEK 293T cells were transfected with FLAG-Gβ1 and HA-Gγ2 along with the indicated constructs. 48 hours later, the cells were lysed and immunoprecipitated with FLAG antibody. The amount of Gβ1 and Gγ2 was quantified compared to the PhLP1 sample. B) HEK 293T cells were treated with negative control or PDCD5 siRNA. 24 hours later, the cells were transfected with FLAG-Gβ1 and HA-Gγ2. 72 hours after the transfection, the cells were pulsed with [^{35}S] methionine for 10 min and chased for 30 min. Cells were then lysed and immunoprecipitated with HA antibody. Folded nascent PhLP1 and nascent Gβ1 were quantified by taking the ratio of folded protein to immunoprecipitated Gγ and normalizing the ratio to the negative control siRNA sample. Bars represent the average ± standard error from at least three experiments. Representative blots and gels are shown below the graphs.

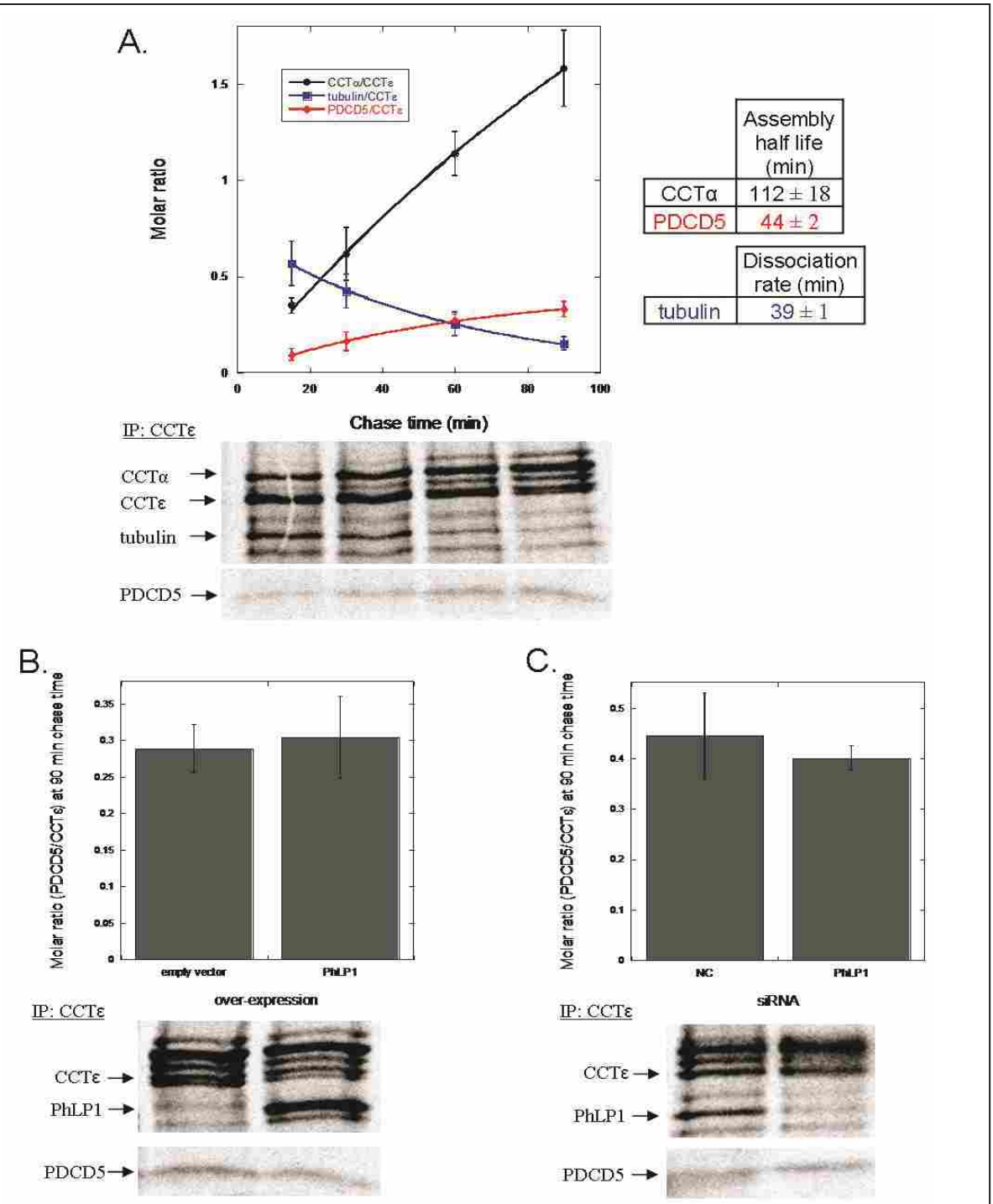

Figure 3-7. PDCD5 is not a substrate of CCT. HEK 293T cells were transfected with PDCD5-FLAG. 48 hours later, cells were pulsed with [^{35}S] methionine and chased for the times indicated. Cells were then lysed and immunoprecipitated with CCTε antibody. The black curve represents the assembly of CCT over time, whereas the blue curve represents the dissociation of tubulin from CCT over time. The red curve indicates that PDCD5 is accumulating on CCT over time. B) HEK 293T cells were transfected with empty vector or PhLP1-myc. 48 hours later, cells were subject to a pulse/chase as in (A) except for only one chase time of 90 min. C) HEK 293T cells were treated with negative control or PhLP1 siRNA. 96 hours later, cells were treated as in (B).

To test whether PhLP1 affects the rate of accumulation of PDCD5 on CCT, PhLP1 was over-expressed and the amount of nascent PDCD5 bound to CCT was measured after a 90 minute chase time. The amount of PDCD5 bound to CCT was also measured when PhLP1 was knocked down using siRNA against PhLP1 or a negative control siRNA. In both cases, the amount of nascent PDCD5 bound to CCT did not change significantly when PhLP1 expression was altered (Fig. 3-7B,C). From these results we conclude that PhLP1 does not affect the amount of PDCD5 that accumulates on CCT.

PDCD5, PhLP1, and CCT expression levels in HEK 293T cells.

It has been estimated that there are between 1×10^5 and 3×10^5 CCT complexes in testis and rapidly growing embryonic cells (*76, 77*). In order to determine the stoichiometry of PDCD5, PhLP1, and CCT in cultured cells, we estimated the number of CCT, PDCD5, and PhLP1 particles in HEK 293T cells. Cell lysates were blotted for CCTε, PDCD5, or PhLP1 along with increasing amounts of standards of known concentration of CCT, PDCD5, and PhLP1. We estimate that there are 3×10^5 CCT complexes, 2×10^6 PDCD5 polypeptides, and 2×10^6 PhLP1 polypeptides in HEK 293T cells. The nearly ten-fold excess of PhLP1 and PDCD5 molecules over CCT complexes in cells indicates that there is ample PhLP1 or PDCD5 to associate with all CCT complexes. The excess PhLP1 and PDCD5 also suggests that they may have other yet-to-be determined cellular functions that are independent of CCT.

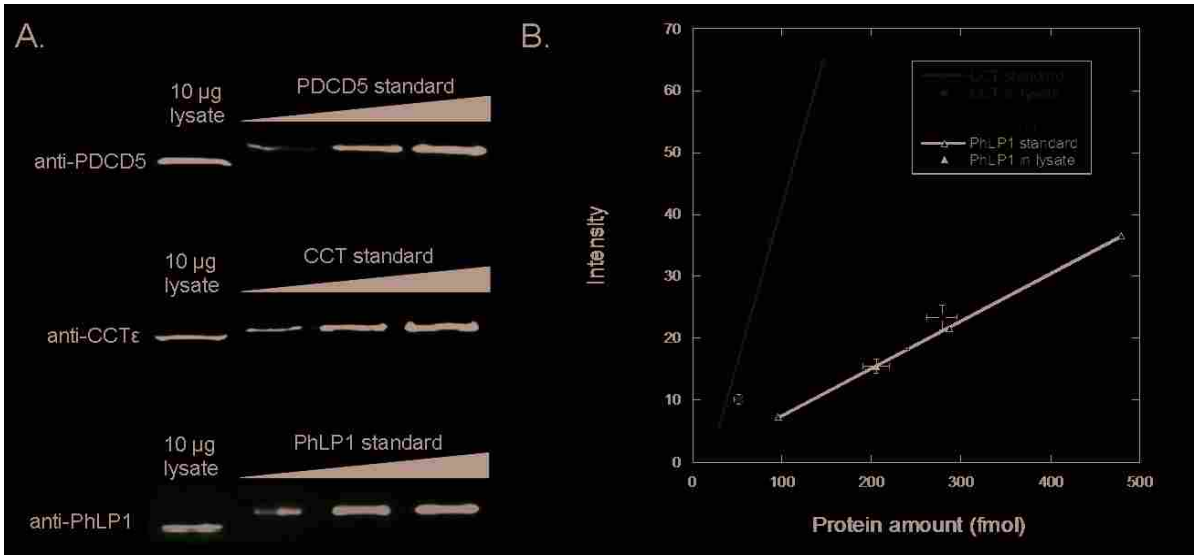

Figure 3-8. PDCD5, PhLP1, and CCT expression levels in HEK 293T cells. A) HEK 293T cells were counted and lysed in immunoprecipitation buffer. 10 µg of cleared cell lysates were immunoblotted along with increasing amounts of PDCD5, CCT, or PhLP1 standard. B) The molar amount of protein standards was plotted against the relative intensities measured on the blots. The molar amount of PDCD5, CCT and PhLP1 found in the cell lysate were interpolated from the standard line. The numbers of molecules were then calculated by mol/cell multiplied by Avogadro's number. Bars represent the average ± standard error from at least three experiments.

PDCD5 does not translocate to the nucleus

It has been suggested that PDCD5 translocates to the nucleus in the early stages of apoptosis (*63*). In order to validate nuclear localization of PDCD5, we induced apoptosis and immunoblotted for PDCD5 in cytosolic and nuclear fractions. The results presented in Figure 3-9 clearly show that PDCD5 does not localize to the nucleus during apoptosis. An increase in phosphorylated H2A.X and PARP cleavage confirm the DNA damage and apoptotic response, but no PDCD5 is found in the nuclear fraction. TATA-binding protein (TBP) is a known nuclear protein that is only present in the nuclear fraction, demonstrating that there is no nuclear cross-contamination in the cytosolic fraction. These data contradict previous reports that PDCD5 is a nuclear protein (*63*). From this result, we propose that the PDCD5 apoptotic activity takes place in the cytosol.

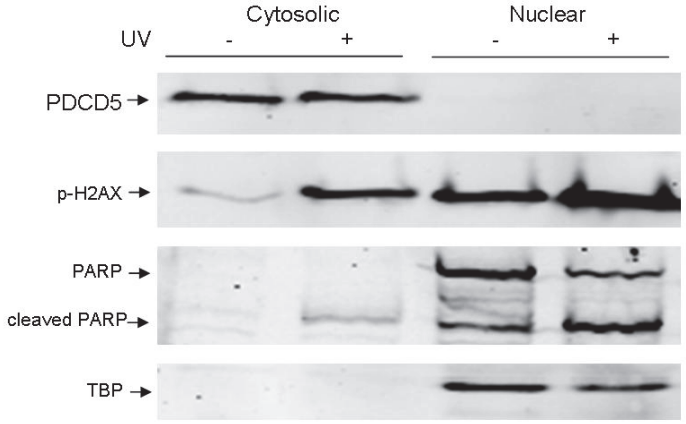

Figure 3-9. Effect of UV-induced DNA damage on the PDCD5-CCT complex. U2OS cells were irradiated with 60 J/m^2 UV-C. They were lysed 14-16 hours later as described in experimental procedures. Cytosolic and nuclear fractions were immunoblotted for the indicated proteins. Representative blots are shown from at least three independent experiments.

The PDCD5-CCT interaction is phosphorylation dependent

CK2 has been shown to phosphorylate PDCD5 on S118. Subsequently, an unphosphorylated S118A PDCD5 variant inhibited apoptotic activity (*65*), suggesting that phosphorylation on S118 is important in the apoptotic activity of PDCD5. To determine whether CCT is also involved in this process, we measured PDCD5 S118 variants binding during apoptosis. UV-induced apoptosis caused a two-fold increase in WT PDCD5 binding to CCT compared to untreated cells (Fig 3-10A). An even greater increase of PDCD5 binding to CCT was observed with the phosphorylation mimetic variant S118E. In contrast, no UV-induced increase was observed with a S118A variant. These results suggest that CK2 phosphorylation in addition to some other unknown event, possibly a second phosphorylation event, causes PDCD5 to bind CCT with greater affinity during apoptosis. The possibility of a second phosphorylation event was subsequently investigated.

We identified a possible phosphorylation site on S99 that is surrounded by a potential Ataxia telangiectasia mutated (ATM) kinase family phosphorylation site. Many amino acid sequences containing an SQ sequence in the phosphorylation site were found to be phosphorylated by ATM kinase family members that are the principle mediators of the DNA

damage response (*78*). PDCD5 harbors an SQ site at residues 99 and 100, thus we hypothesized that this could be another phosphorylation site on PDCD5. In order to determine whether these sites are important in CCT binding, S99 and/or S118 were replaced with alanine (phosphorylation blocking substitution) or aspartic acid (phosphorylation mimetic substitution) resulting in a total of eight single and double point PDCD5 variants. Significant decreases in CCT binding were observed with the S118A variant and the S99D,S118A variant. The S118D variants and all the other S99 A and D variants had little effect on CCT binding (Fig 3-10B). From this data, we can conclude that S118 phosphorylation increases the binding of PDCD5 to CCT and that S99 phosphorylation is not likely to be the other event that contributes to this increased binding.

PDCD5 interacts specifically with β-tubulin

We determined that PDCD5 accumulates on CCT over time and binds with greater affinity during apoptosis (Figures 3-7A and 3-9A). Additionally, we did not observe PDCD5 in the nucleus in healthy nor apoptotic cells (Figure 3-9B). To better understand PDCD5's apoptotic role, we searched for other possible PDCD5 binding partners. We employed a similar immunoprecipitation coupled with mass spectrometry strategy as performed previously with PhLP1. Over-expressed FLAG-TEV-PDCD5 was immunoprecipitated from U2OS cells with and without UV irradiation and analyzed by mass spectrometry. In addition to CCT subunits, PDCD5 was found to bind β-tubulin.

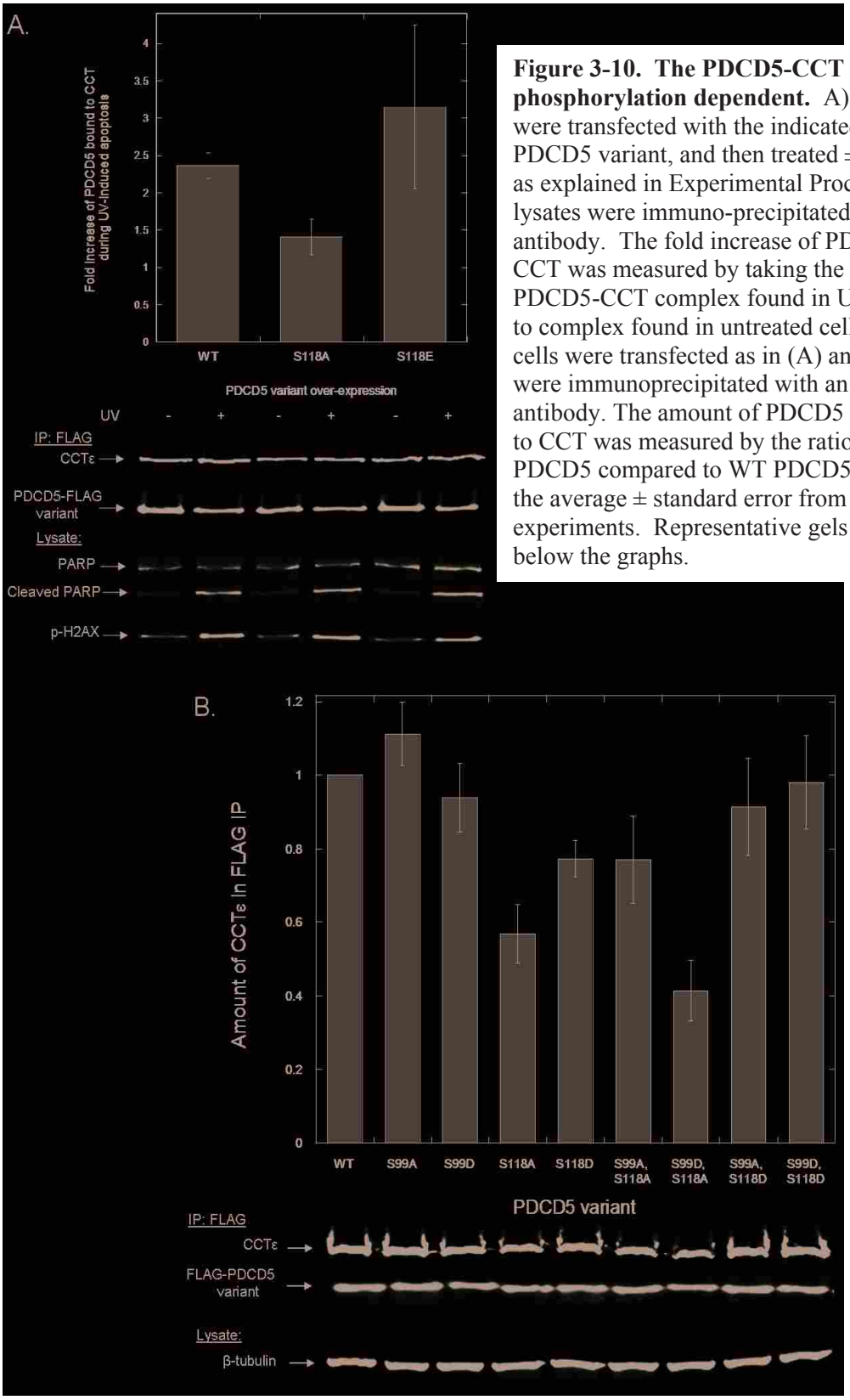

Figure 3-10. The PDCD5-CCT interaction is phosphorylation dependent. A) U2OS cells were transfected with the indicated FLAG-PDCD5 variant, and then treated ± 60 J/m^2 UV as explained in Experimental Procedures. Cells lysates were immuno-precipitated with FLAG antibody. The fold increase of PDCD5 bound to CCT was measured by taking the ratio of PDCD5-CCT complex found in UV treated cells to complex found in untreated cells. B) U2OS cells were transfected as in (A) and cell lysates were immunoprecipitated with an anti-FLAG antibody. The amount of PDCD5 variant bound to CCT was measured by the ratio of CCTε to PDCD5 compared to WT PDCD5. Bars represent the average ± standard error from at least three experiments. Representative gels are shown below the graphs.

Table 3-2. A proteomics search for PDCD5 binding partners.

Control	PDCD5	Significance (decibans)	Gene	Description	UniProt ID
1	174	118.0968	CCT8	T-complex protein 1 subunit theta	P50990
0	155	115.9621	TCP1	T-complex protein 1 subunit alpha	P17987
0	126.2	108.866	CCT3	T-complex protein 1 subunit gamma	P49368
0	105	99.91492	CCT2	T-complex protein 1 subunit beta	P78371
0	96	98.57756	PDCD5	Programmed cell death protein 5	O14737
0	71.5	81.86643	CCT5	T-complex protein 1 subunit epsilon	P48643
0	64.5	77.8806	CCT7	T-complex protein 1 subunit eta	Q99832
0	62.5	75.52574	CCT4	T-complex protein 1 subunit delta	P50991
0	60	74.41963	CCT6A	T-complex protein 1 subunit zeta	P40227
0	15	15.14269	CCT6B	T-complex protein 1 subunit zeta-2	Q92526
0.3333	10.8333	14.26641	TUBB4	Tubulin beta-4 chain	P04350
0.3333	10.1667	13.12643	TUBB2C	Tubulin beta-2C chain	P68371
0.3333	9.08333	10.09961	TUBB	Tubulin beta chain	P07437
0.3333	5.66667	4.224257	TUBB2A	Tubulin beta-2A chain	Q13885

U2OS cells were transfected with empty vector or Flag-TEV-PDCD5 in pcDNA3.1B+. 48 hrs later cells were lysed in an ATP depletion lysis buffer and immunoprecipitated with an anti-FLAG antibody. Proteins were released via TEV protease cleaveage. The co-immunoprecipitates were trypsin digested and analyzed by MS-MS on an Orbitrap mass spectrometer. The table displays a selection of hits found in the proteomics screen. The values in the first two columns indicate the number of peptides indentified in each sample. Values in the third column indicate the significance of the peptide hits (calculated from Bayes factors).

To verify the β-tubulin-PDCD5 interaction, PDCD5 was over-expressed in HEK 293T cells and immunoprecipitated using a FLAG antibody. β-tubulin was found to co-immunoprecipitate with PDCD5, while α-tubulin did not, confirming the specific interaction of PDCD5 with β-tubulin from the MS data (Fig. 3-11A). These data suggest a possible role of PDCD5 in β-tubulin folding. Ongoing work is testing this possibility.

PDCD5 inhibits β-actin folding

The stable interaction of PDCD5 with CCT suggests a role for PDCD5 in the folding of CCT substrates. In addition to tubulins, β-actin is another major substrate of CCT. To investigate the possibility that PDCD5 affects β-actin folding, a pulse-chase assay was employed.

PDCD5 was knocked down in HEK293T cells using RNAi. Cells were pulsed with [^{35}S] methionine for 10 min and chased for 15 min. Folded β-actin was immunoprecipitated with DNase I-coupled beads. When PDCD5 was knocked down 60%, there was no significant change in folded β-actin compared to the negative control (Fig. 3-12A). On the other hand, when PDCD5 was over-expressed, there was a decrease (~30%) in β-actin folding (Fig. 3-12B), suggesting that PDCD5 is inhibiting actin folding. Decreased β-actin folding could be a way in which PDCD5 contributes to the apoptotic response.

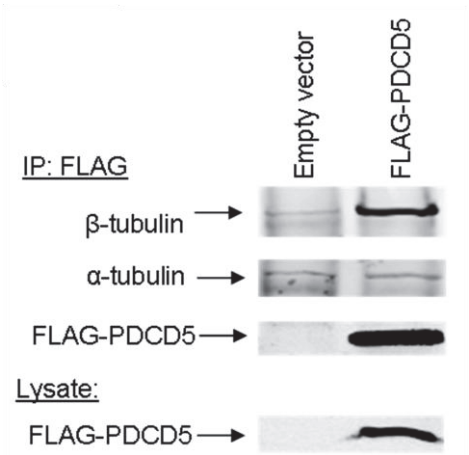

Figure 3-11. PDCD5 interacts specifically with β-tubulin. A) HEK 293T cells were transfected with empty vector or FLAG-PDCD5. Cells were lysed and immunoprecipitated with FLAG antibody. Immunoprecipitates were then immunoblotted for α-tubulin and β-tubulin. Representative blots are shown of three independent experiments.

Discussion

In Chapter 2, PhLP1 was determined to be a general co-chaperone for the assembly of all Gβ and Gγ dimers (*27*). In the current chapter, we sought to identify other functions of PhLP1 by identifying novel protein binding partners or other CCT substrates that utilize PhLP1 in their CCT-mediated folding and assembly. In our proteomics search, PDCD5 was found to be a novel interacting partner of PhLP1 but not any other phosducin-like protein (Fig. 3-1). However, a series of experiments have shown that PhLP1 and PDCD5 do not interact directly, but associate indirectly through CCT (Fig 3-2). This finding is consistent with the effects of PhLP1 phosphorylation on its co-immunoprecipitation with PDCD5. Phosphorylation increases the

binding of PhLP1 to CCT (*38*) and also increased the co-immunoprecipitation of PDCD5 with PhLP1 (Fig 3-1C). Such would be expected if PhLP1 formed a ternary complex with PDCD5 on CCT. Despite the fact that they form a ternary complex with CCT, PhLP1 and PDCD5 were found to bind CCT independently of each other. Consistent with this finding, PDCD5 was found to have no effect on Gβγ assembly.

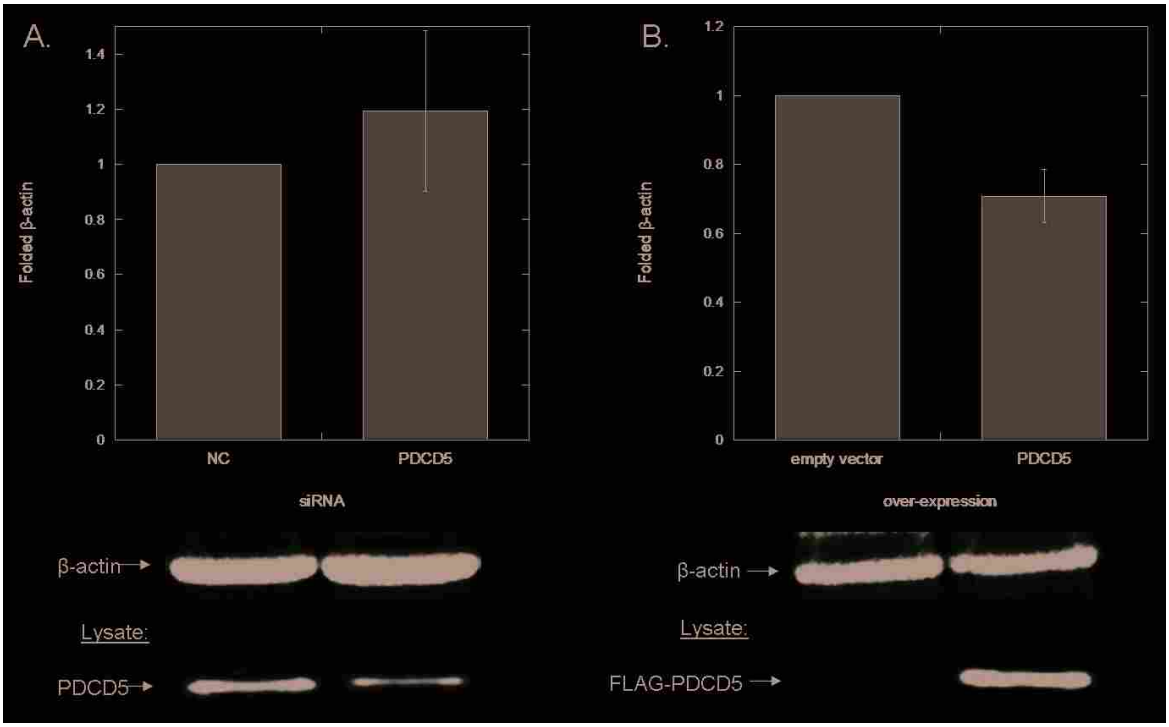

Figure 3-12. **Effect of PDCD5 on β-actin folding.** In HEK 293T cells, PDCD5 was either knocked down (A) or over-expressed (B) as outlined in experimental procedures. Cells were pulsed with [^{35}S] methionine for 10 min and chased for 15 min, and then lysed with actin IP buffer. Cells were immunoprecipitated with DNaseI beads. The amount of folded β-actin was quantified relative to the negative controls. Bars represent the average ± standard error from at least three experiments, and representative gels are shown below the graphs. Cell lysates were blotted for PDCD5 (A) or FLAG-PDCD5 (B) to verify knockdown or over-expression.

Structural data provides greater insight into the interaction between PDCD5 and CCT. Prior cryo-EM analysis of the CCT:PhLP1 complex showed PhLP1 associated with the tips of the CCT apical domains well above the folding cavity. PhLP1 traversed the chaperonin cavity and interacted with three CCT subunits on one side and two on the other (γ, β, ζ, and δ, η, respectively) (*36*). Since PDCD5 binds the CCTδ subunit inside the folding cavity, PhLP1 and

PDCD5 would be able to bind CCT simultaneously with no overlap between the two binding sites. This lack of structural overlap readily explains the observed independence of binding to PhLP1 and PDCD5 to CCT. These findings leave wide open the question of the purpose of the interaction between PDCD5 and CCT.

Our cryo-EM structural analysis revealed PDCD5 binding within the CCT folding cavity, suggesting that PDCD5 might be a CCT substrate (Fig 3-3). However, PDCD5 is a small, 14 kDa protein with a simple structure composed of 5 α-helices (*66*). A typical CCT substrate is larger in size and is usually highly hydrophobic and β-sheet rich (*16, 22, 25*). Thus, PDCD5 does not have the structure of a CCT substrate. Consistent with this observation, we found that PDCD5 is not a CCT substrate when we observed nascent PDCD5 accumulating on CCT over time (Fig 3-7A). What then is the purpose of PDCD5 binding to CCT? We hypothesize that PDCD5 may act either as a co-chaperone for certain CCT substrates or as an inhibitor of other CCT substrates, particularly those involved in apoptotic events.

Previous reported data suggests that PDCD5 translocates to the nucleus in early stages of apoptosis (*63*). This theory was only analyzed by immunohistochemistry, which is notorious for producing false positive results. On the contrary, our data clearly shows that PDCD5 is not a nuclear protein. After successfully extracting the cytosolic and nuclear fractions of U2OS cells, we saw no TBP in the cytosolic fraction. PDCD5 was detected only in the cytoplasmic fraction, whereas no PDCD5 was detected in the nuclear fraction of healthy or apoptotic cells. Furthermore, we were not able to reproduce immunohistochemistry results in favor of PDCD5 nuclear localization (data not shown). These results demonstrate that PDCD5 is not a nuclear protein and that its apoptotic activity is cytosolic, possibly mediated through its interaction with CCT.

The PDCD5-CCT interaction appears to be enhanced during apoptosis by PDCD5 phosphorylation on S118. Transfection of a PDCD5 S118A variant impaired the PDCD5 accelerated apoptotic response in chemical- or UV-induced U2OS cells (*65*). This finding, combined with our structural data, led us to examine the binding of PDCD5 variants to CCT both in healthy and apoptotic cells. We propose that PDCD5 phosphorylation on S118 by CK2 kinase (*65*) is important for CCT binding and that this phosphorylation event causes enhanced binding to CCT during UV-induced apoptosis. Perhaps, the enhanced PDCD5 binding to CCT blocks CCT substrates (particularly those important for cell cycle progression) from entering the folding cavity of CCT. Additional studies will be necessary to determine the signal that triggers the phosphorylation of PDCD5 during apoptosis.

Perhaps one of the apoptotic roles of PDCD5 is to inhibit the folding of CCT substrates as was observed with β-actin. β-actin is a well-known CCT substrate that is delivered to the chaperonin by prefoldin (*22*). It is also known that actin binds inside the chaperonin folding cavity to the CCTδ and CCTβ or CCTε subunits (*72*). In our cryo-EM studies, PDCD5 interacted with the δ subunit within the CCT folding cavity. Therefore, it would not be unreasonable to assume that β-actin and PDCD5 share a binding site on CCT. In agreement with this assumption, over-expression of PDCD5 significantly reduced β-actin folding, while PDCD5 knockdown had no effect. These results indicate that PDCD5 acts as an inhibitor of actin folding by sterically hindering β-actin access to its binding site on CCT. We propose that this reduction of actin folding is due to blockage of the CCTδ subunit (the β-actin binding site) by PDCD5.

In our search for other PDCD5 binding partners, we identified a specific interaction with β-tubulin and confirmed the interaction by co-immunoprecipitation. β-tubulin is a CCT substrate that interacts with α-tubulin to form microtubules, an important component of the cell

cytoskeleton. During microtubule formation, newly synthesized α- and β-tubulin interact with prefoldin and are delivered to CCT. Following ATP hydrolysis on CCT, quasi-native tubulin intermediates interact with tubulin specific co-factors A-E. Finally, native tubulin dimers are released from a super complex that hydrolyzes GTP (*79*). Recently, reports on the crystal structure of the CCT-tubulin complex confirmed previous reports of an interaction of tubulin with the CCTβ subunit inside the chaperonin folding cavity (*71, 80*). We would expect over-expression of PDCD5 to have no effect on β-tubulin binding as they have independent binding sites within the CCT folding cavity. PhLP1 and PDCD5 also have independent binding sites on CCT and were found in a ternary complex with CCT. Therefore, it is not unreasonable to suspect that we found another ternary complex involving PDCD5 and CCT in our MS results with β-tubulin. On-going work is confirming this hypothesis. An alternative function of PDCD5 could be to enhance the folding of pro-apoptotic proteins. A proteomic screen comparing the CCT substrates whose folding is impaired or enhanced during apoptosis and PDCD5 over-expression may provide insight to the apoptotic role of PDCD5.

CHAPTER4:

THE EMERGING FUNCTIONS OF PHOSDUCIN-LIKE PROTEINS 2 AND 3

Summary

Compared to PhLP1, the functions of other members of the phosducin family, PhLP2A, PhLP2B, and PhLP3 are poorly understood. PhLP1 acts as a co-chaperone in CCT-mediated Gβγ assembly. PhLP2 and PhLP3 have no role in G protein signaling, but appear to assist CCT in the folding of actin, tubulin and proteins involved in cell cycle progression. The current chapter investigates the possibility of PhLP2 and/or PhLP3 acting as co-chaperones in the folding and assembly of actins and tubulins. In addition, mass spectrometry results revealed an interaction between PhLP2A and 14-3-3ε, a modulator in cellular signaling. 14-3-3ε was found to interact with PhLP2A in a phosphorylation dependent manner and to relieve the inhibition of β-actin folding caused by PhLP2A over-expression.

Introduction

The phosducin family can be broken up into three homologous families that share an N-terminal helical domain, a central thioredoxin-like fold, and a charged C-terminal extension (*29*). Members of subfamily I, consisting of phosducin and phosducin-like protein 1 (PhLP1), share a Gβγ binding motif that binds Gβγ subunits with high affinity. Phosducin has been shown to act as a chaperone of light-dependent transducin (G_t) translocation from the outer to inner segments in retinal rod cells (*41*). As mentioned before, PhLP1 also plays a Gβγ chaperone role, albeit in an entirely different manner. PhLP1 actually acts as a co-chaperone in the CCT-mediated folding of Gβ and its subsequent assembly with Gγ (*27, 38, 39, 41*). Unlike subfamily I, subfamilies II

and III do not contain a Gβγ binding motif and bind Gβγ poorly. Very little is known regarding the functions of these phosducin subfamilies.

Humans and mice have two phlp2 genes that fall into subfamily II designated as PhLP2A and PhLP2B (*29*). PhLP2A and PhLP2B share 57% homology, yet differ greatly in their expression patterns (*46, 47*). PhLP2A is ubiquitously-expressed (*46*), whereas PhLP2B only expresses in germ cells undergoing meiotic maturation (*47*). However, it is interesting to note that PhLP2B is able to rescue the lethal phenotype of a yeast phlp2 knockout (*47*), demonstrating an evolutionarily conserved function. The yeast ortholog, PLP2, was shown to be essential in *Saccharomyces cerevisiae* when plp2Δ spore products failed to grow (*43*). Additionally, disruption of PhLP2 in *Dictostelium discideum* led to a decreased growth rate followed by a simultaneous collapse of the cell culture after 16-17 cell divisions (*29*). PhLP2 temperature-sensitive alleles in yeast are defective in actin and tubulin function, and PhLP2 has been shown to have an essential function in G1/S phase cell cycle progression (*44*). Temperature-sensitive mutants of CCT subunits also display defects in cell cycle progression (*22*). Together, these observations suggest a possible co-chaperone role for PhLP2 with CCT substrates that are important in cell cycle progression.

Subfamily III contains one member, PhLP3, which has a physiological function distinct from PhLP2. Deletions of PhLP3 in yeast and *Dictyostelium* result in very different phenotypes than PhLP2. PhLP3 knockouts are not lethal, and PhLP3 over-expression cannot rescue the lethality of PhLP2 knockout (*43*), indicating evolutionary distinct roles. However, deletion of PhLP3 protects cells against toxic effects of β-tubulin (*45*). Additionally, siRNA-mediated knockdown of PhLP3 in *C. elegans* results in microtubule architecture defects, suggesting a positive role of PhLP3 in tubulin function (*48*). In contrast, *in vitro* β-tubulin folding assays

show significant effect of PhLP3 (*45*). Recently, PhLP3 studies in mammalian cells have provided more insight into the function of PhLP3. Over-expression of PhLP3 in CHO cells was shown to decrease α-tubulin while increasing β-tubulin levels, thus causing a reorganization of microtubules (*81*). On the other hand, PhLP3 knockdown resulted in cell and nuclei elongation suggesting cytoskeletal changes (*81*). These observations suggest that PhLP3 is involved in microtubule formation.

All phosducin family members except phosducin bind to chaperonin containing tailless complex polypeptide 1 (CCT) in their native form and not as substrates. Recently, the role of PhLP1 as a co-chaperone with CCT in the folding of nascent Gβ and the subsequent association with Gγ has been revealed (*27, 38, 39*). In Chapter 2, PhLP1 was shown to act as a co-chaperone in the assembly of many different Gβγ dimer combinations. It was concluded that PhLP1 acts as general co-chaperone in Gβγ dimer assembly. PhLP2A has also been shown to form ternary complexes with CCT and actin *in vitro*, however these complexes were inactive and inhibited actin folding *(44)*. Cryo-EM studies demonstrated that PhLP3 forms a ternary complex with CCT and either actin or tubulin and negatively regulates their folding (*45*). Additionally, genetic studies have suggested a role for PhLP3 in β-tubulin folding (*49*). Since PhLP2 and PhLP3 also bind CCT in their native form, these other phosducin family members may also act as co-chaperones in the folding of specific substrates.

In addition to co-chaperones, there are several other modulators of cellular signaling. For example, 14-3-3 proteins are essential, highly conserved proteins found in all eukaryotes and are important in modulating many processes including cell cycle control and apoptosis. On the molecular level, 14-3-3 proteins bind specific phosphoserine or phosphothreonine motifs such as RSXpSXP, RX(Y/F)XpSXP or other similar sites (*82*). However, 14-3-3 proteins are also

known to bind targets lacking these consensus sites or even unphosphorylated targets (*83*). Among many other processes, 14-3-3 plays a role in Gβγ signaling in the retina by binding to phosphorylated phosducin (*84*). 14-3-3 interacts with Pdc in a Ca^{2+}/calmodulin-dependent protein kinase II (CaMKII) dependent manner by competing with Gβγ dimers. In a light-adapted retina, Pdc is unphosphorylated and preferentially binds transducin (G_t) βγ dimers, sterically blocking them from interacting with Gα subunits (*85, 86*) or other Gβγ effectors (*87*). Upon dark-adaptation, Ca^{2+} levels rise and Pdc is phosphorylated by CaMKII on S54 and S73. When Pdc is phosphorylated, it preferentially binds 14-3-3, and releases G_tβγ dimers allowing their interaction with G_tα (*84*).

14-3-3 was observed to co-immunoprecipitate with PhLP2B in mouse testicular protein extracts (*47*). The RSSVP motif (amino acids 119-123) of mouse PhLP2B was predicted to be the 14-3-3 binding site which is similar to 14-3-3 binding motifs previously observed (*47*). PhLP2A has a casein kinase II (CKII) consensus sites on S234 and S236 and these residues were recently shown to be phosphorylated in a global phosphoproteome screen (*88, 89*). Thus, it is likely that PhLP2 proteins interact with and are regulated by 14-3-3. Moreover, PhLP2 isoforms could act as co-chaperones in the folding and assembly of 14-3-3 or 14-3-3 could be mediating PhLP2 proteins.

Experimental Procedures

Cell culture

HEK293T cells were cultured in 1:1 DMEM/F-12 growth media containing 2.5 mM L-glutamine and 15 mM HEPES supplemented with 10% fetal bovine serum. The cells were subcultured regularly to maintain growth but were only used to 25 passages.

Preparation of cDNA constructs

Human PhLP1 and PhLP2A were cloned in pcDNA3.1/myc-His B vector (Invitrogen) using PCR. PhLP2A mutants (Δ233-239, S234A, S236, and S234A, S236A) with C-terminal c-myc and His_6 tags were also constructed in pcDNA3.1/myc-His B vector using site-directed mutagenesis. Human 14-3-3ε was constructed in pcDNA3.1/myc-His B vector with a C-terminal FLAG, 3X-FLAG or HA tags using PCR. All sequences were verified by automated DNA sequencing and analysis.

RNA interference experiments

HEK 293T cells were grown in 12-well plates to 50–70% confluency at which point they were transfected with negative control siRNA #1 (Ambion) or CCTζ siRNA (Dharmacon) at 100 nM final concentration using Oligofectamine reagent (Invitrogen) as described previously (*39*). 24 h later, the cells were transfected with 0.5 μg each of 14-3-3ε-FLAG and 14-3-3ε-HA constructs using Lipofectamine 2000 according to the manufacturer's protocol (Invitrogen). The cells were harvested for subsequent immunoprecipitation experiments 72 h later. 10 μg of cell lysates were immunoblotted with an anti-CCTζ antibody (Santa Cruz) to assess the percent CCTζ knockdown.

Transient transfections

HEK 293T cells were grown in 6-well or 12-well plates to 80-90% confluency at which point they were transfected with 1 μg (6-well plate) or 0.5 μg (12-well plate) each of the indicated vectors using Lipofectamine 2000 according to the manufacturer's protocol (Invitrogen). 48 hours later, the cells were harvested for immunoprecipitation experiments.

Radiolabel pulse-chase assays

Transfected HEK 293T cells in 12-well plates were washed and incubated in 1 ml methionine-free DMEM media (Mediatech, Inc.) supplemented with 4 mM $_{L}$-glutamine (Sigma), 0.063 g/l $_{L}$-cystine dihydrochloride (USB) and 10% dialyzed fetal bovine serum (Invitrogen). The media were discarded and the cells were pulsed with 500 µl of new media supplemented with 200 µCi/ml radiolabeled L-[^{35}S] methionine (Perkin-Elmer) for 10 min. After the pulse phase, the cells were washed and incubated in DMEM/F-12 growth media supplemented with an extra 4 mM L-methionine (Sigma) and 4 µM cyclohexamide to stop the [^{35}S] methionine incorporation. After the indicated chase times, the cells were harvested for immunoprecipitation experiments.

Immunoprecipitation experiments

Transfected HEK 293T cells were washed with phosphate-buffered saline (PBS) (Fisher) and solubilized in immunoprecipitation buffer (PBS pH 7.4, 1% NP-40 (Sigma), 0.6 mM PMSF, 6 µl/ml protease inhibitor cocktail per mL buffer (Sigma, P8340)). The lysates were passed through a 25-gauge needle 10 times and centrifuged at maximum speed for 10-12 minutes at 4ºC in an Eppendorf microfuge. The protein concentration for each sample was determined using the DC Protein Assay Kit II (Bio-Rad) and equal amounts of protein were used in the subsequent immunoprecipitations. Approximately 150 µg of total protein were used in immunoprecipitations from cells in 12 well plates and 450 µg from cells in 6 well plates. The clarified lysates were incubated for 30 minutes at 4°C with 1.5 µg anti-FLAG antibody (clone M2, Sigma), for lysates from 12-well plates or with 3 µg of anti-FLAG for lysates from 6-well plates. Next, 30 µl of Protein A/G Plus agarose slurry (Santa Cruz Biotechnology) was added, and the mixture was incubated for 30 minutes at 4°C. In the case of β-actin, DNase I-coupled

beads were used as previously described (*90*). The immunoprecipitated proteins were solubilized in SDS sample buffer and resolved on 10% Tris-Glycine-SDS gels. The proteins were transferred to nitrocellulose and immunoblotted using an anti-FLAG (clone M2, Sigma), anti-c-myc (BioMol), anti-HA (Roche), or anti-CCTζ (Santa Cruz) antibodies. Immunoblots were incubated with the appropriate anti-mouse, anti-rat, or anti-goat (Li-Cor Biosciences) secondary antibody conjugated with an infrared dye. Blots were scanned using an Odyssey Infrared Imaging System (Li-Cor Biosciences), and protein band intensities were quantified using the Odyssey software. The data are presented as the mean value +/- standard error from at least three experiments. In the case of pulse-chase assays, radiolabeled gels were visualized with a Storm 860 phosphorimager, and the band intensities were quantified using Image Quant software (GE Healthcare). The rate data for 14-3-3 assembly were fit to a first-order rate equation with background correction to determine the rate constant for assembly.

Mass spectrometry sample preparation

For immunoprecipitations used in mass spectrometry analysis, the washed protein A/G beads were resuspended in 150 µl AcTEV protease cleavage buffer with 30 units AcTEV protease (Invitrogen) and incubated for 16 hours at 4°C to cleave PhLP2A and co-immunoprecipitating proteins from the beads. Next, each supernatant was reduced with DTT at a final concentration of 4 mM at 60°C for 15 minutes. After the samples had cooled to room temperature, the proteins were alkylated by addition of iodoacetamide at a final concentration of 10 mM and incubated at room temperature for 15 minutes in the dark. The proteins were then acetone precipitated with Acetone-HCL (one drop HCL in 10 ml acetone) at a ratio of 9 parts Acetone-HCl to 1 part sample and incubated at -80°C for 16 hours. The precipitated proteins were pelleted at maximum speed in an Eppendorf microfuge for 20 minutes at 4°C. The

supernatant was removed, and the pelleted proteins dried at room temperature for 20 minutes with the tube lying on its side to prevent dust contamination. The pellet was rehydrated in 20 µl of 8M urea and an additional 73 µl of 25 mM ammonium bicarbonate and 7 µg sequencing grade modified trypsin (Promega) were added. The trypsin digest was incubated for 20 hours at 37°C in a rocking oven and the reaction was quenched by the addition of 1 µl 88% formic acid followed by water bath sonication for 20 minutes. The samples were stored at -20°C until they were used for MS analysis.

Results

Effect of PhLP isoforms on tubulin and actin folding

PhLP2 and PhLP3 have been implicated in actin and tubulin folding (*43-45, 48, 49*). To directly test the role of these PhLP isoforms in actin and tubulin folding, several assays were developed to measure folding in cultured cells. Tubulin binding co-factor B (TBCA or co-factor B) interacts with α-tubulin once α-tubulin is folded and released from CCT. Moreover, co-factor B acts as a reservoir for excess α-tubulin (*79*). Thus, by measuring the binding of nascent α-tubulin to cofactor B in a pulse/chase assay, we were able to examine the effects of PhLP isoforms on α-tubulin folding. When PhLP1, PhLP2A, or PhLP3 were knocked down using siRNA in HEK239T cells, the amount of folded α-tubulin does not change significantly compared to the negative control (Fig 4-1A). Similarly, the amount of folded α-tubulin did not change significantly when PhLP1, PhLP2B, or PhLP3 were over-expressed (Fig. 4-1B). Together, these data indicate that PhLP isoforms do not affect the folding of α-tubulin in HEK 293T cells. In contrast, we have demonstrated that PhLP1 knockdown decreased the rate of Gβ folding and assembly with Gγ 5-fold (*39*) and PhLP1 over-expression increased Gβγ assembly nearly 4-fold using a similar pulse-chase assay (*39*). Therefore, the assay is effective in

detecting co-chaperone activity and it is unlikely that any of the PhLP isoforms are co-chaperones in CCT-mediated α-tubulin folding.

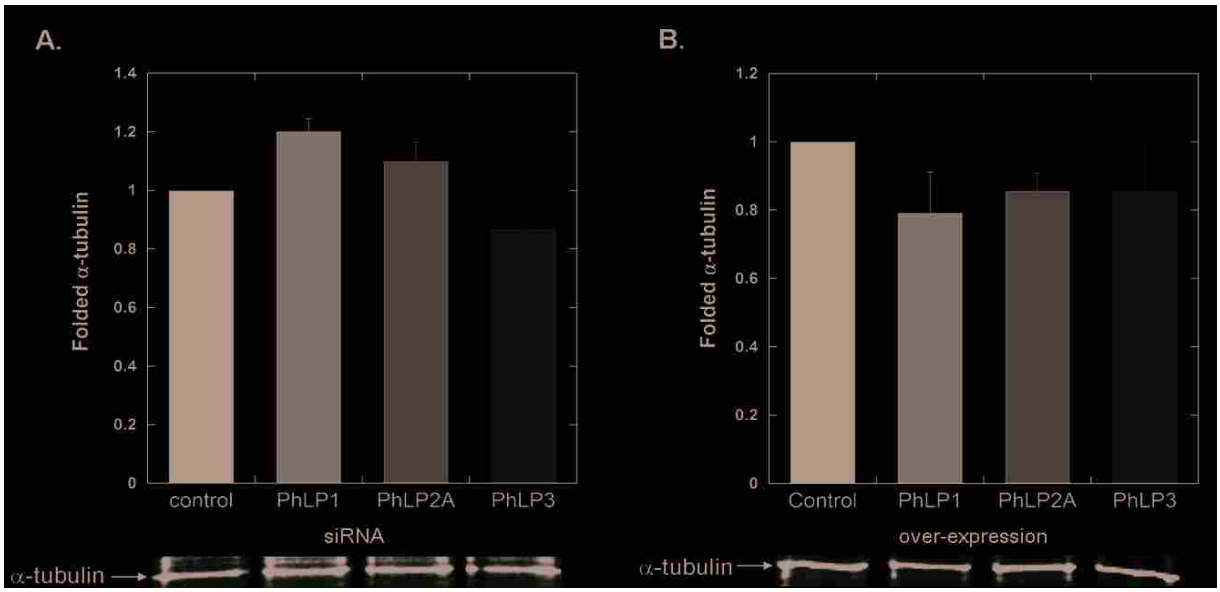

Figure 4-1. Effect of PhLP isoforms on α-tubulin folding. A) HEK-293T cells were treated with siRNA specific to PhLP1, PhLP2A, PhLP3, or negative control siRNA (Ambion) as indicated. After 24 hours, the cells were transfected with an N-terminal FLAG tagged co-factor B. After 72 additional hours, the binding of nascent α-tubulin to co-factor B was determined as a measure of α-tubulin folding in a pulse-chase experimental format as described in Experimental Procedures. In each experiment, the amount of nascent α-tubulin bound to co-factor B was calculated as a fraction of that bound in the negative control siRNA sample. Bars represent the average ± standard error from at least three experiments. A representative gel is shown below the blot. B) HEK-293T cells were transfected with the indicated C-terminal myc-tagged PhLP cDNA constructs. After 48 hours, α-tubulin folding was measured as described in panel A. In each experiment, the amount of nascent α-tubulin bound to co-factor B was calculated as a fraction of that bound in the empty vector control. Bars represent the average ± standard error from at least three experiments. A representative gel is shown below the blot.

A similar pulse-chase assay was used to look at the effect of the different PhLP isoforms on β-actin folding. Folded β-actin binds to DNase I while unfolded β-actin does not (*90*). This fact permitted an analysis of β-actin folding by measuring the amount of ^{35}S-labeld β-actin bound to beads coated with DNase I. When the PhLP isoforms were knocked down using siRNA, the amount of folded β-actin did not change significantly compared to the negative control. Since β-actin is a known CCT substrate (*72*), CCT was also knocked down as a positive

control. A 40% CCT knock down resulted in a proportional 40% decrease in β-actin folding (Fig 4-2A), indicating that the pulse-chase assay was accurately detecting changes in β-actin folding. Not surprisingly, when the PhLP isoforms were over-expressed, the amount of folded β-actin also decreased by 40-60% compared to the empty vector control (Fig 4-2B). This decrease was observed previously with PhLP1 (*35*) and can be attributed to an inability of β-actin to either enter or escape the CCT folding cavity when PhLP isoforms are bound. When bound to CCT, PhLP isoforms span the folding cavity in a manner that would inhibit the folding of CCT substrates that are not assisted by PhLPs (*36, 45*). These data confirm that PhLP isoforms do not act a co-chaperones in CCT-mediated actin folding.

A proteomics search for PhLP2A binding partners

The inability of PhLP isoforms to contribute to α-tubulin and β-actin folding led to a search for other possible substrates for PhLP-assisted folding by CCT. To accomplish this search, an immunoprecipitation coupled with mass spectrometry (MS) strategy was employed to find PhLP binding partners that could be potential folding substrates. Pdc-TEV, PhLP1-TEV, PhLP2A-TEV, each with a C-terminal myc tag, or an empty vector control, were expressed in HEK 293T cells. Each Pdc family member was immunoprecipitated with an antibody against the c-myc tag and the samples were incubated with TEV protease. This procedure freed the PhLP proteins and any interacting partners from the antibody and protein A/G beads, removing these contaminants from the MS analysis. The proteins were reduced, alkylated, acetone precipitated, and then digested with trypsin. The resulting peptides were analyzed by LCMSMS and protein identifications were assigned using the MASCOT software (*68*).

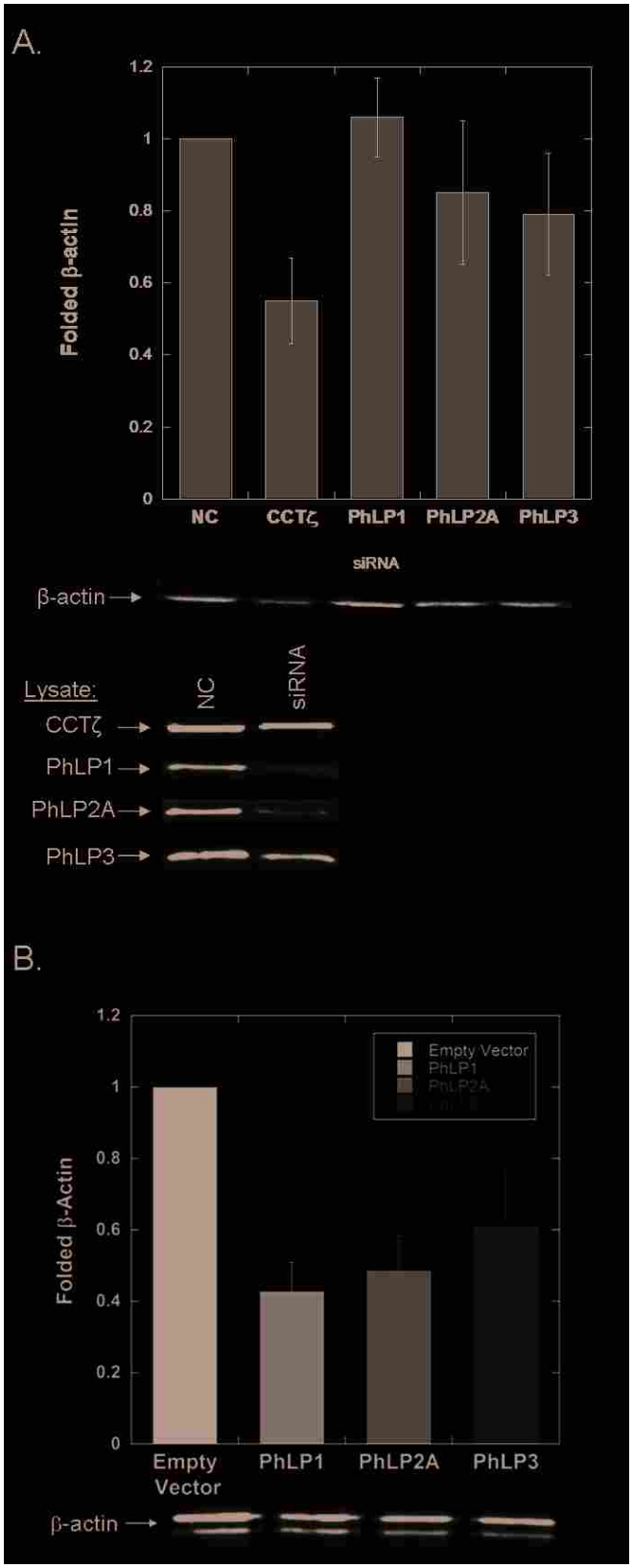

Figure 4-2. Effect of PhLP isoforms on β-actin folding. A) HEK-293T cells were treated with siRNA specific to CCTζ, PhLP1, PhLP2A, or PhLP3, or a negative control siRNA (Ambion) as indicated. Cell extracts were immunoblotted and quantified to determine the efficiency of the siRNA knockdown. B) HEK-293T cells were transfected with cDNA constructs for PhLP1, PhLP2A, PhLP3 or an empty vector control along with a FLAG-β-actin construct as described in Experimental Procedures. The effect of these knockdowns (A) or over-expressions (B) on β-actin folding was determined by measuring the binding of nascent actin to DNase I beads in an [^{35}S] pulse-chase experimental format as described in Experimental Procedures. In each experiment, the amount of β-actin bound to the DNase I beads was calculated as a fraction of that bound in the negative controls. Bars represent the average ± standard error from at least three experiments. Representative gels are shown below the graphs.

The proteins listed in Figure 4-3A were found to interact with either the empty vector control, Pdc, PhLP1 or PhLP2A. Proteins found in the PhLP2A sample that were also found in the Pdc or empty vector controls were treated as false-positive identifications, except for 14-3-3ε which is a known Pdc binding partner (*84*). Several proteins, including elongation factor 1α (eEF1α), NADH-quinone reductase, and S-adenosylmethionine decarboxylase proenzyme 1 were found to interact with PhLP1 and PhLP2A. Six of eight CCT subunits were found in the PhLP2A sample, indicating that PhLP2A interacts with the entire CCT holocomplex and not only with individual CCT subunits. Three proteins, α-tubulin, 14-3-3ε, and ribosomal protein L3, were found to interact specifically with PhLP2A, and not with the negative control.

14-3-3ε co-immunoprecipitates specifically with PhLP2A

Since phosducin is known to be regulated by 14-3-3 and 14-3-3 is predicted to interact with PhLP2B, the interaction of 14-3-3ε with PhLP2A in the MS analysis was intriguing. To confirm the mass spectrometry results, 14-3-3ε was co-immunoprecipitated in HEK 293T cells with each human phosducin family member. PhLP2A was the only phosducin family member to co-immunoprecipitate with 14-3-3ε in HEK 293T cells (Fig. 4-3B). Since S234 and S236 are known phosphorylation sites on PhLP2A (*88*), these sites are possible candidates for a 14-3-3ε binding site. The binding of WT PhLP2A or PhLP2A phosphorylation site variants to 14-3-3ε were measured. This was accomplished by constructing a PhLP2A Δ233-239 truncation variant, a serine to alanine mutation on S234 or S236, and a double mutation where both S234 and S236 were mutated to alanine. All PhLP2A variants co-immunoprecipitated with 14-3-3ε with less affinity than WT PhLP2A (Fig. 4-3C). This observation suggests that the interaction of 14-3-3ε with PhLP2A is phosphorylation dependent. Specifically, phosphorylation of S234 and S236 are important for interaction with 14-3-3ε.

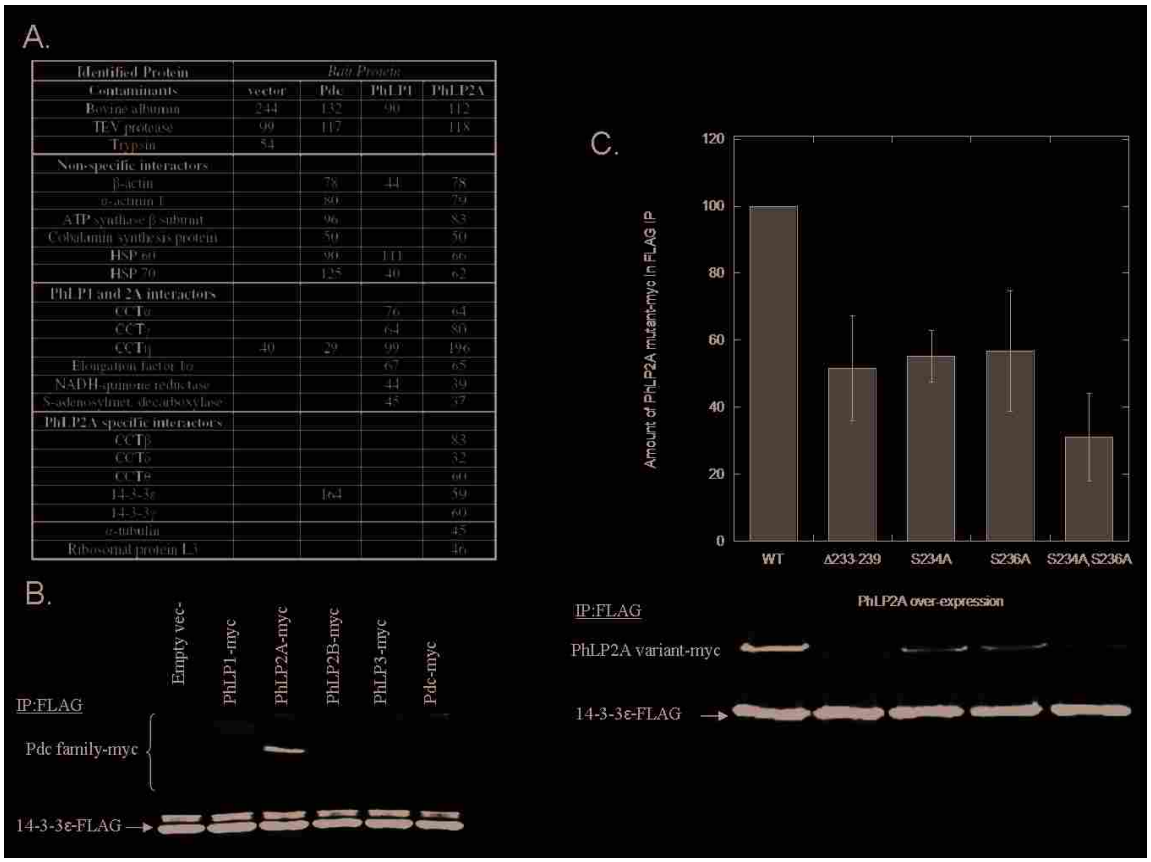

Identified Protein	Bait Protein			
Contaminants	vector	Pdc	PhLP1	PhLP2A
Bovine albumin	244	132	90	112
TEV protease	99	117		118
Trypsin	54			
Non-specific interactors				
β-actin		78	44	78
α-actinin 1		80		79
ATP synthase β subunit		96		83
Cobalamin synthesis protein		50		50
HSP 60		90	111	66
HSP 70		125	40	62
PhLP1 and 2A interactors				
CCTα			76	64
CCTγ			64	80
CCTη	40	29	99	196
Elongation factor 1α			67	65
NADH-quinone reductase			44	39
S-adenosylmet. decarboxylase			45	37
PhLP2A specific interactors				
CCTβ				83
CCTζ				52
CCTε				60
14-3-3ε		164		59
14-3-3ζ				60
α-tubulin				45
Ribosomal protein L3				46

Figure 4-3. 14-3-3ε specifically interacts with PhLP2A. A) HEK 293 cells were transfected with an empty vector control, Pdc-TEV, PhLP1-TEV, or PhLP2A-TEV all with a C-terminal myc tag in pcDNA 3.1 B+. After 48 hours, cells were lysed and immunoprecipitated with an anti-myc antibody. Immunoprecipitated proteins were prepared for MS as described in experimental procedures. LCMSMS was performed on each sample and the spectra were sent to MASCOT. Each protein is listed with its assigned MOWSE (molecular weight search) score which is a weighted probability score based on peptide masses and fragment ions (theoretical values vs. experimental data). Higher MOWSE scores indicate greater confidence in the protein identification. Only those scores with p values <0.05 are listed. B) HEK 293T cells were transfected with 1 μg of each Flag-14-3-3ε and phosducin family members in pcDNA3.1+ myc-His. After 48 hours, the cell lysate was immunoprecipitated with an anti-myc antibody. Each immunoprecipitation was blotted with anti-FLAG or anti-myc antibodies. C) HEK293T cells were transfected with 1μg of FLAG-14-3-3ε in pcDNA3.1+ myc-His and different PhLP2A variants as indicated. After 48 hours, the cells were lysed, immunoprecipitated with an anti-FLAG antibody, and then immunoblotted with anti-myc or anti-FLAG. The amount of the PhLP2A variant bound to 14-3-3ε was calculated by taking to ratio of PhLP2A and 14-3-3ε immunoprecipitated compared to WT PhLP2A. Bars represent the average ± standard error from at least three experiments. Representative gels are shown below the graph.

PhLP2A does not affect 14-3-3ε homodimerization

PhLP1 functions as a co-chaperone with CCT in the folding of Gβ and its subsequent association with Gγ (*39*). One important aspect to note is that PhLP1 must be phosphorylated for Gβγ assembly to occur (*38*). By analogy, we hypothesized that PhLP2A may also interact with CCT as a co-chaperone to assist in the folding of certain CCT substrates (*44, 91*). The interaction between PhLP2A and 14-3-3 suggested the possibility that PhLP2 might somehow be involved in 14-3-3 folding. Like Gβγ, 14-3-3 proteins are obligate dimers (*82*), raising the possibility that PhLP2A assisted in the assembly of 14-3-3 dimers. These observations led us to investigate the role of PhLP2A in 14-3-3 dimer assembly. Dimer formation was measured by co-immunoprecipitation of two differently tagged 14-3-3ε variants. A 3X-FLAG- and an HA-tagged 14-3-3ε were over-expressed in HEK 293T cells, and the assembly of 14-3-3ε homodimers was measured via immunoprecipitation. When PhLP2A was over-expressed, there was no change in the amount of 14-3-3ε-3X-FLAG/14-3-3ε-HA complex that was formed compared to the empty vector control (Fig. 4-4A). The rate of dimer assembly was also measured using a radiolabel pulse-chase experiment. The rate of 14-3-3ε-3X-FLAG/14-3-3ε-HA dimer assembly in the presence of PhLP2A over-expression was not significantly different than in the empty vector control (Fig. 4-4B).

If 14-3-3ε was a CCT substrate, then the assembly of the 14-3-3ε dimer should be affected in the absence of CCT. To test this idea, CCT levels were knocked down using siRNA against the CCTζ subunit and the assembled 14-3-3 dimer was measured using immunoprecipitation. There was no significant change in the amount of 14-3-3ε-3X-FLAG/14-3-3ε-HA dimer that formed (Fig 4-5). These data combined suggest that 14-3-3ε is not a CCT substrate nor is the assembly of 14-3-3ε dimer dependent on PhLP2A.

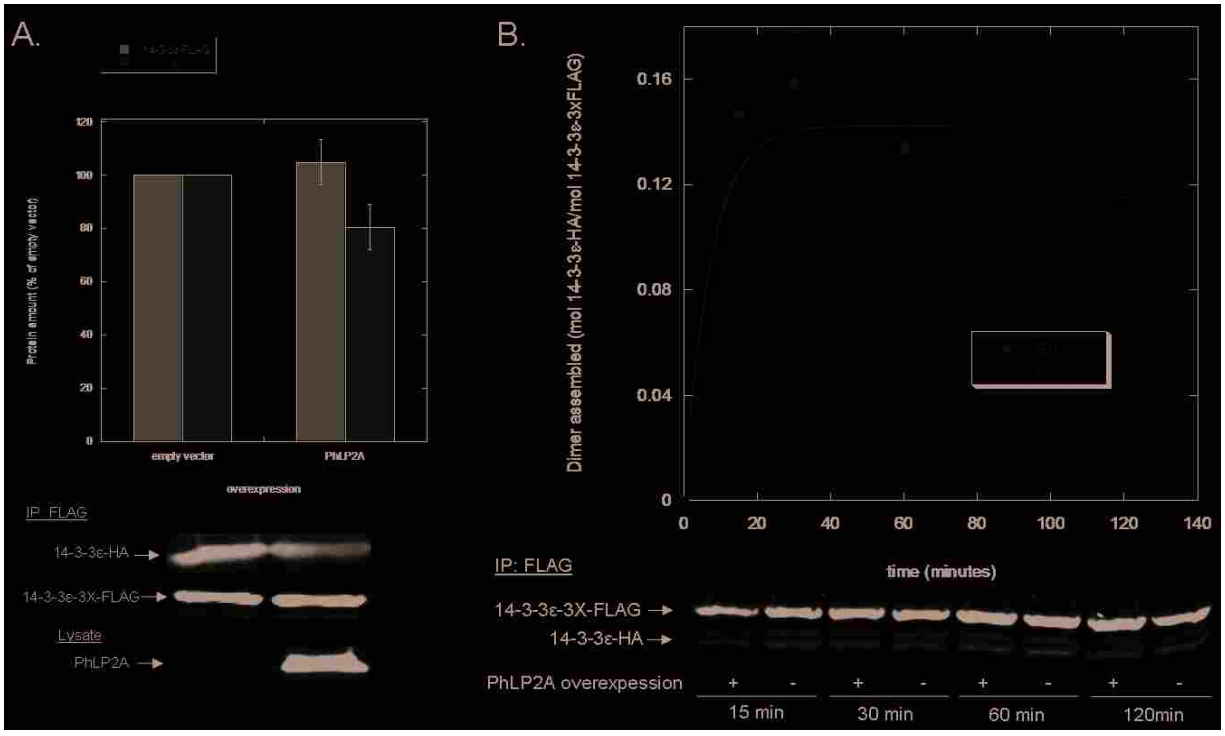

Figure 4-4. PhLP2A does not affect 14-3-3ε homodimerization. A) HEK293T cells were transfected with 1 μg 14-3-3ε-HA and 14-3-3ε-3XFLAG along with 1 μg empty vector or PhLP2A-myc. After 48 hours, cells were lysed and immunoprecipitated with anti-FLAG antibody, and then immunoblotted with HA, FLAG, or myc antibodies. The percentage of protein immunoprecipitated is compared to the empty vector control. Bars represent the average ± standard error from at least three experiments. Representative gels are shown below the graph. B) HEK293T cells were transfected as in (A) and were pulsed with [^{35}S]-methionine and chased with cold methionine for the times indicated. Cells were then lysed and immunoprecipitated with FLAG antibody. The molar ratio of 14-3-3ε-HA to 14-3-3ε-3XFLAG is graphed for each time point. Bars represent the average ± standard error from at least three experiments. Representative gels are shown below the graph.

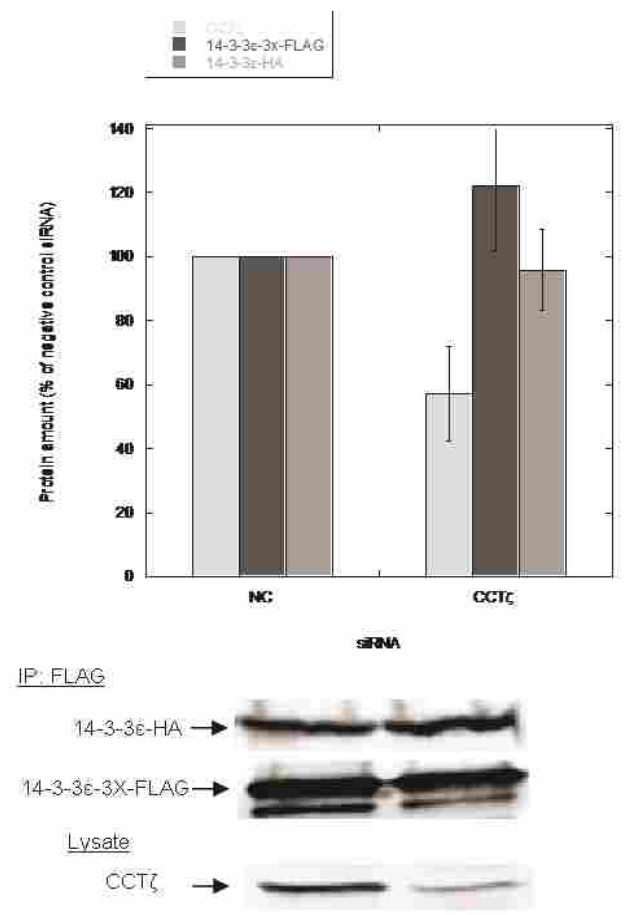

Figure 4-5. 14-3-3ε is not a CCT substrate. HEK293T cells were treated with negative control siRNA or CCTζ siRNA as indicated. 24 hours later, cells were transfected with 1 μg 14-3-3ε-HA and 14-3-3ε-3XFLAG. 72 hours after transfection, cells were lysed and immunoprecipitated with FLAG antibody, and immunoblotted with FLAG or HA antibodies. Cell lysates were immunoblotted for CCTζ to access the knockdown percentage. Bars represent the average ± standard error from at least three experiments. Representative gels are shown below the graph.

14-3-3ε regulates PhLP2A on CCT

When PhLP2A is over-expressed, there is a significant decrease in β-actin folding (Fig. 4-2B). We were also curious to see if phosphorylation of PhLP2A or 14-3-3ε had an effect on β-actin folding. Therefore, we measured the effect of over-expression of PhLP2A, PhLP2A Δ233-239, 14-3-3ε, or different combinations of these on β-actin folding. As observed before, PhLP2A over-expression inhibited β-actin folding. Moreover, PhLP2A Δ233-239 caused a similar effect exhibiting a 60% decrease in β-actin folding (Fig 4-6). 14-3-3ε over-expression did not affect β-actin folding; however, when PhLP2A and 14-3-3ε were over-expressed together, β-actin inhibition by PhLP2A was abolished. Interestingly, when 14-3-3ε and PhLP2A

Δ233-239 were over-expressed inhibition of β-actin folding was the same as when PhLP2A Δ233-239 over-expressed alone. To test whether 14-3-3 influences the CCT-PhLP2A interaction, we measured the effect of 14-3-3ε over-expression on PhLP2A binding to CCT. When 14-3-3ε was over-expressed, PhLP2A binding to CCT did not change compared to the empty vector control (Fig. 4-6B). These results indicate that 14-3-3ε regulates the co-chaperone function of PhLP2A in such a way that does not change PhLP2A's affinity for CCT.

Discussion

For some time, the role of PhLP1 has been understood as a co-chaperone in CCT-mediated folding of Gβ and its subsequent assembly with Gγ (*27, 38, 39*). In comparison, the functions of other members of the phosducin family, namely, PhLP2A, PhLP2B, and PhLP3, are poorly understood. It is clear that the PhLP2 homologs in yeast and *Dictostelium* are essential (*29, 43*), but their function appears to be unrelated to Gβγ signaling(*43*). Temperature sensitive PhLP2 mutants displayed defects in cell cycle progression and cytoskeletal function, suggesting a role in actin or tubulin function (*44*). In the case of PhLP3, genetic studies have pointed to a role for PhLP3 in β-tubulin folding (*49*), and cryo-EM studies demonstrated the formation of a ternary complex between PhLP3, tubulin, and CCT. However, our data revealed no effect of any mammalian PhLP isoform on α-tubulin folding (Fig. 4-1). Recent studies have shown that mammalian PhLP3 over-expression promotes a decrease in α-tubulin and an increase in β-tubulin, which leads to microtubule disassembly and eventual cell death (*81*), suggesting that additional folding assays measuring β-tubulin are necessary to determine whether PhLP3 is a co-chaperone in tubulin folding.

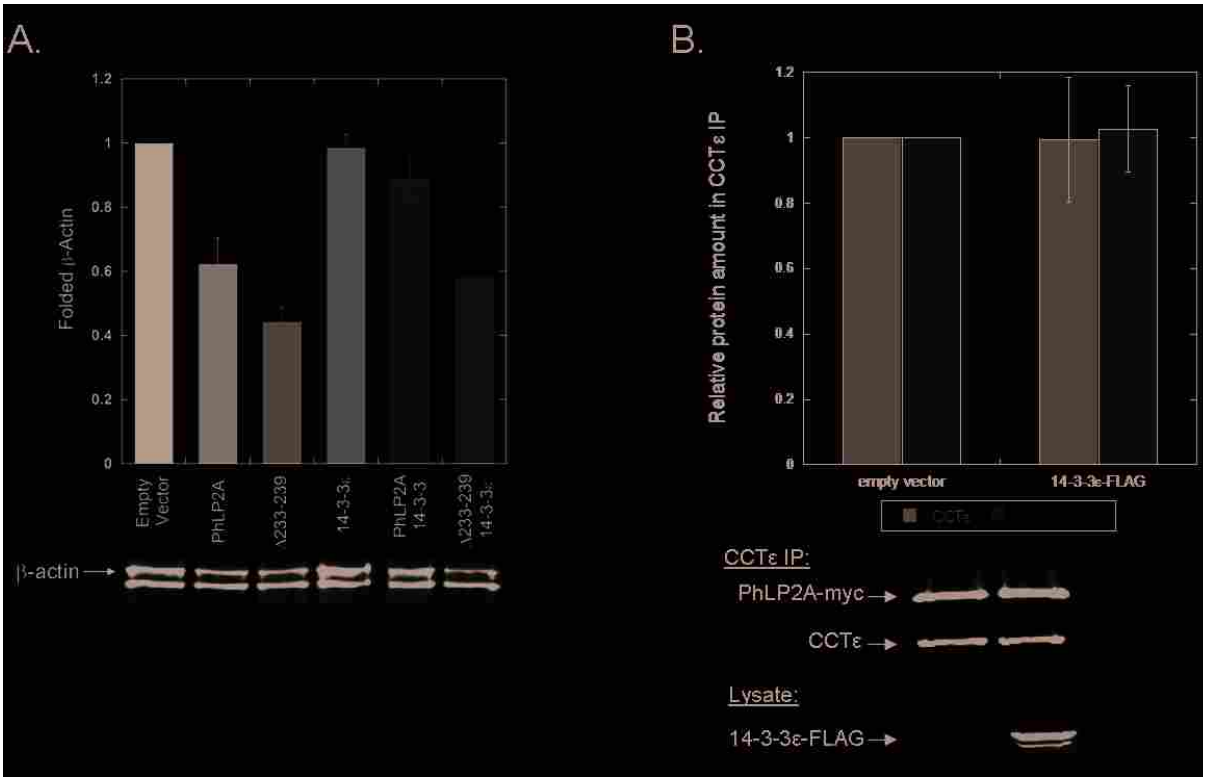

Figure 4-6. Effect of the PhLP2A/14-3-3ε interaction on β-actin folding. A) β-actin and different combinations of PhLP2A variants and 14-3-3ε were over-expressed in HEK 293T cells as indicated. β-actin folding was measured as in Fig. 4-2. B) HEK 293T cells were transfected with PhLP2A-myc along with emtpy vector or 14-3-3ε-FLAG as indicated. Cell lysates were immunoprecipitated with anti-CCTε antibody. Relative protein expressions were measured compared to the empty vector control. Bars represent the average ± standard error from at least three experiments. A representative gel (A) or blots (B) are shown below the graphs.

Although PhLP2A forms a ternary complex with CCT and actin, this complex is inactive and inhibits actin folding *in vitro* (*44*). On the other hand, PLP2 (yeast ortholog of PhLP2A) forms a ternary complex with yeast CCT and actin while highly promoting actin folding *in vitro*, whereas human PhLP2A would not (*91*) . Replacement of the PLP2 C-terminus on human PhLP2A restored actin folding in this system. Consequently, it was suggested that human PhLP2 may require phosphorylation of the C-terminus in order to promote actin folding (*91*). In agreement with the earliest stated data (*44*), knockdown of the PhLPs in the current study resulted in no significant change in actin folding (Fig 4-2A). Moreover, our studies yielded

similar results where over-expression of PhLP1, PhLP2A, or PhLP3 inhibited the folding of actin (Fig. 4-2B). Since the knockdown yielded no change and the over-expression inhibited actin folding, we consider that over-expressed PhLP produces excess PhLP which interacts with CCT, thus blocking actin from entering the CCT folding cavity (Fig. 4-2A). However, in the case of PhLP2A, it is possible that phosphorylation is necessary for PhLP2A to promote actin folding.

Two 14-3-3 isoforms (ε and γ) were identified as PhLP2A binding partners by the MS analysis, but oddly, PhLP2A does not contain a 14-3-3 consensus binding site. Other proteins containing no 14-3-3 consensus site have been shown to interact with 14-3-3 (*83*). The data presented clearly show that PhLP2A does bind 14-3-3ε and that phosphorylation at S234 and S236 is important for the interaction. The 14-3-3 dimer assembly data clearly show that 14-3-3ε is not a CCT substrate nor does PhLP2A regulate the folding and assembly of 14-3-3ε. Interestingly, 14-3-3ε relieves the inhibition of β-actin folding caused by PhLP2A (Fig 4-6), most likely by blocking the binding of PhLP2A to CCT. This finding suggests that 14-3-3ε may regulate the folding of a yet-to-be-determined substrate of PhLP2A and CCT. Despite a concerted effort on our part, the identification of such a substrate has not yet been achieved. Future work to isolate more transient folding intermediates associated with PhLP2A and CCT might be more productive in identifying these elusive substrates of PhLP2A.

REFERENCES

1. Gomez-Puertas, P., Martin-Benito, J., Carrascosa, J. L., Willison, K. R., and Valpuesta, J. M. (2004) The substrate recognition mechanisms in chaperonins, *Journal of molecular recognition : JMR 17*, 85-94.
2. Hartl, F. U., Bracher, A., and Hayer-Hartl, M. (2011) Molecular chaperones in protein folding and proteostasis, *Nature 475*, 324-332.
3. Anfinsen, C. B. (1973) Principles that govern the folding of protein chains, *Science 181*, 223-230.
4. Chen, W. J., and Douglas, M. G. (1987) The role of protein structure in the mitochondrial import pathway. Unfolding of mitochondrially bound precursors is required for membrane translocation, *The Journal of biological chemistry 262*, 15605-15609.
5. Cheng, M. Y., Hartl, F. U., Martin, J., Pollock, R. A., Kalousek, F., Neupert, W., Hallberg, E. M., Hallberg, R. L., and Horwich, A. L. (1989) Mitochondrial heat-shock protein hsp60 is essential for assembly of proteins imported into yeast mitochondria, *Nature 337*, 620-625.
6. McMullin, T. W., and Hallberg, R. L. (1988) A highly evolutionarily conserved mitochondrial protein is structurally related to the protein encoded by the Escherichia coli groEL gene, *Mol Cell Biol 8*, 371-380.
7. Ostermann, J., Horwich, A. L., Neupert, W., and Hartl, F. U. (1989) Protein folding in mitochondria requires complex formation with hsp60 and ATP hydrolysis, *Nature 341*, 125-130.
8. Langer, T., Lu, C., Echols, H., Flanagan, J., Hayer, M. K., and Hartl, F. U. (1992) Successive action of DnaK, DnaJ and GroEL along the pathway of chaperone-mediated protein folding, *Nature 356*, 683-689.
9. Hartl, F. U., and Hayer-Hartl, M. (2002) Molecular chaperones in the cytosol: from nascent chain to folded protein, *Science 295*, 1852-1858.
10. Hartl, F. U. (1996) Molecular chaperones in cellular protein folding, *Nature 381*, 571-579.
11. Frydman, J. (2001) Folding of newly translated proteins in vivo: the role of molecular chaperones, *Annual review of biochemistry 70*, 603-647.
12. Spiess, C., Meyer, A. S., Reissmann, S., and Frydman, J. (2004) Mechanism of the eukaryotic chaperonin: protein folding in the chamber of secrets, *Trends Cell Biol 14*, 598-604.
13. Kim, S., Willison, K. R., and Horwich, A. L. (1994) Cystosolic chaperonin subunits have a conserved ATPase domain but diverged polypeptide-binding domains, *Trends in biochemical sciences 19*, 543-548.
14. Sigler, P. B., Xu, Z., Rye, H. S., Burston, S. G., Fenton, W. A., and Horwich, A. L. (1998) Structure and function in GroEL-mediated protein folding, *Annual review of biochemistry 67*, 581-608.
15. Thulasiraman, V., Yang, C. F., and Frydman, J. (1999) In vivo newly translated polypeptides are sequestered in a protected folding environment, *The EMBO journal 18*, 85-95.

16. Valpuesta, J. M., Martin-Benito, J., Gomez-Puertas, P., Carrascosa, J. L., and Willison, K. R. (2002) Structure and function of a protein folding machine: the eukaryotic cytosolic chaperonin CCT, *FEBS Lett 529*, 11-16.
17. Cong, Y., Baker, M. L., Jakana, J., Woolford, D., Miller, E. J., Reissmann, S., Kumar, R. N., Redding-Johanson, A. M., Batth, T. S., Mukhopadhyay, A., Ludtke, S. J., Frydman, J., and Chiu, W. (2010) 4.0-A resolution cryo-EM structure of the mammalian chaperonin TRiC/CCT reveals its unique subunit arrangement, *Proceedings of the National Academy of Sciences of the United States of America 107*, 4967-4972.
18. Dekker, C., Roe, S. M., McCormack, E. A., Beuron, F., Pearl, L. H., and Willison, K. R. (2011) The crystal structure of yeast CCT reveals intrinsic asymmetry of eukaryotic cytosolic chaperonins, *The EMBO journal 30*, 3078-3090.
19. Wells, C. A., Dingus, J., and Hildebrandt, J. D. (2006) Role of the chaperonin CCT/TRiC complex in G protein betagamma-dimer assembly, *The Journal of biological chemistry 281*, 20221-20232.
20. Llorca, O., Martin-Benito, J., Gomez-Puertas, P., Ritco-Vonsovici, M., Willison, K. R., Carrascosa, J. L., and Valpuesta, J. M. (2001) Analysis of the interaction between the eukaryotic chaperonin CCT and its substrates actin and tubulin, *J Struct Biol 135*, 205-218.
21. Martin-Benito, J., Boskovic, J., Gomez-Puertas, P., Carrascosa, J. L., Simons, C. T., Lewis, S. A., Bartolini, F., Cowan, N. J., and Valpuesta, J. M. (2002) Structure of eukaryotic prefoldin and of its complexes with unfolded actin and the cytosolic chaperonin CCT, *The EMBO journal 21*, 6377-6386.
22. Siegers, K., Bolter, B., Schwarz, J. P., Bottcher, U. M., Guha, S., and Hartl, F. U. (2003) TRiC/CCT cooperates with different upstream chaperones in the folding of distinct protein classes, *The EMBO journal 22*, 5230-5240.
23. Vainberg, I. E., Lewis, S. A., Rommelaere, H., Ampe, C., Vandekerckhove, J., Klein, H. L., and Cowan, N. J. (1998) Prefoldin, a chaperone that delivers unfolded proteins to cytosolic chaperonin, *Cell 93*, 863-873.
24. Dekker, C., Stirling, P. C., McCormack, E. A., Filmore, H., Paul, A., Brost, R. L., Costanzo, M., Boone, C., Leroux, M. R., and Willison, K. R. (2008) The interaction network of the chaperonin CCT, *The EMBO journal 27*, 1827-1839.
25. Ho, Y., Gruhler, A., Heilbut, A., Bader, G. D., Moore, L., Adams, S. L., Millar, A., Taylor, P., Bennett, K., Boutilier, K., Yang, L., Wolting, C., Donaldson, I., Schandorff, S., Shewnarane, J., Vo, M., Taggart, J., Goudreault, M., Muskat, B., Alfarano, C., Dewar, D., Lin, Z., Michalickova, K., Willems, A. R., Sassi, H., Nielsen, P. A., Rasmussen, K. J., Andersen, J. R., Johansen, L. E., Hansen, L. H., Jespersen, H., Podtelejnikov, A., Nielsen, E., Crawford, J., Poulsen, V., Sorensen, B. D., Matthiesen, J., Hendrickson, R. C., Gleeson, F., Pawson, T., Moran, M. F., Durocher, D., Mann, M., Hogue, C. W., Figeys, D., and Tyers, M. (2002) Systematic identification of protein complexes in Saccharomyces cerevisiae by mass spectrometry, *Nature 415*, 180-183.
26. Humrich, J., Bermel, C., Bunemann, M., Harmark, L., Frost, R., Quitterer, U., and Lohse, M. J. (2005) Phosducin-like protein regulates G-protein betagamma folding by interaction with tailless complex polypeptide-1alpha: dephosphorylation or splicing of PhLP turns the switch toward regulation of Gbetagamma folding, *The Journal of biological chemistry 280*, 20042-20050.

27. Howlett, A. C., Gray, A. J., Hunter, J. M., and Willardson, B. M. (2009) Role of molecular chaperones in G protein beta5/regulator of G protein signaling dimer assembly and G protein betagamma dimer specificity, *The Journal of biological chemistry 284*, 16386-16399.
28. Kubota, S., Kubota, H., and Nagata, K. (2006) Cytosolic chaperonin protects folding intermediates of Gbeta from aggregation by recognizing hydrophobic beta-strands, *Proceedings of the National Academy of Sciences of the United States of America 103*, 8360-8365.
29. Blaauw, M., Knol, J. C., Kortholt, A., Roelofs, J., Ruchira, Postma, M., Visser, A. J., and van Haastert, P. J. (2003) Phosducin-like proteins in Dictyostelium discoideum: implications for the phosducin family of proteins, *The EMBO journal 22*, 5047-5057.
30. Savage, J. R., McLaughlin, J. N., Skiba, N. P., Hamm, H. E., and Willardson, B. M. (2000) Functional roles of the two domains of phosducin and phosducin-like protein, *The Journal of biological chemistry 275*, 30399-30407.
31. Miles, M. F., Barhite, S., Sganga, M., and Elliott, M. (1993) Phosducin-like protein: an ethanol-responsive potential modulator of guanine nucleotide-binding protein function, *Proceedings of the National Academy of Sciences of the United States of America 90*, 10831-10835.
32. Lee, R. H., Lieberman, B. S., and Lolley, R. N. (1987) A novel complex from bovine visual cells of a 33,000-dalton phosphoprotein with beta- and gamma-transducin: purification and subunit structure, *Biochemistry 26*, 3983-3990.
33. Reig, J. A., Yu, L., and Klein, D. C. (1990) Pineal transduction. Adrenergic----cyclic AMP-dependent phosphorylation of cytoplasmic 33-kDa protein (MEKA) which binds beta gamma-complex of transducin, *The Journal of biological chemistry 265*, 5816-5824.
34. Schroder, S., and Lohse, M. J. (2000) Quantification of the tissue levels and function of the G-protein regulator phosducin-like protein (PhlP), *Naunyn Schmiedebergs Arch Pharmacol 362*, 435-439.
35. McLaughlin, J. N., Thulin, C. D., Hart, S. J., Resing, K. A., Ahn, N. G., and Willardson, B. M. (2002) Regulatory interaction of phosducin-like protein with the cytosolic chaperonin complex, *Proceedings of the National Academy of Sciences of the United States of America 99*, 7962-7967.
36. Martin-Benito, J., Bertrand, S., Hu, T., Ludtke, P. J., McLaughlin, J. N., Willardson, B. M., Carrascosa, J. L., and Valpuesta, J. M. (2004) Structure of the complex between the cytosolic chaperonin CCT and phosducin-like protein, *Proceedings of the National Academy of Sciences of the United States of America 101*, 17410-17415.
37. Knol, J. C., Engel, R., Blaauw, M., Visser, A. J., and van Haastert, P. J. (2005) The phosducin-like protein PhLP1 is essential for G{beta}{gamma} dimer formation in Dictyostelium discoideum, *Mol Cell Biol 25*, 8393-8400.
38. Lukov, G. L., Baker, C. M., Ludtke, P. J., Hu, T., Carter, M. D., Hackett, R. A., Thulin, C. D., and Willardson, B. M. (2006) Mechanism of assembly of G protein betagamma subunits by protein kinase CK2-phosphorylated phosducin-like protein and the cytosolic chaperonin complex, *The Journal of biological chemistry 281*, 22261-22274.
39. Lukov, G. L., Hu, T., McLaughlin, J. N., Hamm, H. E., and Willardson, B. M. (2005) Phosducin-like protein acts as a molecular chaperone for G protein betagamma dimer assembly, *The EMBO journal 24*, 1965-1975.

40. Humrich, J., Bermel, C., Grubel, T., Quitterer, U., and Lohse, M. J. (2003) Regulation of phosducin-like protein by casein kinase 2 and N-terminal splicing, *The Journal of biological chemistry 278*, 4474-4481.
41. Willardson, B. M., and Howlett, A. C. (2007) Function of phosducin-like proteins in G protein signaling and chaperone-assisted protein folding, *Cell Signal 19*, 2417-2427.
42. Dupre, D. J., Robitaille, M., Richer, M., Ethier, N., Mamarbachi, A. M., and Hebert, T. E. (2007) Dopamine receptor-interacting protein 78 acts as a molecular chaperone for Ggamma subunits before assembly with Gbeta, *The Journal of biological chemistry 282*, 13703-13715.
43. Flanary, P. L., DiBello, P. R., Estrada, P., and Dohlman, H. G. (2000) Functional analysis of Plp1 and Plp2, two homologues of phosducin in yeast, *The Journal of biological chemistry 275*, 18462-18469.
44. Stirling, P. C., Srayko, M., Takhar, K. S., Pozniakovsky, A., Hyman, A. A., and Leroux, M. R. (2007) Functional interaction between phosducin-like protein 2 and cytosolic chaperonin is essential for cytoskeletal protein function and cell cycle progression, *Molecular biology of the cell 18*, 2336-2345.
45. Stirling, P. C., Cuellar, J., Alfaro, G. A., El Khadali, F., Beh, C. T., Valpuesta, J. M., Melki, R., and Leroux, M. R. (2006) PhLP3 modulates CCT-mediated actin and tubulin folding via ternary complexes with substrates, *The Journal of biological chemistry 281*, 7012-7021.
46. Wilkinson, J. C., Richter, B. W., Wilkinson, A. S., Burstein, E., Rumble, J. M., Balliu, B., and Duckett, C. S. (2004) VIAF, a conserved inhibitor of apoptosis (IAP)-interacting factor that modulates caspase activation, *The Journal of biological chemistry 279*, 51091-51099.
47. Lopez, P., Yaman, R., Lopez-Fernandez, L. A., Vidal, F., Puel, D., Clertant, P., Cuzin, F., and Rassoulzadegan, M. (2003) A novel germ line-specific gene of the phosducin-like protein (PhLP) family. A meiotic function conserved from yeast to mice, *The Journal of biological chemistry 278*, 1751-1757.
48. Ogawa, S., Matsubayashi, Y., and Nishida, E. (2004) An evolutionarily conserved gene required for proper microtubule architecture in Caenorhabditis elegans, *Genes Cells 9*, 83-93.
49. Lacefield, S., and Solomon, F. (2003) A novel step in beta-tubulin folding is important for heterodimer formation in Saccharomyces cerevisiae, *Genetics 165*, 531-541.
50. Wettschureck, N., and Offermanns, S. (2005) Mammalian G proteins and their cell type specific functions, *Physiol Rev 85*, 1159-1204.
51. Cabrera-Vera, T. M., Vanhauwe, J., Thomas, T. O., Medkova, M., Preininger, A., Mazzoni, M. R., and Hamm, H. E. (2003) Insights into G protein structure, function, and regulation, *Endocr Rev 24*, 765-781.
52. Reiter, E., and Lefkowitz, R. J. (2006) GRKs and beta-arrestins: roles in receptor silencing, trafficking and signaling, *Trends Endocrinol Metab 17*, 159-165.
53. Willars, G. B. (2006) Mammalian RGS proteins: multifunctional regulators of cellular signalling, *Semin Cell Dev Biol 17*, 363-376.
54. Marrari, Y., Crouthamel, M., Irannejad, R., and Wedegaertner, P. B. (2007) Assembly and trafficking of heterotrimeric G proteins, *Biochemistry 46*, 7665-7677.
55. Gautam, N., Downes, G. B., Yan, K., and Kisselev, O. (1998) The G-protein betagamma complex, *Cell Signal 10*, 447-455.

56. Robishaw, J. D., and Berlot, C. H. (2004) Translating G protein subunit diversity into functional specificity, *Curr Opin Cell Biol 16*, 206-209.
57. Watson, A. J., Katz, A., and Simon, M. I. (1994) A fifth member of the mammalian G-protein beta-subunit family. Expression in brain and activation of the beta 2 isotype of phospholipase C, *The Journal of biological chemistry 269*, 22150-22156.
58. Downes, G. B., and Gautam, N. (1999) The G protein subunit gene families, *Genomics 62*, 544-552.
59. Ray, K., Hansen, C. A., and Robishaw, J. D. (1996) Gbetagamma-Mediated signaling in the heart: Implications of beta and gamma subunit heterogeneity, *Trends Cardiovasc Med 6*, 115-121.
60. Dingus, J., Wells, C. A., Campbell, L., Cleator, J. H., Robinson, K., and Hildebrandt, J. D. (2005) G Protein betagamma dimer formation: Gbeta and Ggamma differentially determine efficiency of in vitro dimer formation, *Biochemistry 44*, 11882-11890.
61. Witherow, D. S., and Slepak, V. Z. (2003) A novel kind of G protein heterodimer: the G beta5-RGS complex, *Receptors Channels 9*, 205-212.
62. Liu, H., Wang, Y., Zhang, Y., Song, Q., Di, C., Chen, G., Tang, J., and Ma, D. (1999) TFAR19, a novel apoptosis-related gene cloned from human leukemia cell line TF-1, could enhance apoptosis of some tumor cells induced by growth factor withdrawal, *Biochem Biophys Res Commun 254*, 203-210.
63. Chen, Y., Sun, R., Han, W., Zhang, Y., Song, Q., Di, C., and Ma, D. (2001) Nuclear translocation of PDCD5 (TFAR19): an early signal for apoptosis?, *FEBS Lett 509*, 191-196.
64. Chen, L. N., Wang, Y., Ma, D. L., and Chen, Y. Y. (2006) Short interfering RNA against the PDCD5 attenuates cell apoptosis and caspase-3 activity induced by Bax overexpression, *Apoptosis 11*, 101-111.
65. Salvi, M., Xu, D., Chen, Y., Cabrelle, A., Sarno, S., and Pinna, L. A. (2009) Programmed cell death protein 5 (PDCD5) is phosphorylated by CK2 in vitro and in 293T cells, *Biochem Biophys Res Commun 387*, 606-610.
66. Yao, H., Xu, L., Feng, Y., Liu, D., Chen, Y., and Wang, J. (2009) Structure-function correlation of human programmed cell death 5 protein, *Archives of biochemistry and biophysics 486*, 141-149.
67. Hong, J., Zhang, J., Liu, Z., Qin, S., Wu, J., and Shi, Y. (2009) Solution structure of S. cerevisiae PDCD5-like protein and its promoting role in H(2)O(2)-induced apoptosis in yeast, *Biochemistry 48*, 6824-6834.
68. Perkins, D. N., Pappin, D. J., Creasy, D. M., and Cottrell, J. S. (1999) Probability-based protein identification by searching sequence databases using mass spectrometry data, *Electrophoresis 20*, 3551-3567.
69. Thulin, C. D., Howes, K., Driscoll, C. D., Savage, J. R., Rand, T. A., Baehr, W., and Willardson, B. M. (1999) The immunolocalization and divergent roles of phosducin and phosducin-like protein in the retina, *Mol Vis 5*, 40.
70. Wang, Y., Li, D., Fan, H., Tian, L., Zhong, Y., Zhang, Y., Yuan, L., Jin, C., Yin, C., and Ma, D. (2006) Cellular uptake of exogenous human PDCD5 protein, *The Journal of biological chemistry 281*, 24803-24817.
71. Llorca, O., Martin-Benito, J., Ritco-Vonsovici, M., Grantham, J., Hynes, G. M., Willison, K. R., Carrascosa, J. L., and Valpuesta, J. M. (2000) Eukaryotic chaperonin CCT

stabilizes actin and tubulin folding intermediates in open quasi-native conformations, *The EMBO journal 19*, 5971-5979.
72. Llorca, O., McCormack, E. A., Hynes, G., Grantham, J., Cordell, J., Carrascosa, J. L., Willison, K. R., Fernandez, J. J., and Valpuesta, J. M. (1999) Eukaryotic type II chaperonin CCT interacts with actin through specific subunits, *Nature 402*, 693-696.
73. Liou, A. K., and Willison, K. R. (1997) Elucidation of the subunit orientation in CCT (chaperonin containing TCP1) from the subunit composition of CCT micro-complexes, *The EMBO journal 16*, 4311-4316.
74. Martin-Benito, J., Grantham, J., Boskovic, J., Brackley, K. I., Carrascosa, J. L., Willison, K. R., and Valpuesta, J. M. (2007) The inter-ring arrangement of the cytosolic chaperonin CCT, *EMBO reports 8*, 252-257.
75. Yam, A. Y., Xia, Y., Lin, H. T., Burlingame, A., Gerstein, M., and Frydman, J. (2008) Defining the TRiC/CCT interactome links chaperonin function to stabilization of newly made proteins with complex topologies, *Nature structural & molecular biology 15*, 1255-1262.
76. Kubota, H., Hynes, G., Carne, A., Ashworth, A., and Willison, K. (1994) Identification of six Tcp-1-related genes encoding divergent subunits of the TCP-1-containing chaperonin, *Curr Biol 4*, 89-99.
77. Lewis, V. A., Hynes, G. M., Zheng, D., Saibil, H., and Willison, K. (1992) T-complex polypeptide-1 is a subunit of a heteromeric particle in the eukaryotic cytosol, *Nature 358*, 249-252.
78. Kim, S. T., Lim, D. S., Canman, C. E., and Kastan, M. B. (1999) Substrate specificities and identification of putative substrates of ATM kinase family members, *The Journal of biological chemistry 274*, 37538-37543.
79. Lopez-Fanarraga, M., Avila, J., Guasch, A., Coll, M., and Zabala, J. C. (2001) Review: postchaperonin tubulin folding cofactors and their role in microtubule dynamics, *J Struct Biol 135*, 219-229.
80. Munoz, I. G., Yebenes, H., Zhou, M., Mesa, P., Serna, M., Park, A. Y., Bragado-Nilsson, E., Beloso, A., de Carcer, G., Malumbres, M., Robinson, C. V., Valpuesta, J. M., and Montoya, G. (2011) Crystal structure of the open conformation of the mammalian chaperonin CCT in complex with tubulin, *Nature structural & molecular biology 18*, 14-19.
81. Hayes, N. V., Josse, L., Smales, C. M., and Carden, M. J. (2011) Modulation of phosducin-like protein 3 (PhLP3) levels promotes cytoskeletal remodelling in a MAPK and RhoA-dependent manner, *PloS one 6*, e28271.
82. Yaffe, M. B., Rittinger, K., Volinia, S., Caron, P. R., Aitken, A., Leffers, H., Gamblin, S. J., Smerdon, S. J., and Cantley, L. C. (1997) The structural basis for 14-3-3:phosphopeptide binding specificity, *Cell 91*, 961-971.
83. Bridges, D., and Moorhead, G. B. (2005) 14-3-3 proteins: a number of functions for a numbered protein, *Science's STKE : signal transduction knowledge environment 2005*, re10.
84. Thulin, C. D., Savage, J. R., McLaughlin, J. N., Truscott, S. M., Old, W. M., Ahn, N. G., Resing, K. A., Hamm, H. E., Bitensky, M. W., and Willardson, B. M. (2001) Modulation of the G protein regulator phosducin by Ca2+/calmodulin-dependent protein kinase II phosphorylation and 14-3-3 protein binding, *The Journal of biological chemistry 276*, 23805-23815.

85. Gaudet, R., Bohm, A., and Sigler, P. B. (1996) Crystal structure at 2.4 angstroms resolution of the complex of transducin betagamma and its regulator, phosducin, *Cell 87*, 577-588.
86. Yoshida, T., Willardson, B. M., Wilkins, J. F., Jensen, G. J., Thornton, B. D., and Bitensky, M. W. (1994) The phosphorylation state of phosducin determines its ability to block transducin subunit interactions and inhibit transducin binding to activated rhodopsin, *The Journal of biological chemistry 269*, 24050-24057.
87. Ford, C. E., Skiba, N. P., Bae, H., Daaka, Y., Reuveny, E., Shekter, L. R., Rosal, R., Weng, G., Yang, C. S., Iyengar, R., Miller, R. J., Jan, L. Y., Lefkowitz, R. J., and Hamm, H. E. (1998) Molecular basis for interactions of G protein betagamma subunits with effectors, *Science 280*, 1271-1274.
88. Dephoure, N., Zhou, C., Villen, J., Beausoleil, S. A., Bakalarski, C. E., Elledge, S. J., and Gygi, S. P. (2008) A quantitative atlas of mitotic phosphorylation, *Proceedings of the National Academy of Sciences of the United States of America 105*, 10762-10767.
89. Kim, J. E., Tannenbaum, S. R., and White, F. M. (2005) Global phosphoproteome of HT-29 human colon adenocarcinoma cells, *J Proteome Res 4*, 1339-1346.
90. Rosenblatt, J., Peluso, P., and Mitchison, T. J. (1995) The bulk of unpolymerized actin in Xenopus egg extracts is ATP-bound, *Molecular biology of the cell 6*, 227-236.
91. McCormack, E. A., Altschuler, G. M., Dekker, C., Filmore, H., and Willison, K. R. (2009) Yeast phosducin-like protein 2 acts as a stimulatory co-factor for the folding of actin by the chaperonin CCT via a ternary complex, *Journal of molecular biology 391*, 192-206.